UNIVERSITY OF CALIFORNIA SAN DIEGO

Regulation of *FSHB* Transcription by a Novel Distal Enhancer

A dissertation submitted in partial satisfaction of the requirements for the degree Doctor of Philosophy

in

Neurosciences

by

Stephanie Claire Bohaczuk

Committee in Charge:

Professor Pamela Mellon, Chair
Professor Alexander Kauffman
Professor Francesca Telese
Professor Varykina Thackray
Professor Nicholas Webster

2021

The dissertation of Stephanie Claire Bohaczuk is approved, and it is acceptable in quality and form for publication on microfilm and electronically.

University of California San Diego

2021

DEDICATION

I would like to dedicate my dissertation to those who made it possible. First, to my parents and sister, who nurtured my passion for science from an early age. Second, to my good friend Elad Idan, for encouraging me not only to succeed but to find happiness and balance in the process.

EPIGRAPH

Share your knowledge. It is a way to achieve immortality.

Dalai Lama

TABLE OF CONTENTS

LIST OF ABBREVIATIONS

ChIP	Chromatin immunoprecipitation
Enh	Enhancer
FSH	Follicle-stimulating hormone
FSHB	FSH beta-subunit gene
GnRH	Gonadotropin-releasing hormone
GWAS	Genome-wide association study
HPG axis	Hypothalamic-pituitary-gonadal axis
Luc	Luciferase
LH	Luteinizing hormone
PCOS	Polycystic ovary syndrome
scATAC-seq	Single-cell Assay for Transposase Accessible Chromatin using sequencing
SF1	Steroidogenic factor 1
SNP	Single-nucleotide polymorphism

LIST OF FIGURES

LIST OF TABLES

ACKNOWLEDGEMENTS

I would first like to thank my thesis advisor, Pamela Mellon, who always supported me whenever needed but also offered me independence to learn how to become a scientist. I would also like to thank my high school mentor, Donna Leonardi, and undergraduate mentors, Elliot Meyerowitz and Paul Tarr, for teaching me the fundamentals of molecular biology. I am especially grateful for members of the Mellon lab, especially Shanna Newton Lavalle, Erica Schoeller, and Jessica Cassin, for technical support, advice, and comfort in the face of difficulties, as well as for our lab manager, Ichiko Saotome, who performed spectacular feats in the face of COVID-19 to keep the lab running as smoothly as ever. I would also like to thank Theresa Slaiwa for her assistance with experiments and patience as I learned how to be a research mentor. Additionally, I would like to thank my committee member and NRSA co-mentor, Varykina Thackray, for her advice and support through all stages of my studies, as well as my other committee members, Alexander Kauffman, Francesca Telese, and Nicholas Webster, for their helpful insights.

I would also like to thank the Neurosciences Graduate program at UCSD for providing me with a solid foundation to succeed in my studies. I am endlessly grateful for the support of my peers who entered the program with me in 2015. Together, we faced and overcame challenges more extreme than I ever could have expected. I admire you all and feel honored to have been a part of such a group.

Finally, I would like to thank my family and friends for their support extending long before my graduate studies. In particular, my parents, Phyllis and Anthony Bohaczuk, for their encouragement to value knowledge and making it possible for me to pursue science even before I could drive myself to the lab. I would also like to thank my sister, Sonya Bohaczuk, for many

years of entertainment, advice, and for making sure that all the teachers I had after her were grateful, and not afraid, to have me in their classes. I am so grateful for my friend Elad Idan, who has always encouraged me to chase not just success, but happiness, no matter what form it might take. Finally, I would like to thank my husband, Antonín Pavelka, for countless hours of interesting discussions, embracing our individuality, and for traveling across the world during a pandemic so that we could be together while I finished my Ph.D.

Chapter 1 has been published in *Endocrinology* (Bohaczuk, Stephanie. C.; Thackray, Varykina. G.; Shen, Jia; Skowronska-Krawczyk, Dorota; Mellon, Pamela. L. 2021. *FSHB* Transcription is Regulated by a Novel 5' Distal Enhancer with a Fertility-Associated Single Nucleotide Polymorphism. *Endocrinology* 162(1)). The dissertation author was the primary investigator and author of this paper. Jia Shen and Dorota Skowronska-Krawczyk contributed single-cell ATAC sequencing for whole pituitary. Dorota Skowronska-Krawczyk also assisted with experimental design of chromatin immunoprecipitation experiments. Varykina Thackray assisted with experimental design and paper composition. Pamela Mellon supervised the project and provided advice.

Chapter 2 has been resubmitted for publication in *Endocrinology* (Bohaczuk, Stephanie. C.; Cassin, Jessica; Slaiwa, Theresa I.; Thackray, Varykina. G.; Mellon, Pamela. L. 2021. Distal Enhancer Potentiates Activin- and GnRH-Induced Transcription of FSHB. *Endocrinology* [Resubmitted]). The dissertation author was the primary investigator and author of this paper. Jessica Cassin contributed the DNA pull-down. Theresa Slaiwa provided technical assistance with the follistatin luciferase experiment. Varykina Thackray assisted with experimental design and paper composition. Pamela Mellon supervised the project and provided advice.

Chapter 3 is currently in preparation for submission of this material for publication. (Bohaczuk, Stephanie C.; Slaiwa, Theresa I.; Thackray, Varykina G.; Mellon, Pamela L. Mouse Fertility Is Not Impaired by Deletion of or Point Mutation within an Upstream *Fshb* Enhancer). The dissertation author was the primary investigator and author of this paper. Theresa Slaiwa provided technical assistance. Varykina Thackray assisted with experimental design. Pamela Mellon supervised the project and provided advice.

VITA

2013 Bachelor of Science, Biology, California Institute of Technology

2021 Doctor of Philosophy, Neurosciences, University of California San Diego

PUBLICATIONS

Bohaczuk, Stephanie C.; Cassin, Jessica; Slaiwa, Theresa I.; Thackray, Varykina G.; Mellon, Pamela L. 2021. Distal Enhancer Potentiates Activin- and GnRH-Induced Transcription of FSHB. *Endocrinology* [Resubmitted].

Ryan, Genevieve E.; **Bohaczuk, Stephanie C.**; Cassin, Jessica; Witham, Emily A.; Shojaei, Shadi; Ho, Emily H.; Thackray, Varykina G.; Mellon, Pamela L. (2021). Androgen Receptor Positively Regulates Gonadotropin-releasing Hormone Receptor in Pituitary Gonadotropes. *Molecular and Cellular Endocrinology* [Resubmitted].

Bohaczuk, Stephanie C.; Thackray, Varykina G.; Shen, Jia; Skowronska-Krawczyk, Dorota; Mellon, Pamela L. (2021). FSHB Transcription is Regulated by a Novel 5' Distal Enhancer with a Fertility-Associated Single Nucleotide Polymorphism. *Endocrinology*, *162*(1), bqaa181. https://doi.org/10.1210/endocr/bqaa181

ABSTRACT OF THE DISSERTATION

Regulation of *FSHB* transcription by a Novel Distal Enhancer

by

Stephanie Claire Bohaczuk

Doctor of Philosophy in Neurosciences

University of California San Diego, 2021

Professor Pamela Mellon, Chair

Follicle- stimulating hormone (FSH) is a glycoprotein hormone that is an essential regulator of mammalian fertility. Produced within gonadotrope cells in the anterior pituitary, FSH, along with the other pituitary gonadotropin, luteinizing hormone, act on the gonads to regulate pubertal maturation, hormone synthesis, and gametogenesis. Genome-wide association studies (GWAS) link a 130 Kb locus at 11p14.1 that encompasses the FSH beta-subunit gene

(*FSHB*) with fertility-related traits including polycystic ovary syndrome, age of natural menopause, and dizygotic twinning. The rate-limiting step in FSH synthesis is transcription of the beta subunit. Therefore, understanding the transcriptional regulation of *FSHB* is critical to understand how *FSHB* dysregulation contributes to infertility. The lead single nucleotide polymorphism from several studies is rs11031006, which resides within a highly evolutionarily conserved, ~450 base pair element located 26 Kb upstream of the *FSHB* transcriptional start site in humans. We hypothesized that the highly conserved element is an enhancer of *FSHB* and that the minor allele of the rs11031006 polymorphism would impair *FSHB* transcription. Chapter 1 describes the conserved element in the context of basal regulation and demonstrates that it is, indeed, an enhancer of *FSHB* transcription in human and mouse. Counter to our initial hypothesis, the rs11031006 variant increased, rather than decreased, *FSHB* transcription, likely through creation of a higher affinity binding site for the transcription factor Steroidogenic factor 1. Chapter 2 describes the role of the novel *FSHB* enhancer in the context of hormone regulation. The enhancer potentiated activin- and gonadotropin-releasing hormone- induction of *FSHB*, dependent upon a binding site within the enhancer for SMAD transcription factors, which are downstream effectors of activin signaling. Chapter 3 examines the *in vivo* necessity of the *Fshb* enhancer in a mouse model and the effect of the rs11031006 minor allele. Neither deletion of the enhancer or the rs11031006 minor allele impaired adult fertility, possibly indicating that other enhancers of *Fshb* can compensate. Overall, we identified a novel enhancer of basal and hormone-stimulated *FSHB* transcription and demonstrate that the rs11031006 allele increases the activity of the enhancer, although the role of the enhancer and rs11031006 variant *in vivo* requires further resolution.

INTRODUCTION

The hypothalamic-pituitary-gonadal (HPG) axis

The HPG axis regulates mammalian fertility. At the apex is the hypothalamus, which releases pulsatile gonadotropin-releasing hormone (GnRH) through the hypophyseal portal to gonadotrope cells in the anterior pituitary. GnRH binds its receptor on the cell surface of gonadotrope cells and stimulates synthesis and secretion of the gonadotropins, follicle-stimulating hormone (FSH) and luteinizing hormone (LH). The gonadotropins act on the gonads to regulate reproductive function and sex steroid synthesis. Sex steroids are secreted and travel to the hypothalamus through the bloodstream to regulate GnRH secretion. In this way, appropriate control of the HPG axis is maintained to regulate fertility.

Differential regulation of FSH and LH

LH and FSH are glycoprotein hormones, each consisting of a heterodimer including a common alpha subunit (αGSU) and a unique beta subunit. While transcription and release of LH and FSH occurs within the same cell and are both stimulated by the pulsatile release of GnRH from the hypothalamus, the differential regulation of LH and FSH is critical for ovulation and ovarian steroidogenesis.

One mechanism of differential regulation is GnRH pulse frequency and amplitude. High amplitude, high frequency GnRH pulses favor LH synthesis and secretion, whereas slower pulses stimulate FSH synthesis and secretion (1-4). FSH is also upregulated by activin (5). Activin is synthesized in the gonads and gonadotrope cells themselves, forming an autocrine loop (5, 6). Activin signaling phosphorylates SMAD proteins, which bind to the proximal promoter of the

gene encoding the beta subunit of FSH (*FSHB)* and activate its transcription (7). Inhibin and follistatin inhibit activin signaling and sequester activin, respectively (5, 8, 9).

Altered FSH levels impair fertility

The importance of FSH in reproduction is underscored by loss-of function (LOF) mutations, which result in infertility in both sexes (10). In males, FSH is critical for spermatogenesis and Sertoli cell differentiation and proliferation (11, 12). In females, FSH is critical for folliculogenesis and estrogen synthesis. FSH drives oocyte maturation by promoting estrogen synthesis and preparing granulosa cell responsiveness to the ovulatory LH surge by inducing expression of LH receptors (13, 14). FSH accelerates the conversion of testosterone to estrogen through its action on granulosa cells, where it upregulates aromatase, the enzyme responsible for this conversion (15). Extremes of FSH can lead to infertility, as low FSH levels halt follicular growth and high FSH levels are associated with premature ovarian failure (16). Therefore, FSH serum levels, primarily limited by the rate of FSHβ transcription (17, 18), must be tightly controlled to maintain female fertility.

GWAS links gonadotropins and their receptors to female fertility

Multiple GWAS studies in European and Chinese populations identified the chr 11p14.1 locus, which spans 130 kb and contains the 5' upstream and coding sequence of *FSHB*, in association with traits of female fertility including PCOS risk, gonadotropin levels, age of natural menopause, and dizygotic twinning (19-24). The lead SNP identified in several studies, rs11031006 (rs06), resides ~26 kB upstream of *FSHB* in humans within an element that is highly conserved among mammals. The minor allele frequency is approximately 8% (25). It is

interesting to note that the rs06 SNP minor allele correlates with a copy-number dependent increase in LH serum levels and LH to FSH ratio in women, a feature of PCOS (26). Additionally, as high levels of FSH result in premature ovarian failure and a higher dizygotic twin rate, it is consistent that the rs06 minor allele (A) is correlated with an older age of natural menopause and a lower rate of dizygotic twin births (23, 27).

GWAS provides important correlative evidence to identify variants that contribute to disease etiology but does not directly test causality or mechanism. The rs11031006 SNP is in linkage disequilibrium with many other polymorphisms. From GWAS alone, it is unknown whether rs11031006 itself affects *FSHB* or merely correlates with a variant that does. Furthermore, regulatory elements can act over many kilobases, so even if a causal variant were known, it still may not act directly on *FSHB.* Finally, GWAS cannot identify the mechanism by which a variant affects fertility. To fully understand how regulatory regions containing polymorphisms contribute to expression of their target genes, detailed mechanistic studies, as presented in the chapter below, are an essential basis for the development of personalized and effective treatments.

CHAPTER 1: *FSHB* TRANSCRIPTION IS REGULATED BY A NOVEL 5' DISTAL ENHANCER WITH A FERTILITY-ASSOCIATED SINGLE NUCLEOTIDE POLYMORPHISM

Abstract

The pituitary gonadotropins, follicle-stimulating hormone (FSH) and luteinizing hormone, signal the gonads to regulate male and female fertility. FSH is critical for female fertility as it regulates oocyte maturation, ovulation, and hormone synthesis. Multiple genome-wide association studies (GWAS) link a 130 Kb locus at 11p14.1, which encompasses the FSH beta-subunit (*FSHB*) gene, with fertility-related traits including polycystic ovary syndrome, age of natural menopause, and dizygotic twinning. The most statistically significant single-nucleotide polymorphism from several GWAS studies (rs11031006) resides within a highly conserved 450 bp region 26 Kb upstream of the human *FSHB* gene. Given that sequence conservation suggests an important biological function, we hypothesized that the region could regulate *FSHB* transcription. In luciferase assays, the conserved region enhanced *FSHB* transcription and gel shifts identified a binding site for Steroidogenic factor 1 (SF1) contributing to its function. Analysis of mouse pituitary single-cell ATAC-seq demonstrated open chromatin at the conserved region exclusive to a gonadotrope cell-type cluster. Additionally, enhancer-associated histone markers were identified by immunoprecipitation of chromatin from mouse whole pituitary and an immortalized mouse gonadotrope-derived LβT2 cell line at the conserved region. Furthermore, we found that the rs11031006 minor allele upregulated *FSHB* transcription via increased SF1 binding to the enhancer. All together, these results identify a novel upstream regulator of *FSHB* transcription and indicate that rs11031006 can modulate FSH levels.

Introduction

Follicle-stimulating hormone (FSH) is a key regulator of fertility. In females, FSH is critical for folliculogenesis and steroidogenesis. FSH drives oocyte maturation by promoting estrogen synthesis and preparing granulosa cell responsiveness to the ovulatory luteinizing hormone (LH) surge by inducing the expression of LH receptors (13, 14). FSH accelerates the conversion of testosterone to estrogen through its action on granulosa cells, where it regulates the expression of aromatase, the enzyme responsible for this conversion (15). In males, FSH stimulates Sertoli cell differentiation and proliferation during development and promotes spermatogenesis (11, 12). FSH is a glycoprotein hormone consisting of a unique beta subunit (FSHβ), encoded by the *FSHB* gene, and a common alpha subunit (αGSU), encoded by the *CGA* gene, which also is a component of the other glycoprotein hormones including LH, thyroid-stimulating hormone, and human chorionic gonadotropin. The gonadotropins, FSH and LH, are both synthesized and secreted by gonadotrope cells within the anterior pituitary.

Constitutive FSH secretion is maintained throughout the cycle. Studies using immortalized mouse gonadotrope-derived LβT2 cells (28) have shown that transcription factors including Paired-like homeodomain 1 (PTX1), LIM homeobox gene 3 (LHX3), and Steroidogenic factor 1 (SF1, encoded by *NR5A1*) in cooperation with Nuclear transcription factor Y (NFY) bind to the *Fshb* proximal promoter to regulate basal transcription (29-31). FSH serum levels are primarily limited by the rate of *Fshb* transcription (17, 18).

In the human menstrual cycle, *FSHB* mRNA synthesis and FSH serum levels peak midcycle at the time of the LH surge and rise again during the late luteal/early follicular phase to initiate follicular maturation (32). Similarly, in rodents, there is a primary rise that occurs during LH-induced ovulation and a secondary rise that occurs during estrus (33). These increases in

FSH have been shown to be mediated, in part, by gonadotropin-releasing hormone (GnRH) and activin. While hypothalamic GnRH and steroid hormones regulate FSH and LH transcription and secretion, FSH is also regulated by activins, inhibins, and follistatin (5, 8, 9). Activin signaling phosphorylates SMAD proteins, which bind to the proximal promoter of *FSHB* and activate its transcription in conjunction with the FOXL2 transcription factor (7, 34).

In humans, inactivating (loss-of-function) mutations in *FSHB* result in infertility in both sexes (10). Females fail to go through puberty (35-38), while both normal and absent puberty have been reported in males (37, 39, 40). Female, but not male, *Fshb* knock-out mutant mice are infertile, and the phenotype of the female recapitulates failure to ovulate and reduced uterine and ovarian weight (41). Conversely, high FSH levels in females are associated with premature ovarian failure (16). Therefore, FSH serum levels must be tightly controlled to maintain female fertility.

Recent genome-wide association studies (GWAS) from both Caucasian and Han Chinese populations identified a 130 Kb locus, mapping to the chromosome 11p14.1 region containing *FSHB*, that is associated with polycystic ovary syndrome (PCOS) (19-22), age of natural menopause (ANM) (23), and dizygotic twinning (24). Notably, these fertility-associated traits and diseases are all linked with FSH levels (19-24). PCOS is the most common cause of anovulatory infertility, affecting up to 10-15% of reproductive-age women (42). PCOS diagnosis with the Rotterdam criteria requires two of three diagnostic features: elevated androgens, anovulation, or the presence of ovarian cystic follicles (43). The 11p14.1 locus has also been associated with decreased FSH, increased LH, and an elevated LH/FSH ratio, characteristic of some PCOS patients (19-22, 27, 44). Strikingly, LH levels are also elevated in FSH-deficient female mouse models and in women with inactivating mutations of *FSHB* (10, 35, 36, 38, 41,

45), suggesting that FSH insufficiency may contribute to elevated LH in women with PCOS. Additionally, GWAS studies for PCOS identified risk loci encompassing the FSH and LH receptors (46, 47), suggesting that disturbances in gonadotropin production and action are potential mechanisms that contribute to PCOS etiology and pathophysiology.

The lead single nucleotide polymorphism (SNP) identified in ANM, dizygotic twinning, and a subset of PCOS GWAS studies is rs11031006 (G/A) (19, 20), which is located approximately 26 Kb upstream of the human *FSHB* transcriptional start site (TSS). The worldwide minor (A) allele frequency is approximately 8% (25). As of yet, the only polymorphism associated with *FSHB* to be functionally interrogated is the rs10835638 (G/T) SNP, located 211 base pairs upstream of the *FSHB* TSS in the proximal promoter. In humans, the rs10835638 minor (T) allele has been associated with lower FSH levels in males and infertility in both sexes (48-52). The minor (T) allele was found to decrease the binding of the LHX3 homeodomain transcription factor to the proximal promoter and reduce basal *FSHB* transcription in cell culture (53).

The rs11031006 SNP resides within a non-coding region highly conserved among vertebrates (Fig. 1.1A). We hypothesized that this conserved intergenic region is an enhancer of *FSHB* transcription, and that *FSHB* expression would be decreased by the disease-associated variant. Consistent with our hypothesis, we determined that the conserved enhancer region increased transcription driven by the *FSHB* proximal promoter via binding of the SF1 transcription factor to the enhancer region. This region also possessed markers of an enhancer including open chromatin exclusively in gonadotrope cells within the pituitary and enrichment of the histone markers H3K4me1 and H3K27Ac, which are associated with active enhancers (54, 55). Contrary to our expectations, conversion to the rs11031006 minor (A) allele increased SF1

binding to the enhancer and increased, rather than decreased, *FSHB* expression, indicating that the mechanism linking this SNP to fertility-related traits still remains to be elucidated.

Methods

Plasmids

The human -1028/+7 *FSHB* luciferase reporter plasmid (-1028/+7 *FSHB*-luc) in a pGL3 backbone (Promega) was provided by Daniel Bernard (56). A conserved intergenic region 26 Kb upstream of *FSHB*, spanning 450 base pairs (chr11:30,204,683-30,205,132, hg38 assembly), was amplified by PCR from a human fosmid template (GenBank accession number: AL358944.12) containing the major allele of the rs11031006 SNP (G) using primers "FW human enh-KpnI" and "RV human enh-SacI" to add each restriction site (Table 1.1). It was ligated into the human -1028/+7 *FSHB*-luc reporter plasmid between the KpnI/SacI sites, directly upstream of the proximal promoter, to create the hEnh/G:1028 *FSHB*-luc plasmid. Truncations of the upstream region were constructed in the same way, with primers designed for intermediate sites (Table 1.1). To restore restriction sites within the pGL3 backbone, the mouse -1000/-1 *Fshb*-luc plasmid was constructed by amplifying the promoter region of the previously described mouse -1000FSHβluc plasmid (57) with PCR using primers "FW mouse pro-MluI" and "RV mouse pro-XhoI" (Table 1.1) to add each restriction site. The amplicon was ligated into the MluI/XhoI sites of the pGL3-Basic plasmid. The mouse equivalent, conserved 450 base-pair element 17 Kb upstream of *Fshb* (chr2:107,076,909-107,077,358, mm10) was amplified from C57BL/6 genomic mouse DNA with primers "FW mouse enh-KpnI" and "RV mouse enh-SacI" (Table 1.1) and subcloned into the -1000/-1 *Fshb*-luc plasmid at the KpnI/SacI sites to create the mEnh/G:1000 *Fshb*-luc plasmid. Plasmids with the human and mouse enhancer in reverse

orientation (RV-hEnh/G:1028 *FSHB*-luc and RV-mEnh/G:1000 *Fshb*-luc) were constructed exactly as the forward enhancer plasmids except using primers with the KpnI and SacI sites switched. Plasmids containing the herpes simplex thymidine kinase (-81/+52 TK) promoter were constructed by subcloning the enhancer variants referenced above into the KpnI/SacI sites upstream of the TK promoter in a pGL3 backbone (58). Plasmids containing the mouse -523/+6 Lhb and -493/+9 Gnrhr promoters were constructed by amplifying each region with the "FW mouse Lhb-MluI" and "RV mouse Lhb-XhoI" or "FW mouse Gnrhr-MluI" and "RV mouse Gnrhr-XhoI" primer sets from C57BL/6 mouse genomic DNA and cloning into the MluI/XhoI sites in the human enhancer construct in place of the *FSHB* promoter to create hEnh/G:*Lhb*-luc and hEnh/G:*Gnrhr*-luc. The SF1 expression vector in pcDNA3 (Invitrogen) was cloned from a pCMV expression vector originally provided by Bon-Chu Chung (59). All plasmids were confirmed by Sanger sequencing (Eton Bioscience).

Mutagenesis

Construction of the SF1 site mutation plasmids, the rs11031006 (G>A) minor allele plasmids, and 10 base-pair deletions within the human conserved region was performed using the Quikchange II Site-Directed Mutagenesis Kit (Agilent, Cat # 200523) according to the manufacturer's protocol. The hEnh/G:1028 *FSHB*-luc and the RV-mEnh/G:1000 *Fshb*-luc plasmids were used as templates. Primers were designed using the "Quikchange Primer Design Program" from the manufacturer's website (60). Forward primer sequences are listed in Table 1.2; reverse primer sequences are the reverse complement.

Cell Culture and Transient Transfection

LβT2 and NIH 3T3 cells were maintained in DMEM (Corning, cat # 10-013-CV) supplemented with 10% fetal bovine serum (Omega Scientific, cat # FB-01) and 1% penicillin-streptomycin (GE Life Sciences, cat # SV30010), and incubated at 37°C, 5% CO_2. They were passaged at approximately 80% confluency by dissociating cells with 0.25% trypsin-EDTA (Gibco, cat # 25200056). Prior to transfection, $4.25x10^5$ LβT2 cells or $5x10^4$ NIH 3T3 cells were plated into 12 well plates (Thermo Scientific, cat # 150628) and cultured overnight. The following morning, cells were transfected using Polyjet (Sygnagen Laboratories, cat # SL100688) according to the manufacturer's protocol. Each well was co-transfected with 500 ng of the luciferase reporter construct and 200 ng of a reporter plasmid encoding β-galactosidase driven by the herpes virus thymidine kinase promoter to control for transfection efficiency. NIH 3T3 cells were also transfected with 20 ng of SF1 expression vector or the same amount of the pcDNA3 backbone. After 5 hours, the transfection agent was removed and replaced with supplemented DMEM. Three technical replicates were included for each reporter.

Luciferase Assay

Approximately 48 hours after transfection, cells were washed with 1x PBS and incubated for 5 minutes at room temperature in lysis buffer [0.1 M potassium phosphate (pH 7.8) and 0.2% Triton-X-100]. Lysate was transferred into two 96-well plates. Luciferase and β-Galactosidase activity were measured using a Veritas Microplate Luminometer (Turner BioSystems). For luciferase activity, 25 μL of lysate was treated with 100 μL of luciferase buffer [25 mM Tris-HCl (pH 7.8), 15 mM MgSO4, 10 mM ATP, and 65 μM luciferin] with a one-second delay before measuring luminescence over one second. β-Galactosidase activity was assayed using Galacto-Light Plus reagents (Tropix, cat# T1009) according to the manufacturer's protocol.

Single-Cell Assay for Transposase-Accessible Chromatin using Sequencing (scATAC-seq)

Pituitaries were collected from two adult male mice. Nuclei isolation for scATAC-seq was performed following the instruction provided by 10xGenomics (scATAC-V1) with some modifications. Briefly, 100,000 cells were added to a 2 mL microcentrifuge tube and centrifuged (300 x g for 5 min at 4°C). The supernatant was removed without disrupting the cell pellet. Lysis Buffer [10 mM Tris-HCl (pH 7.4), 10 mM NaCl, 3 mM $MgCl_2$, 0.1% Tween-20, 0.1% Nonidet P40 Substitute, 0.01% Digitonin, and 1% BSA] was diluted by Lysis Dilution Buffer [10 mM Tris-HCl (pH 7.4), 10 mM NaCl, 3 mM $MgCl_2$, 1% BSA] to make 0.1x Lysis Buffer. 100 µL chilled 0.1x Lysis Buffer was added to the cell pellet, and then pipette-mixed 10 times. The microcentrifuge tube was then incubated on ice for 5 min. Next, 1 mL of chilled Washing Buffer [10 mM Tris-HCl (pH 7.4), 10 mM NaCl, 3 mM $MgCl_2$, 0.1% Tween-20, and 1% BSA] was added and gently pipette-mixed 5 times. Nuclei were centrifuged (500 x g for 5 min at 4°C) to remove the supernatant, and the wash was repeated. An appropriate volume of chilled Diluted Nuclei Buffer (10xGenomics) was added to resuspend nuclei at 2,500 nuclei/µL to retrieve/target 6,000 nuclei per library following the standard protocol provided by Chromium Single Cell ATAC Library and Gel Bead kit (10x Genomics, v1). Each sample library was uniquely barcoded. Libraries were then pooled and loaded on a NovaSeq Illumina sequencer and sequenced to ~50% saturation on average.

scATACseq Analysis

Raw sequencing data were converted to fastq format using cell ranger atac mkfastq (10x Genomics, v.1.0.0). Read counts of single library were aligned to mm10 reference genome for

quantification and analyzed by cellranger-atac count (10x Genomics, v.1.0.0). To ensure identical detection sensitivity across libraries, we performed cellranger-atac aggr on integrated libraries and normalized all the data to identical sequencing depth. Pituitary cell-type clusters were obtained using t-SNE (61) to cluster together cells with similar open chromatin profiles. Processed and raw data have been deposited and can be downloaded from NCBI GEO (GSE158070) .

Chromatin Immunoprecipitation (ChIP)

ChIP was performed using the Active Motif ChIP-IT High Sensitivity kit (cat # 53040). LβT2 cells were cultured in DMEM supplemented with 10% fetal bovine serum and 1% penicillin-streptomycin in 15 cm tissue culture dishes. Cells were harvested at approximately 80% confluency and fixed with "Complete Cell Fixation Solution" containing 1.3% formaldehyde for 10 minutes. Chromatin was extracted according to the manufacturer's protocol, with the following modifications: After addition of the "Chromatin Prep Buffer" supplemented with 100 nM PMSF and 1 μL/mL of "Protease Inhibitor Cocktail", cells were lysed by passing through a 25-gauge needle four times. Prior to sonication, nuclei were diluted with "ChIP Buffer" to a density of approximately 3 million per 100 μL. Cells were sonicated in 300 μL aliquots in 1.5 mL Bioruptor Pico Microtubes (Diagenode, cat# C30010016) using the Bioruptor Pico (Diagenode, cat# B01060010), 30 sec on/30 sec off for 20 minutes total. Following centrifugation at 16,000 x g for two minutes to remove cellular debris, 25 μL of chromatin was collected as input. Immunoprecipitation was performed according to manufacturer's protocol, using approximately 10 μg of chromatin per reaction. 5 μg of each antibody targeting histone H3 lysine 27 acetylation (H3K27Ac) (Active Motif, cat # 93133) (62), and histone 3 lysine 27

trimethylation (H3K27me3) (Active Motif, cat # 39155) (63) were compared to a normal rabbit IgG control (Cell Signaling, cat # 2729) (64). 10 μL of antibody targeting histone H3 lysine 4 monomethylation (H3K4me1) (Active Motif, cat # 39297) (65) was compared to a normal rabbit serum control (Molecular Probes, cat # PLN5001). ChIP DNA was eluted in a total volume of 200 μL. Input chromatin was treated with RNAse A and Proteinase K. DNA was purified using the Active Motif Chromatin IP DNA Purification Kit (cat # 58002) and eluted in a total volume of 200 μL.

For the whole pituitary ChIP, 4-12 pituitaries from randomly-cycling adult C57BL/6 female mice were pooled in a glass dounce and homogenized in "Complete Tissue Fixation Solution" containing 1% formaldehyde in PBS for 10 minutes. Chromatin was extracted as above. Prior to sonication, nuclei were diluted with "ChIP Buffer" to a density of approximately 2 million per 100 μL. Cells were sonicated in 150-300 μL aliquots in 1.5 mL Bioruptor Pico Microtubes (Diagenode, cat# C30010016) using the Bioruptor Pico (Diagenode, cat# B01060010), 30 sec on/30 sec off for 10 minutes total. Immunoprecipitation was performed according to manufacturer's protocol, using approximately 25 μg of chromatin per reaction. 5 μg of each antibody targeting H3K27Ac (Active Motif, cat # 93133) (62) or H3K4me1 (Active Motif, cat # 61633) (66) were compared to a normal rabbit IgG control (Cell Signaling, cat # 2729) (64). Input was collected from the flow-through of the IgG immunoprecipitation. Input and samples were treated with Proteinase K, purified using the QIAquick PCR Purification kit (Qiagen, cat# 28104), and eluted in a total volume of 100 μL.

Quantitative PCR Analysis

Primers targeting the mouse conserved intergenic region (putative enhancer), *Fshb* proximal promoter, and control regions (Table 1.3) were designed using IDT PrimerQuest (67) and NCBI Primer-BLAST (68). DNA from input and immunoprecipitated samples were measured using iQ SYBR Green Supermix (Bio-Rad Laboratories, cat # 1708880) in a CFX Connect Detection System (Bio-Rad Laboratories). A standard curve of serial input dilutions was constructed for each plate and used to compute the concentration of each sample as % input. A dissociation curve was performed following PCR to ensure the presence of a single product. Three technical replicates were included per experiment.

Electrophoretic mobility shift assay

To prepare nuclear extracts, LβT2 cells were washed once with PBS and lysed in a buffer containing 20 mM Tris pH 7.4, 10 mM NaCl, 1 mM $MgCl_2$, 1 mM PMSF, 10 mM NaF, and 10 µL/mL of protease inhibitor cocktail (Sigma, cat # P8340). Cells swelled on ice for 15 minutes before they were passed four times through a 25G needle. Nuclei were collected by centrifugation at 3750 x g for 4 minutes at 4°C. Nuclei were lysed in a hypertonic buffer containing 20 mM HEPES pH 7.9, 20% glycerol, 420 mM KCl, 1.5 mM $MgCl_2$, 0.5 mM EDTA, 0.1 mM EGTA, 1 mM PMSF, 10 mM NaF, and 10 µL/mL of protease inhibitor cocktail. Complementary oligonucleotides (Table 1.4) were annealed and ATP γ-32P end-labelled with T4 Polynucleotide Kinase (New England Biolabs, cat# M0201). 2 µg of nuclear extract was incubated with labelled probes for 30 minutes in a buffer containing 10 mM HEPES pH 7.8, 50 mM KCl, 5 mM $MgCl_2$, 0.1% NP-40, 10% glycerol, 1 mM DTT, 0.1 mg/mL poly dI-dC, and 2 µg anti-SF1 (Millipore, cat # 07-618) (69), 2 µg rabbit IgG (Santa Cruz Biotechnology Cat# sc-2027) (70), or excess of cold competitor oligonucleotides where specified. Complexes were

separated on a 5% acrylamide gel with 2.5% glycerol in 0.25X TBE. Gels were dried and exposed at -80°C or RT as indicated. Images are representative of at least three experiments yielding the same results.

Statistical Analysis

Differences were analyzed via Student t-test or ANOVA. One-way and two-way ANOVAs were followed by post-hoc Tukey-Kramer honestly significant difference test when comparing all samples or Dunnett test when comparing to the mean of a control sample. Residuals were checked for normality using the Shapiro-Wilk test with $p>0.05$ as the threshold for normality. As needed, data were subsequently log or square transformed and reanalyzed where indicated. For transient transfection, luciferase values were normalized to β-galactosidase values from the same tissue culture well. Triplicates were averaged, and results were expressed relative to pGL3 backbone levels from the same experimental replicate except where indicated. Prism 8 (GraphPad) was used for all analysis, and $p <0.05$ was the threshold for statistical significance.

Results

Conserved putative enhancer region increases transcription from the FSHB promoter

The highly conserved, putative enhancer region containing the rs11031006 SNP spans approximately 450 base pairs (Fig. 1.1A). In the human genome, it is located ~26 Kb upstream of the *FSHB* TSS, with the equivalent region ~17 Kb upstream of the *Fshb* TSS in the mouse genome. To determine whether the human conserved intergenic region containing the major rs11031006 allele (G) can function as an enhancer of *FSHB* transcription, we transfected

gonadotrope-derived LβT2 cells (28) with hEnh/G:1028 *FSHB*-luc. The conserved element subcloned in the forward direction (hEnh/G) increased luciferase activity 2.4-fold compared to the *FSHB* promoter alone (Fig. 1.1B). Additionally, the conserved element subcloned in the reverse direction (RV-hEnh/G) increased luciferase activity 2.2-fold compared to the *FSHB* promoter alone (Fig. 1.1B). Reversibility is a classical property of enhancers (71). The results with the analogous mouse construct mEnh/G:1000 *Fshb*-luc were similar to the human construct, with a 1.7-fold (forward orientation) and 2.5-fold (reverse orientation) increase in luciferase activity compared to the *Fshb* promoter alone (Fig. 1.1C). Overall, these results demonstrated that the conserved intragenic element from both the human and mouse genomes enhanced expression driven from the *FSHB* promoter. From here onward, we will refer to the conserved region as the human *FSHB* enhancer or mouse *Fshb* enhancer.

To test whether the mouse and human enhancers are promoter-specific, we transfected LβT2 cells with hEnh/G:TK and mEnh/G:TK, which contain the herpes simplex virus thymidine kinase (TK) promoter driving luciferase expression. The human *FSHB* enhancer increased luciferase activity in the forward orientation (4.5-fold) (Fig. 1.1D), but the mouse *Fshb* enhancer did not (Fig. 1.1E). Because the mouse enhancer was stronger in the reverse orientation upstream of the *Fshb* promoter, we assessed whether it could act as an enhancer in this orientation on TK and found that reversing the enhancer restored its activity (1.6-fold).

To determine if the *FSHB* enhancer can also function upstream of other mammalian-derived promoters, we transfected LβT2 cells with constructs containing hEnh/G upstream of the *Lhb* (Fig. 1.1F) and *Gnrhr* promoters (Fig. 1.1G), both representing genes actively transcribed in gonadotropes. As with the TK promoter, the human *FSHB* enhancer increased expression driven

by the *Lhb* and *Gnrhr* promoters. Overall, the enhancer is not promoter-specific, and its reversibility may be context-dependent.

Fshb enhancer is characterized by open chromatin exclusively in gonadotropes

Open chromatin structure facilitates gene expression by allowing transcriptional regulators and RNA polymerases to access DNA, while closed chromatin typically inhibits these interactions (72). To evaluate chromatin status in gonadotropes, scATAC-seq data from whole pituitary was analyzed by t-distributed stochastic neighbor embedding (t-SNE) (61) to cluster cells based on similar regions of accessible chromatin (Fig. 1.2). A gonadotrope cell-type cluster (Fig. 1.2A) was identified by open chromatin at genes expressed solely in pituitary gonadotropes such as *Fshb*, *Lhb* (encoding the LH beta subunit), and *Gnrhr* (encoding the GnRH receptor). The coding regions of all three genes were open exclusively in this cluster which included 3.3% of cells, consistent with previous reports of the gonadotrope cell population size relative to total number of pituitary cells (73) (Fig. 1.2B,C). Because the closed chromatin status at *Fshb*, *Lhb*, and *Gnrhr* was consistent among all other clusters identified by t-SNE (74), we combined them into one group ("other") for simplicity (Fig. 1.2). To evaluate whether the *Fshb* enhancer was specifically open in gonadotropes, we compared the chromatin status in this region between the gonadotrope cell-type cluster and all other pituitary cell-type clusters (Fig. 1.2C). The enhancer was only accessible in gonadotrope cells. All findings were replicated in a second experiment (74).

H3K4me1 is enriched near the Fshb enhancer

Specific histone modifications in a region of chromatin correlate with its function. As enhancers are marked by H3K4me1, we used a ChIP assay to assess the presence of this marker at the *Fshb* enhancer in LβT2 cells (Fig. 1.3A). As compared to the negative (gene desert) control, H3K4me1 was enriched at the enhancer and the positive control region (β-actin intron 1). At the proximal *Fshb* promoter, H3K4me1 was also slightly elevated as compared to the negative control region, although it did not reach statistical significance. H3K4me1 has been reported to be highest at enhancers, moderately elevated immediately downstream of the TSS, and lowest at proximal promoters and nonregulatory intergenic regions (75), consistent with our results.

Next, we asked whether the enhancer is active in this cell line, especially given that endogenous basal *Fshb* expression is low in LβT2 cells (76). Active enhancers and promoters are characterized by enrichment of H3K27Ac and an absence of the repressive marker H3K27me3, whereas poised or inactivated enhancers show the opposite pattern (54, 55). As predicted from low *Fshb* expression levels in LβT2 cells, H3K27Ac was not enriched at the *Fshb* enhancer, *Fshb* proximal promoter, or negative (gene desert) control in LβT2 cells as compared to the positive control region (β-actin intron 1) (Fig. 1.3B). Interestingly, H3K27me3 was also absent at the *Fshb* enhancer, *Fshb* promoter, and negative control region (β-actin intron 1) compared to the positive control MyoD, which is not expressed in LβT2 cells (Fig. 1.3C). Enhancers negative for both H3K27me3 and H3K27Ac have been classified as "intermediate" between active and poised and are correlated with lower expression levels of their target genes than observed from active enhancers, but are not correlated with Polycomb repression proteins typical of "poised" enhancers, possibly indicative of a transitionary stage (77).

Because we did not observe H3K27Ac enrichment in LβT2 cells, we performed ChIP in female whole pituitary to assess H3K27Ac recruitment and also to confirm the presence of H3K4me1 at the *Fshb* enhancer. The repressive marker H3K27me3 is expected to be present in non-*Fshb* cell linages, so it could not be measured in this context. As compared to the negative (gene desert) control region, H3K4me1 was elevated at the *Fshb* enhancer as well as the *Fshb* proximal promoter in whole pituitary (Fig. 1.3D). In contrast to LβT2 cells, H3K27Ac was enriched at the *Fshb* enhancer and *Fshb* proximal promoter compared to the negative (gene desert) control (Fig. 1.3E). A well-characterized enhancer 10 Kb upstream of the *POU1F1* TSS (expressing PIT1) was selected as a positive control for H3K4me1 and H3K27Ac immunoprecipitation in whole pituitary, but levels were not directly compared to the *Fshb* enhancer and promoter because *POU1F1* is expressed in most pituitary cells (Fig. 1.3F) (78). Together, these results confirm that the *Fshb* enhancer is positive for the active enhancer markers H3K4me1 and H3K27Ac in adult female pituitary.

216-341 region within the enhancer is sufficient to increase transcription

To narrow the search for regulatory sites within the conserved enhancer region, we cloned subregions of the human *FSHB* enhancer upstream of the -1028/+7 *FSHB*-luc promoter and assessed luciferase expression (Fig. 1.4A). Subregions were selected to divide the enhancer into halves and quarters to identify the minimal region sufficient for enhancer activity. A reporter including the subregion spanning 216-341 (chr11:30,204,898-30,205,023, hg38) significantly enhanced luciferase expression 2.2-fold over the promoter alone. This result was comparable to the 2.4-fold increase by the full 450 bp enhancer and 1.9-fold increase by 216-450. The 216-341 subregion maintained enhancer function in the reverse orientation, although its activity was

reduced as compared to the forward orientation (Fig. 1.4B). Together, these results indicate that 216-341 is sufficient for basal enhancer function.

Putative ZEB1, PTX1, SMAD, and SF1 binding sites are important for enhancer function

We next used site-directed mutagenesis to create a series of plasmids containing the 450 bp human *FSHB* enhancer with sequential 10 base-pair deletions within the identified minimal region sufficient for basal enhancer activity, 216-345. Compared to the intact human *FSHB* enhancer, one deletion increased and three decreased enhancer activity (Fig. 1.4C), demonstrating that several regulatory elements within the 216-345 region of enhancer contribute to its activity. Using Match 1.0 software (GeneXplain) to search the TRANSFAC database, we identified putative transcription factor binding motifs corresponding to each region including ZEB1 (Δ226-235), PTX1 (Δ246-255), SMAD (Δ256-265), and SF1 (Δ296-305) (Fig. 1.4C). Interestingly, the deletion from 296-305 contains the rs11031006 SNP, suggesting that the SNP resides within, and could possibly alter, a functional element. Given its potential relevance for *FSHB* regulation in health and in disease, we further investigated the role of SF1 binding at this element.

rs11031006 G>A increases Steroidogenic Factor 1 (SF1) binding to the enhancer

The rs11031006 SNP falls within an element with striking similarity to the SF1 consensus sequence (79) (Fig. 1.5A). SF1 is a transcriptional activator that is critical for fertility in both sexes and regulates multiple genes at all levels of the hypothalamic-pituitary-gonadal (HPG) axis (80). SF1 has been shown to bind to the proximal promoters of *Lhb*, *Fshb*, and *Cga* to regulate basal expression of the gonadotropin genes (81). The human minor (A) allele of

rs11031006 corrects a mismatch between the SF1 consensus sequence and the sequence with the major (G) allele, creating a full SF1 consensus sequence (Fig. 1.5A). To test whether SF1 can bind the putative SF1 binding element at 296-305 and to compare binding between the major and minor allele, we performed an electrophoretic mobility shift assay (EMSA) using 30 bp radiolabeled double-stranded DNA oligonucleotides (Table 1.3) from mouse and human containing the rs11031006 SNP. Incubation of the probe containing the rs11031006 major (G) allele with nuclear extracts isolated from LβT2 cells resulted in a DNA-protein complex that was supershifted when it was incubated with a SF1 antibody, indicating that SF1 binds to this region of the enhancer (Fig. 1.5B). Notably, binding of SF1 increased when the labelled probe contained the rs11031006 minor (A) allele. A similar pattern was seen for probes corresponding to both human and mouse enhancer sequences encompassing the SF1 binding element.

To further confirm that the DNA protein complex contained SF1, competition with various probes in excess was utilized. A labelled probe containing an SF1 consensus sequence (also called gonadotrope-specific element, GSE) (82) from the *CGA* promoter was competed by cold human major (G) allele or minor (A) allele probe or the corresponding probes from mouse (Fig. 1.5C). All human and mouse probes were able to outcompete GSE. In agreement with SF1 binding in Fig. 1.4B, the minor (A) allele outcompeted the labelled probe at a lower concentration than was needed for competition by the major (G) allele for both human and mouse. Furthermore, SF1 binding to the probe was eliminated by a two base-pair mutation (CAGGGTCA >CAG**TT**TCA) within the SF1 motif (Fig. 1.5D). This mutation does not target the rs11031006 base pair. These findings confirm that SF1 binds to this region of this enhancer and suggests that rs11031006 could affect *FSHB* expression by altering SF1 binding.

rs11031006 increases enhancer activity

Because the rs11031006 minor allele G>A increases SF1 binding to the enhancer in the gel-shift assay (Fig. 1.5), it is important to determine whether this SNP affects enhancer activity. We used site-directed mutagenesis to create hEnh/A:1028 *FSHB*-luc, containing the minor (A) allele at the rs11031006 site. Activity from the rs11031006 minor allele construct (hEnh/A) was increased 1.5-fold compared to the major allele construct (hEnh/G) and 4.3-fold compared to promoter alone (Fig. 1.6A). An equivalent mutation was created in the reversed mouse *Fshb* enhancer since it had higher activity than the forward direction, and it produced a similar increase in transcription compared to the wild-type enhancer (2.4-fold) or promoter alone (4.2-fold) (Fig. 1.6B). These results indicate that the rs11031006 minor (A) allele has a distinct effect on gene expression driven from the *FSHB* promoter compared to the major (G) allele.

SF1 binding site contributes to enhancer function

We next sought to further assess how the SF1 site affects function of the human *FSHB* enhancer. To expand upon the effect of the deletion from 296-305 (Fig. 1.4B), the SF1 binding site was more narrowly targeted by creating the same two base-pair mutation in the human *FSHB* enhancer as in Fig. 1.5D. The SF1 mutation significantly decreased luciferase activity to 0.8-fold WT levels (Fig. 1.6C). This result was consistent with the deletion from 296-305, although luciferase activity driven by the SF1 mutant human *FSHB* enhancer was still greater than from the promoter alone (1.8-fold). An equivalent mutation in the mouse enhancer similarly decreased luciferase activity to 0.8-fold WT levels but was still elevated 1.5-fold relative to promoter alone (Fig. 1.6D). To determine if SF1 overexpression would increase transcription from the TK promoter linked to the *FSHB* enhancer, NIH 3T3 cells were transfected with an SF1 expression

vector (Fig. 1.6E). NIH 3T3 cells do not express endogenous SF1. As compared to the empty pcDNA3 expression vector, SF1 produced a small but significant increase in transcription (1.2 fold), suggesting that it is sufficient for activation of transcription through the enhancer. These results indicate that the SF1 binding site contributes to both the human and mouse enhancer activity *in vitro*.

Discussion

Precise regulation of FSH is critical for optimal fertility. For this reason, identifying *FSHB* transcriptional regulatory elements is necessary to understand how genetic variants within these elements might contribute to the pathophysiology of disease. In this study, we identified a novel upstream enhancer of *FSHB*, confirming that it is reversible, accessible in gonadotropes, and marked by histone modifications associated with active enhancers.

As of yet, there are no ENCODE ChIP-seq databases for gonadotropes. It was previously reported that a potential enhancer, marked by open chromatin and H3K27Ac and H3K1me1 peaks in ENCODE data, resides about 2 Kb downstream of the rs11031006 variant (21). However, these data were from a lymphoblastoid cell line, which is not expected to express *FSHB*, and our scATAC-seq analysis did not show that this region is accessible to transposase in gonadotropes. In contrast, our results clearly demonstrated that the chromatin was accessible at the enhancer region 17 Kb upstream of the *Fshb* promoter and that H3K4me1 and H3K27Ac were enriched at this element. While enrichment of the enhancer-specific histone marker H3K27me1 and an absence of the repressive marker H3K27me3 were detected at the 450 bp upstream region in LβT2 cells, the active regulatory marker H3K27Ac was not enriched, although levels were comparable to the proximal promoter. This result contrasted with the results

in whole pituitary in which both H3K4me1 and H3K27Ac were enriched. Enhancers positive for H3K4me1 and negative for H3K27 acetylation or methylation have been termed “intermediate” and can be activated by stimulatory cues (77). Bulk ATAC-seq of GnRH-treated LβT2 cells showed that the *Fshb* enhancer was not accessible in LβT2 cells (83). Consistent with that finding, *Fshb* mRNA expression in LβT2 cells was relatively low in the absence of activin stimulation (76). Thus, stimulatory cues, such as activin and/or steroid hormones, potentially signaling through the putative SMAD binding site, may be necessary for H3K27Ac recruitment and chromatin accessibility in gonadotropes. How this affects enhancer accessibility with regards to sex, developmental stage, and estrous cycle stage remains an intriguing question for future studies.

To mechanistically interrogate the enhancer, we used systematic deletion and sequence analysis to identify an SF1 binding site that overlaps with a fertility-associated variant and contributes to the function of the enhancer. We also predicted binding sites for the transcription factors PTX1 and SMADs. Deletion of each individual element reduced enhancer-mediated transcription to promoter-only levels, potentially indicating that physical interactions between SF1, PTX1, and SMADs are necessary for *FSHB* upregulation by the enhancer. In gonadotropes, PTX1/SMAD have been demonstrated to interact on the *Fshb* and *Lhb* proximal promoters and PTX1/SF1 interact on the *Lhb* proximal promoter (29, 84-86). Together, SF1 and PTX1 may confine enhancer activity to gonadotropes while the SMAD site could confer activin responsiveness, although this remains to be tested experimentally.

It was previously shown that a randomly integrated, 10 Kb human transgene encoding *FSHB* flanked by 4 Kb of upstream and 2 Kb of downstream sequence was sufficient to restore gonadotrope-specific expression and fertility in *Fshb* knockout mice (87). While this implies that

regulatory elements within the transgene were sufficient to localize *FSHB* expression to gonadotropes and restore fertility, this study was not designed to evaluate *FSHB* expression levels driven by the transgene, as copy number of the *FSHB* transgene and the effect of any regulatory elements near the site of random transgene integration were not able to be controlled. Therefore, it is difficult to infer whether additional intragenic sequences not incorporated in the human transgene can also modulate *FSHB* gene expression levels. Our findings widen the scope of *FSHB* regulation beyond the boundaries of the transgene, raising the potential for this element or additional novel regulatory regions to explain unanswered questions related to *FSHB* gene regulation. In addition to the enhancer element described in this study, scATAC-seq revealed an additional region of open chromatin located 4 Kb more proximal to the *Fshb* TSS and possibly indicative of an additional enhancer to be considered in future studies.

GWAS is a powerful technique for identifying genetic correlants of specific diseases or physiological phenotypes, but it is limited because it does not provide a direct assessment of causality. Variants in high linkage disequilibrium segregate together, confounding whether a disease-correlated SNP has a functional effect or merely segregates with a variant that does. For this reason, there is a growing need for mechanistic studies to evaluate specific genetic variants (88). Variants within protein-coding regions are obvious candidates for further evaluation, but comprise only a small fraction of disease-associated SNPs (89). Therefore, it is essential to also evaluate genetic variants in noncoding regions for regulatory function. Our results show that the rs11031006 minor allele has a demonstrable effect on *FSHB* gene expression, suggesting that genetic variation in the *FSHB* locus may result in changes in *FSHB* gene expression and FSH serum levels that impact the reproductive axis. Furthermore, gel-shift and transcriptional assays

support SF1 binding as a mechanism to explain how the rs11031006 minor allele may alter *FSHB* expression.

Evolutionary conservation is a well-established tool for finding novel regulatory regions (90-92). In this study, we demonstrate that evolutionary conservation can also be used as a tool to prioritize genomic variants for functional analysis. Although in this case, the hypothesized causal variant rs11031006 was also the most statistically significant SNP in several PCOS GWAS studies, this is not always true. While fine-mapping of variants within a disease-associated region of linkage disequilibrium can further refine candidate causal variants, these experiments are costly and require a large sample size (93). Prioritizing variants that occur in putative regulatory elements, marked by evolutionary conservation, histone markers, and/or open chromatin, provides a straightforward method to narrow down functional candidates, and can be evaluated using publicly available databases such as phyloP for conservation and ENCODE for indicative histone modifications, when available.

The chromosome 11p14.1 region containing rs11031006 and *FSHB* is of particular interest for PCOS research as it is also associated with levels of FSH, LH, and a female-specific effect on testosterone levels (19-22, 44, 94). LH levels, also elevated in FSH-deficiency female mouse models and women with *FSHB* loss-of-function mutations, may be increased due to reduced negative feedback on the hypothalamic-pituitary-gonadal axis (10, 35, 36, 38, 41, 45). The observed effect of rs11031006 on *FSHB* transcription could either directly contribute to PCOS etiology through FSH dysregulation, possibly contributing to anovulation, or indirectly through altering LH levels. Increased LH is associated with an array of problems, including elevated testosterone levels (95).

Our results strongly support the conclusion that the enhancer targets *FSHB* given that the open chromatin status at the enhancer is exclusive to gonadotropes within the pituitary and that FSH is an important regulator of fertility. Additionally, LH levels and the LH/FSH ratio in women show a copy number correlation, with higher serum LH levels and LH/FSH ratio when both copies of the rs11031006 minor allele are present compared to one or no copies (26, 27). Therefore, any contribution of rs11031006 to gonadotropin levels most likely results from changes to *FSHB* regulation mediated by the enhancer. While *FSHB* is the most likely target of the enhancer, located within the chromosome 11p14.1 locus 122 Kb downstream of the enhancer is *ARL14EP*, an effector protein that regulates MHC Class II export and is co-expressed with SF1 in the gonads. Our studies do not rule out that the enhancer could target *ARL14EP* or another gene outside the 11p14.1 locus in FSHβ-positive cell populations in the pituitary or in non-pituitary tissues.

Given that some women with PCOS exhibit low FSH and that even a single copy of the rs11031006 minor allele was associated with an increase in the LH/FSH ratio (19, 20), we were surprised that the minor allele increased *FSHB* transcription *in vitro* in our study. One possibility is that the direction of response was altered by the DNA context; in our study, the enhancer was subcloned directly upstream of the *FSHB* proximal promoter and studied in a gonadotrope cell culture model. In the *in vivo* context, it is possible that increased binding of SF1 to the enhancer with the rs11031006 minor allele results in a differential transcriptional response especially since other regulatory elements and factors could interact with the enhancer to alter its effect on the promoter. An alternative possibility is that the rs11031006 minor allele increases *FSHB* transcription during development, resulting in organizational changes to the HPG axis that contribute to PCOS pathogenesis and potentially, other fertility-related traits. It is intriguing that

infants small for their gestational age have been shown to have elevated FSH levels during the "mini-puberty" that occurs in infancy (96) and an increased risk for PCOS in adulthood (97) that may correlate with increased follicle development and anti-mullerian hormone (AMH) levels, as has been observed in premature infants who also have elevated peak FSH levels (98). In women, elevated AMH has been hypothesized to contribute to hyperandrogenism by inhibiting FSH-stimulated aromatase expression or by directly increasing GnRH neuron excitability (99-102), which favors the synthesis of LH over FSH (1-4). Whether increased *FSHB* synthesis driven by the minor allele could elevate AMH and promote later development of PCOS is unknown and would need to be tested experimentally.

Finally, further appreciation of the role of the upstream enhancer in the regulation of *FSHB* gene expression will require the use of mouse models to delineate whether the putative enhancer region is necessary for appropriate regulation of FSH levels and fecundity. Deletion of the enhancer may be sufficient to reduce *Fshb* levels and mirror the phenotype of other FSH deficiency models, such as reduced fecundity, elevated LH, and/or reduced number of corpora lutea. In addition, creation of a mouse model with a point mutation to represent the rs11031006 minor allele will help determine whether genetic variation at the *Fshb* locus is an important factor in reproductive function. Studies in infancy and adulthood may help clarify the discrepancy between the observed increase in *Fshb* expression due to the minor allele versus the decrease in *Fshb* expression that would be predicted to be associated with PCOS. As the function of the conserved region is maintained in mouse, the rs11031006 SNP model has the potential to emerge as an innovative tool providing a genetic model to facilitate future fertility research.

Acknowledgements

This work was supported by National Institutes of Health (NIH) Eunice Kennedy Shriver National Institute of Child Health and Human Development (NICHD) Grants R01 HD082567, HD100580, and HD072754 to P.L.M., as well as P50 HD012303 (to P.L.M. and V.G.T.) as part of the National Centers for Translational Research in Reproduction and Infertility. P.L.M. was also partially supported by NIH P30 DK063491, P30 CA023100, and P42 ES010337. S.C.B. was partially supported by NIH F31 HD096838 and NIH T32 NS061847. V.G.T. was partially supported by NIH R01 HD095412. D.S.K. was partially supported by NIH R01 EY027011 and RPB Special Scholar Award. The content is solely the responsibility of the authors and does not necessarily represent the official views of the National Institutes of Health.

Chapter 1 has been published in *Endocrinology* (Bohaczuk, Stephanie. C.; Thackray, Varykina. G.; Shen, Jia; Skowronska-Krawczyk, Dorota; Mellon, Pamela. L. 2021. FSHB Transcription is Regulated by a Novel 5' Distal Enhancer with a Fertility-Associated Single Nucleotide Polymorphism. *Endocrinology* 162(1)). The dissertation author was the primary investigator and author of this paper. Jia Shen and Dorota Skowronska-Krawczyk contributed single-cell ATAC sequencing for whole pituitary. Dorota Skowronska-Krawczyk also assisted with experimental design of chromatin immunoprecipitation experiments. Varykina Thackray assisted with experimental design and paper composition. Pamela Mellon supervised the project and provided advice.

Figures

Figure 1.1: Conserved intergenic region enhances *FSHB* transcription. (A) 100 Vertebrates Basewise Conservation (Cons 100 Verts) by phyloP, UCSC Browser, (GRCh38/hg38 assembly). The y-axis indicates conservation comparing 100 representative vertebrates at each base pair, expressed as -log (p-value of neutral evolution), with positive and negative values respectively assigned to higher or lower conservation than expected by chance due to genetic drift. (B) Luciferase expression from a reporter containing the major allele 450 bp conserved region (Enh) from human upstream of the -1028/+7 *FSHB* promoter (P) compared to a reporter containing the -1028/+7 *FSHB* promoter alone transfected into LβT2 mouse gonadotrope cells. The putative enhancer was subcloned in the forward (FW) (hEnh/G) or reverse (RV) (RV-hEnh/G) orientations onto the human *FSHB* promoter driving Luciferase (Luc) (n=3). (C) Luciferase expression from the mouse 450 bp conserved region subcloned in the forward (mEnh/G) and reverse (RV-mEnh/G) orientations upstream of the mouse -1000/-1 *Fshb* promoter compared to a luciferase reporter containing the mouse -1000/-1 *Fshb* promoter alone (n=4). (D) Luciferase expression from the human 450 bp conserved region subcloned in the forward and reverse orientations upstream of the -81/+52 TK promoter compared to a reporter containing the TK promoter alone (n=4). (E) Luciferase expression from the mouse 450 bp conserved region subcloned in the forward and reverse orientations upstream of the TK promoter compared to a reporter containing the TK promoter alone (n=4). (F) Luciferase expression from the human 450 bp conserved region subcloned in the forward orientation upstream of the mouse -523/+6 Lhb promoter or (G) mouse -493/+9 Gnrhr promoter compared to each promoter alone (n=4). Luciferase values were normalized to the β-galactosidase internal control and are expressed relative to the empty reporter vector. Values represent mean ± SEM. Data were analyzed by one-way ANOVA, post-hoc Dunnett multiple comparisons test (A-E) or Student t-test (F and G). A log transform was used prior to statistical analysis for D and E (*- $p<0.05$, **- $p<0.01$, ***- $p< 0.005$). P, promoter; Enh, enhancer; Luc, luciferase.

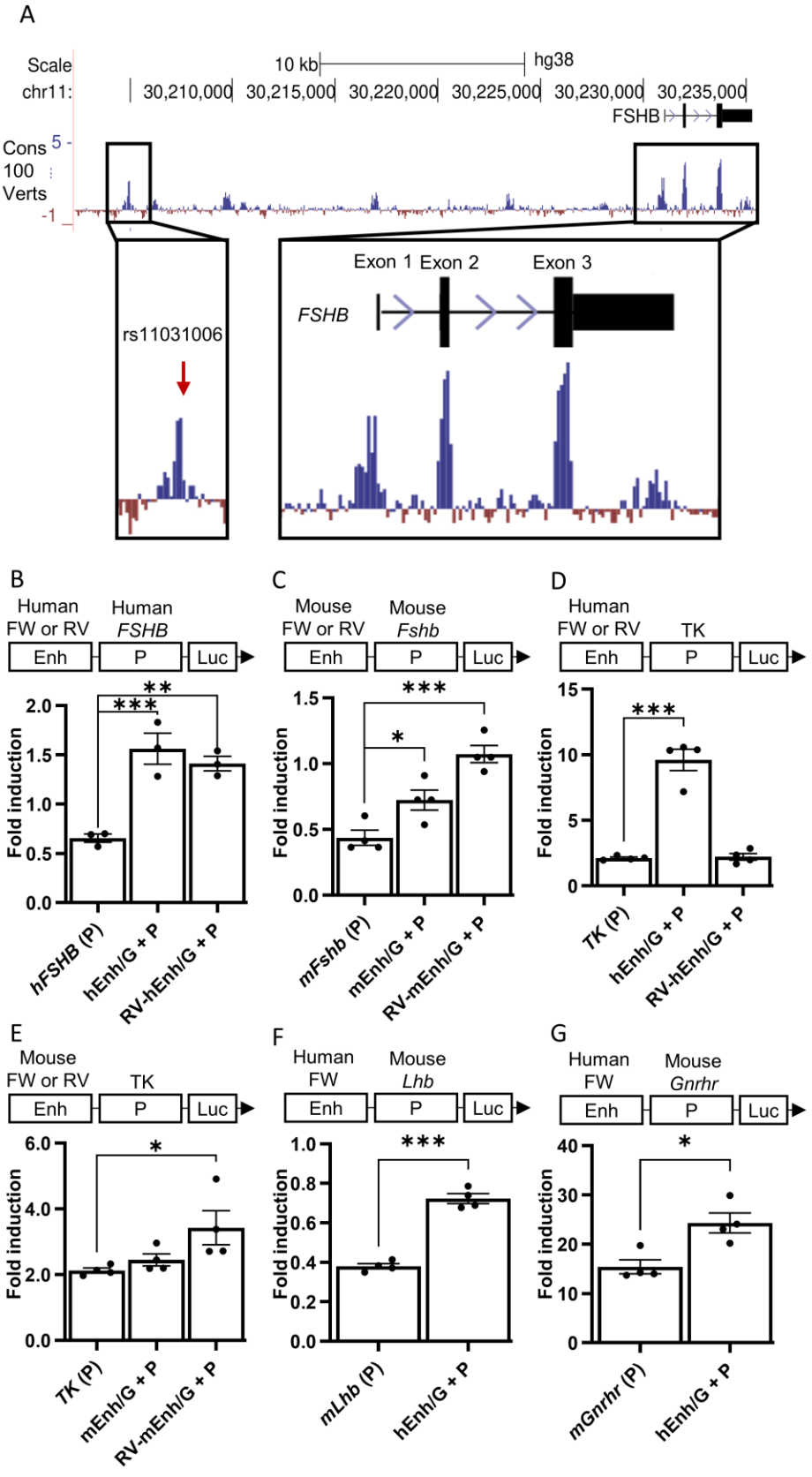
A
Scale
10 kb
hg38
chr11:
30,210,000
30,215,000
30,220,000
30,225,000
30,230,000
30,235,000
FSHB
Cons 100 Verts
5
-1
rs11031006
Exon 1
Exon 2
Exon 3
FSHB
B
Human FW or RV
Human FSHB
Enh
P
Luc
Fold induction
hFSHB (P)
hEnh/G + P
RV-hEnh/G + P
C
Mouse FW or RV
Mouse Fshb
mFshb (P)
mEnh/G + P
RV-mEnh/G + P
D
Human FW or RV
TK
TK (P)
hEnh/G + P
RV-hEnh/G + P
E
Mouse FW or RV
TK
TK (P)
mEnh/G + P
RV-mEnh/G + P
F
Human FW
Mouse Lhb
mLhb (P)
hEnh/G + P
G
Human FW
Mouse Gnrhr
mGnrhr (P)
hEnh/G + P

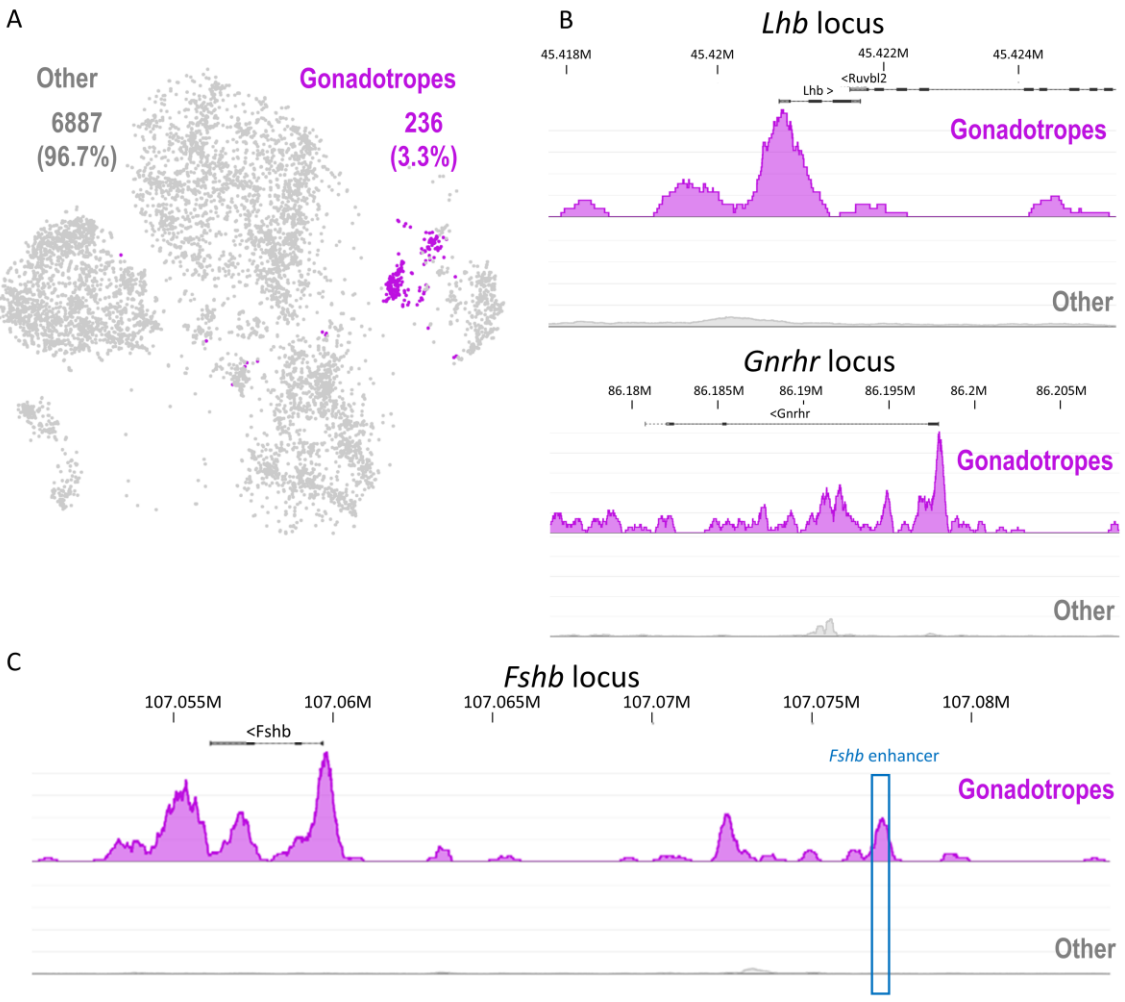

Figure 1.2: *Fshb* enhancer is marked by open chromatin exclusively in gonadotropes. scATAC-seq was performed on single cells from adult male pituitary to evaluate chromatin accessibility to transposase digestion. (A) t-SNE analysis identified a cluster of gonadotopes (purple) marked by (B) chromatin accessibility at *Lhb*, *Gnrhr*, and (C) *Fshb*. *Fshb* enhancer chromatin was open in gonadotropes (boxed in blue) but not in other pituitary cell-types ("other", depicted in gray).

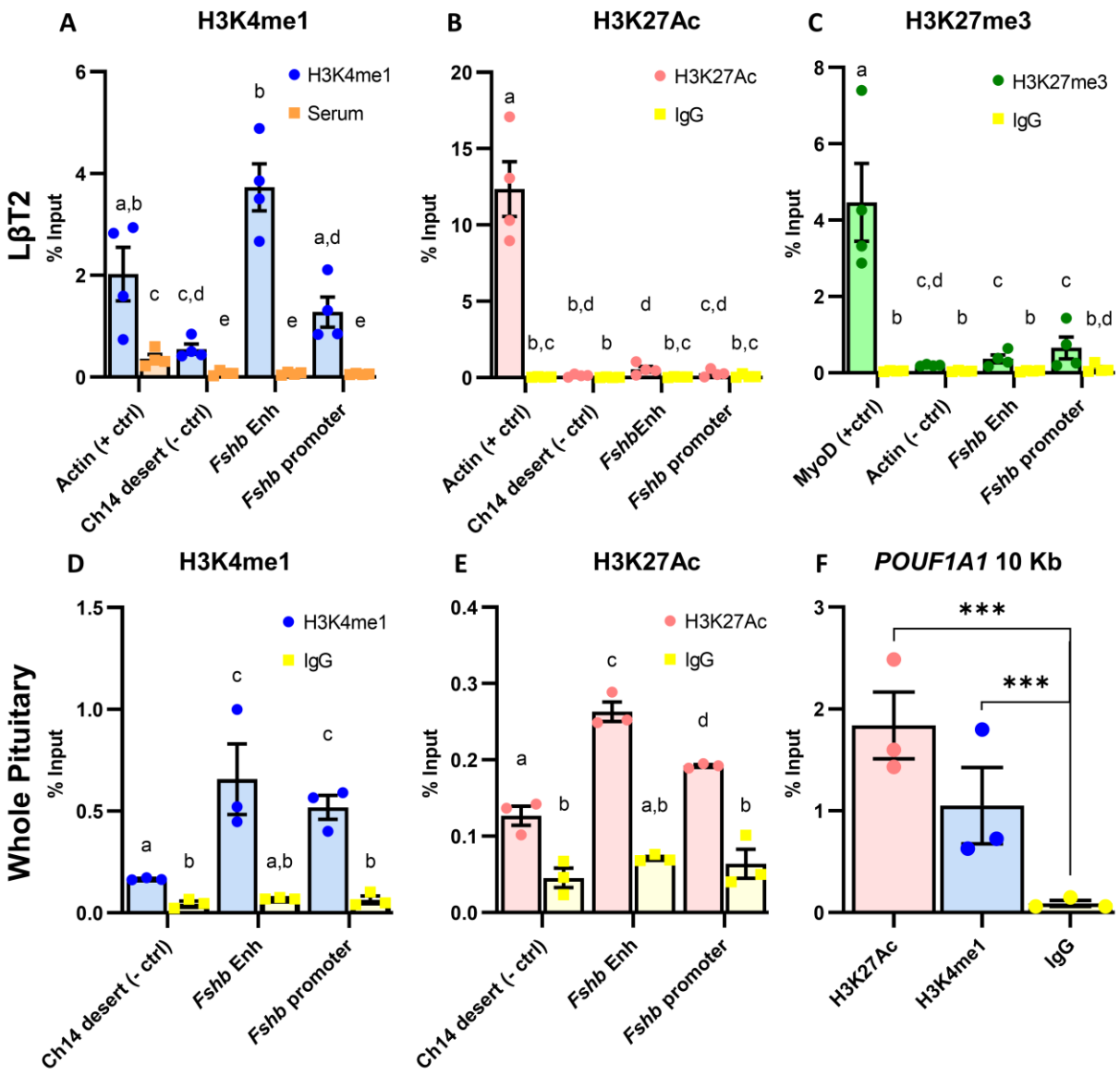

Figure 1.3: The conserved region is marked by the enhancer-specific H3K4me1 histone modification in LβT2 cells and whole pituitary. From LβT2-derived chromatin, enrichment of (A) H3K4Me1 (enhancer-specific marker), (B) H3K27Ac (active marker), and (C) H3K27me3 (repressive marker) at the *Fshb* enhancer and *Fshb* proximal promoter are expressed as percent input. For H3K4me1 and H3K27Ac, β-Actin intron 1 (Actin) was used as a positive control, and a gene desert on chromosome 14 (Ch14 desert) was used as a negative control. For H3K27me3, the MyoD proximal promoter was used as a positive control and the β-actin intron 1 was used as a negative control. From whole female pituitary-derived chromatin, enrichment of (D) H3K4me1 or (E) H3K27Ac is expressed as percent input. The *POUF1A1* 10 Kb enhancer (F) was used as positive control and the chromosome 14 (Ch14 desert) as a negative control. Values represent mean ± SEM. Data from A-E were analyzed by one-way ANOVA, post-hoc Tukey HSD. Different letters denote significant differences among groups $p < 0.05$. Data from F were analyzed by one-way ANOVA, post-hoc Dunnett multiple comparisons test (***- $p < 0.005$). A log transform was used on A-C and F prior to analysis. Enh, enhancer.

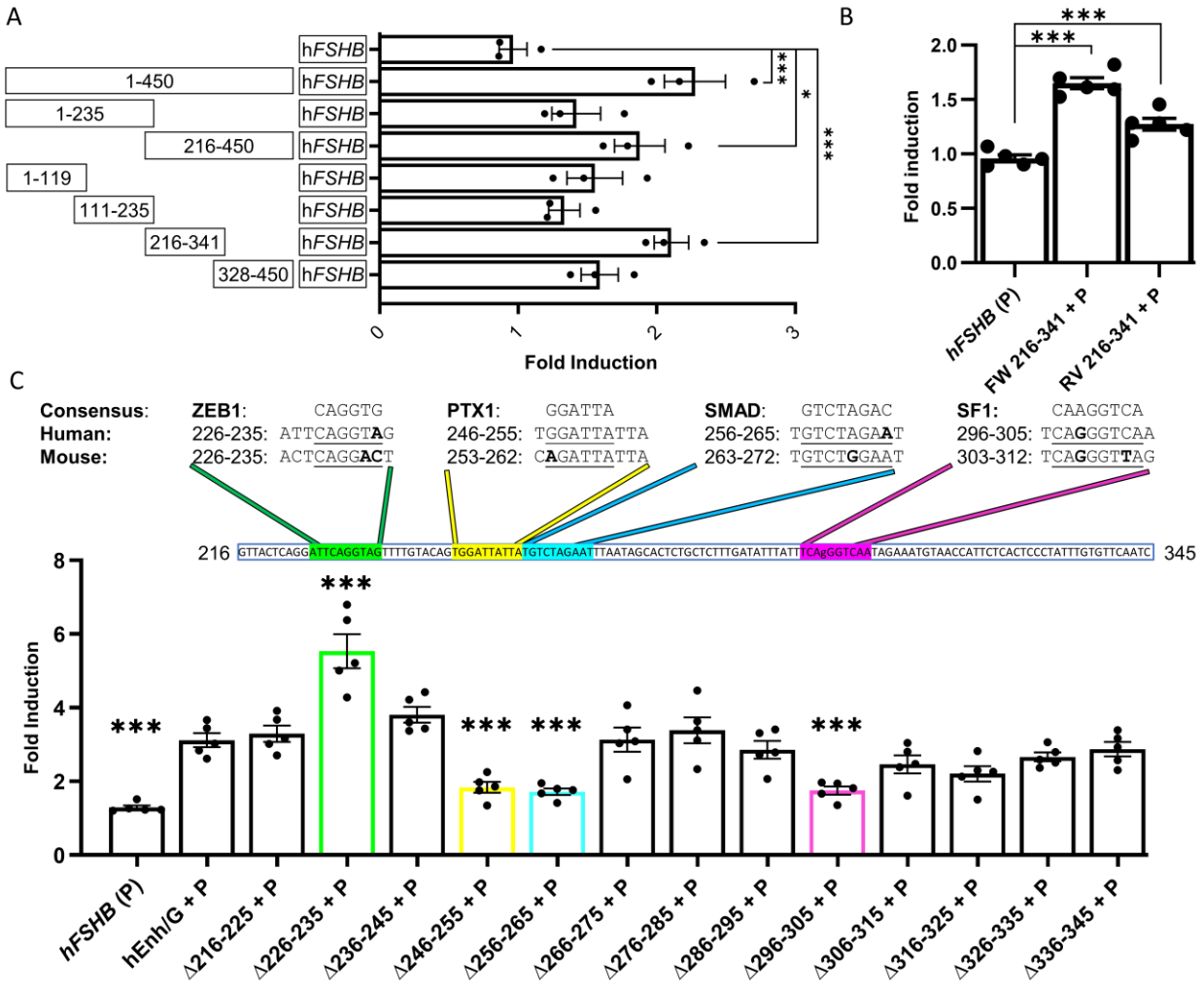

Figure 1.4: Enhancer mapping identifies putative transcription factor binding sites necessary for enhancing *FSHB* transcription. (A) Luciferase expression after transfection into LβT2 cells from subregions (halves or quarters) of the human 450 bp enhancer subcloned upstream of the human -1028/+7 *FSHB* promoter. A subregion spanning 216-341 was sufficient for enhancer function (n=3). (B) Luciferase expression from the human 216-341 subregion cloned in the reverse orientation (RV 216-341) compared to the forward orientation (FW 216-341) and human -1028/+7 *FSHB* promoter alone (n=5). (C) From the 450 base-pair enhancer subcloned upstream of the human -1028/+7 *FSHB* promoter, a series of constructs were created with 10 base-pair deletions spanning 216-345. Δ indicates the span of the 10 base-pair deletion in each construct. Expression levels from four deletion constructs were significantly different from the full-length construct (n=5). Putative transcription factor binding sites were identified from the TRANSFAC database using the Match program and each consensus sequence is shown compared to the mouse and human genomic sequences at the corresponding region. The consensus motif is underlined in each genomic sequence. Bases that differ from the consensus are bolded. Luciferase values were normalized to the β-galactosidase internal control and are expressed relative to the empty reporter vector. Values represent mean ± SEM. Data were analyzed by one-way ANOVA, post-hoc Dunnett multiple comparisons test. A square transform was used on data from A and a log transform on B prior to statistical analysis (*- p<0.05, ***- p< 0.005). P, promoter.

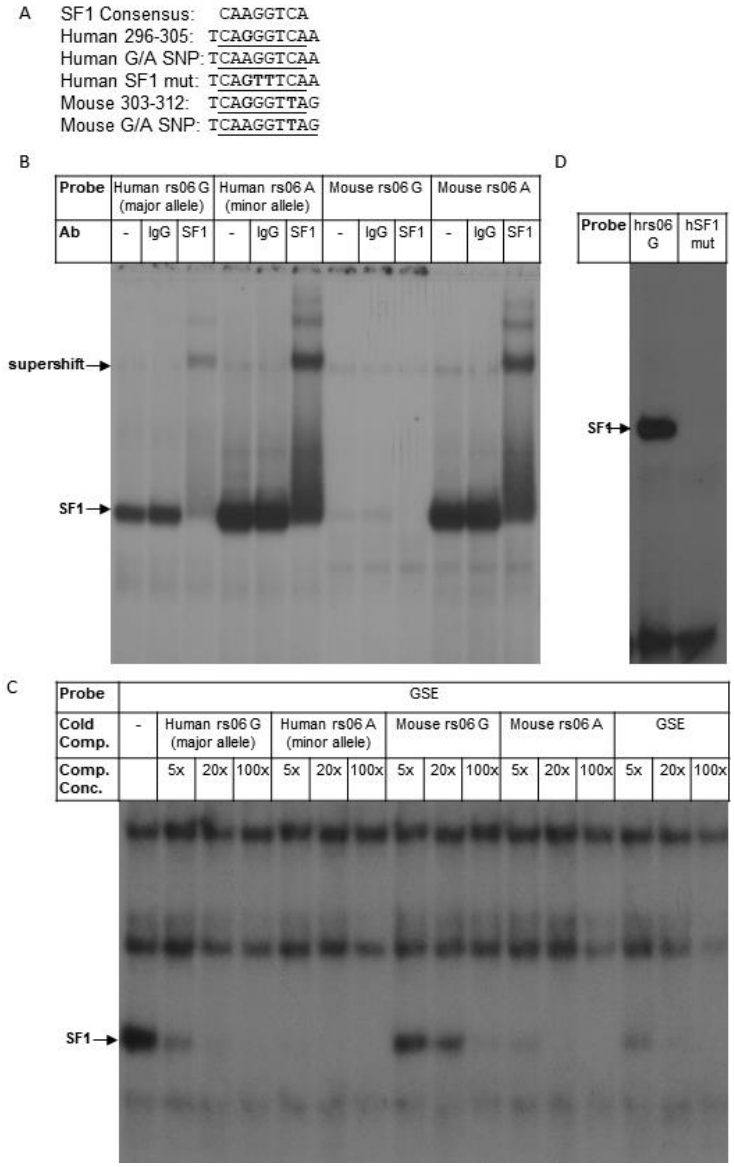

Figure 1.5: SF1 binds to the *FSHB* enhancer and rs11031006 G>A increases SF1 binding to the enhancer. The major and minor allele sequences from human and mouse at the putative SF1 binding site are compared to the SF1 consensus sequence. The consensus motif is underlined. Bases that differ from the consensus are bolded. The 2 base-pair mutation used in Fig. 1.5D and Fig. 1.6 is also shown. (B) Gel shift using 30 base-pair radiolabeled oligonucleotide probes from human containing the rs11031006 site major (G) and minor (A) alleles, or the equivalent region from mouse. Probes were incubated with LβT2 nuclear extracts and no antibody (-), normal rabbit IgG (IgG), or rabbit anti-SF1 antibody (SF1) (exposure: RT for one week). (C) The radiolabelled SF1 consensus probe (Gonadotrope-specific element, abbreviated GSE, from the human *CGA* promoter) (82) was competed by excess cold rs11031006 human major and minor alleles and mouse equivalent probes. (exposure: -80°C, four days.) (D) Gel shift with probes containing the wild-type major allele or a two base-pair mutation in the SF1 consensus sequence (exposure: -80°C, one day). Supershifted bands and complexes containing SF1 are noted with arrows. Images are representative of at least three experiments. Ab, antibody; GSE, gonadotrope specific element (SF1 consensus); cold comp., cold competitor; comp. conc., competitor concentration.

Figure 1.6: rs11031006 G>A regulates *FSHB* expression through an SF1 binding site. (A) Luciferase expression from the forward human enhancer containing the minor allele (hEnh/A) upstream of human -1028/+7 *FSHB* promoter, compared to the major (hEnh/G) allele and promoter alone (n=6). (B) Luciferase expression from the reversed mouse enhancer with a (G>A) mutation equivalent to rs11031006 minor allele (RV-mEnh/A) upstream of the mouse -1000/-1 *Fshb* promoter, compared to the wild-type reversed enhancer (RV-mEnh/G) and promoter alone. The reversed enhancer from mouse was chosen as it showed higher expression in Fig. 1.1C. (C) Luciferase expression from the human enhancer upstream of human -1028/+7 *FSHB* promoter (n=4) or (D) mouse enhancer upstream of -1000/-1 *Fshb* promoter (n=6) with a two base-pair mutation in the SF1 consensus site (same mutation as in Fig. 1.5A,D). (E) Luciferase expression from the hEnh/G:TK reporter in 3T3 cells transfected with SF1 expression vector or pcDNA3 backbone (Empty vector). Luciferase values were normalized to the β-galactosidase internal control for all experiments and are expressed relative to the empty pGL3 reporter vector (A-D) or as a ratio of normalized luciferase expression from the enhancer-promoter construct divided by the promoter alone (E). Values represent mean ± SEM. Data were analyzed by one-way ANOVA, post-hoc Tukey HSD (A-D) or Student t-test (E) (**- $p<0.01$). Different letters denote significant differences among groups $p < 0.05$. P, promoter; Enh, enhancer; Luc, luciferase.

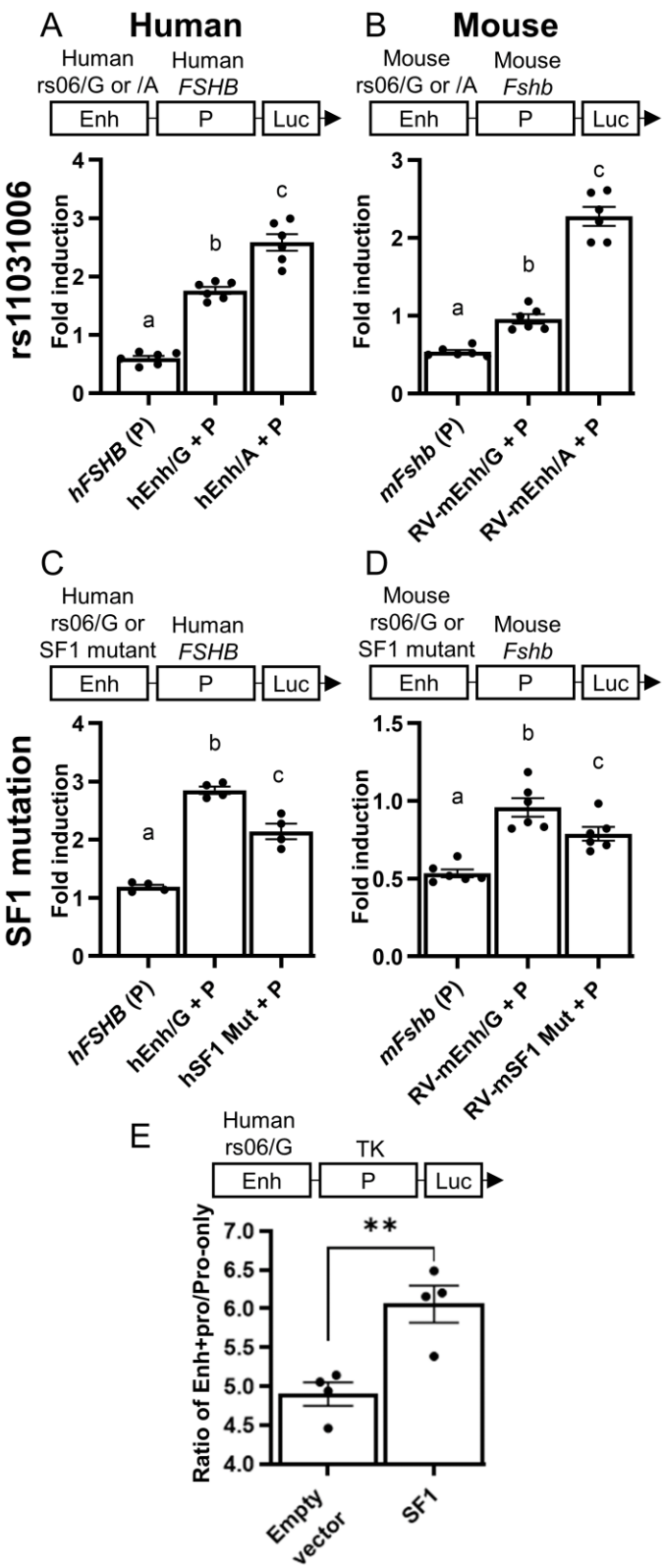
A
Human
Human rs06/G or /A
Human FSHB
Enh
P
Luc
rs11031006
Fold induction
hFSHB (P)
hEnh/G + P
hEnh/A + P
B
Mouse
Mouse rs06/G or /A
Mouse Fshb
mFshb (P)
RV-mEnh/G + P
RV-mEnh/A + P
C
Human rs06/G or SF1 mutant
SF1 mutation
hSF1 Mut + P
D
Mouse rs06/G or SF1 mutant
RV-mSF1 Mut + P
E
Human rs06/G
TK
Ratio of Enh+pro/Pro-only
**
Empty vector
SF1

Tables

Table 1.1: Cloning primer sequences

Primer Name	Sequence
FW human enh-KpnI	GCCGGTACCGCTCAAAAAATGGCTTTTTGAATC
RV human enh-SacI	CCCGAGCTCTGCCTGTGAATGTATTTGG
FW mouse pro-MluI	GCCACGCGTTTAGCAACAAAGAAATGAGAAGG
RV mouse pro-XhoI	GCCCTCGAGCACTGAGTCAAGTTACACCTC
FW mouse enh -KpnI	GCCGGTACCACTCAAAAAAAAAAAAAATGGTC
RV mouse enh-SacI	GCCGAGCTCTATTAAAAATGCACAAGTGTTAAAG
FW rev human enh-KpnI	GCCGGTACCTGCCTGTGAATGTATTTGG
RV rev human enh-SacI	GCCGAGCTCGCTCAAAAAATGGCTTTTTGAATC
FW rev mouse enh -KpnI	GCCGGTACCTATTAAAAATGCACAAGTGTTAAAG
RV rev mouse enh-SacI	GCCGAGCTCACTCAAAAAAAAAAAAAATGGTC
FW mouse Lhb-MluI	GCCACGCGTACAGTGTACCCAAGGCCTAC
RV mouse Lhb-XhoI	GCCCTCGAGACAAGGTCAGGGAAGCCAG
FW mouse Gnrhr-MluI	GCCACGCGTTTGGTATTAGAACAGGCTGCTT
RV mouse Gnrhr-XhoI	GCCCTCGAGCGAAGCGCTGTTGATGTCTG
FW human enh111-KpnI	GCCGGTACCTGTTTGGGGGAAGGGATAAG
RV human enh119-SacI	GCCGAGCTCCCCAAACAGGTGAG
FW human enh216-KpnI	GCCGGTACCGTTACTCAGGATTCAGGTAG
RV human enh235-SacI	GCCGAGCTCCTACCTGAATCCTGAGTAAC
FW human enh328-KpnI	GCCGGTACCCCCTATTTGTGTTCAATCTAACC
RV human enh341-SacI	GCCGAGCTCGAACACAAATAGGGAGTGAG
RV human enh216-SacI (for 216-341 reverse orientation)	GCCGAGCTCGTTACTCAGGATTCAGGTAG
FW human enh341-KpnI (for 216-341 reverse orientation)	GCCGGTACCGAACACAAATAGGGAGTGAG

Table 1.2: Site-directed mutagenesis primer sequences

Primer Name	Sequence
FW human enh SF1 mut	GCACTCTGCTCTTTGATATTTATTTCAGTTTCAATA GAAATGTAACCATTCTCACTCCC
FW mouse enh SF1 mut	CTGCCCTGTGATATTTATTTCAGTTTTAGTAGAAAT GTAGCTACCTCC
FW human enh G/A mut	GCACTCTGCTCTTTGATATTTATTTCAAGGTCAATA GAAATGTAACCATTCTCACTCCC
FW mouse enh G/A mut	TGCTCTGCCCTGTGATATTTATTTCAAGGTTAGTAG AAATGTAG
FW human enh del 216-225	GTTGCTTATTACAAGGAGAAACAATTCAGGTAGTT TTGTACAGTGG
FW human enh del 226-235	TACAAGGAGAAACAGTTACTCAGGTTTTGTACAGT GGATTATTATGTC
FW human enh del 236-245	GAAACAGTTACTCAGGATTCAGGTAGTGGATTATT ATGTCTAGAATTTAATA
FW human enh del 246-255	CAGGATTCAGGTAGTTTTGTACAGTGTCTAGAATTT AATAGCACTCTG
FW human enh del 256-265	ATTCAGGTAGTTTTGTACAGTGGATTATTATTAATA GCACTCTGCTCT
FW human enh del 266-275	GGTAGTTTTGTACAGTGGATTATTATGTCTAGAATT CTGCTCTTTGATATTTA
FW human enh del 276-285	GGATTATTATGTCTAGAATTTAATAGCACGATATTT ATTTCAGGGTCAATAGAAATGT
FW human enh del 286-295	TATGTCTAGAATTTAATAGCACTCTGCTCTTTTCAG GGTCAATAGAAAT
FW human enh del 296-305	TAATAGCACTCTGCTCTTTGATATTTATTTAGAAAT GTAACCATTCTCACTC
FW human enh del 306-315	TGCTCTTTGATATTTATTTCAGGGTCAAACCATTCT CACTCCCTATT
FW human enh del 316-325	CTTTGATATTTATTTCAGGGTCAATAGAAATGTACT CCCTATTTGTGTTCAA
FW human enh del 326-335	TCAATAGAAATGTAACCATTCTCAGTGTTCAATCT AACCATTTAGCAG
FW human enh del 336-345	ATAGAAATGTAACCATTCTCACTCCCTATTTTAACC ATTTAGCAGGAG

Table 1.3: qPCR primer sequences (mouse)

Putative enhancer	FW:	TGCTCACTGCAAGAAGAGACAG
	RV:	ATAAATATCACAGGGCAGAGCAA
Fshb proximal promoter	FW:	CCCTGTGGATTTACTGGGTGT
	RV:	CGAGGCTTGATCTCCCTGTC
β-actin intron 1	FW:	GGTTTGGACAAAGACCCAGA
	RV:	GCCGTATTAGGTCCATCTTGAG
Ch14 gene desert	FW:	GTCACAGAAACGCAAAGGTTTA
	RV:	CCCAAAGTCATGTTGTACTTGATAG
MyoD promoter	FW:	ACTTCTATGATGACCCGTGTTT
	RV:	GTGCTCCTCCGGTTTCAG
POU1F1 10 Kb enhancer	FW:	GCTGGACATGGCTTTGAATATG
	RV:	ATGAGCATGGGCGCATAA

Table 1.4: EMSA probe sequences (FW, rs11031006 is bolded.)

Human rs06 G	TTGATATTTATTTCA**G**GGTCAATAGAAATG
Human rs06 A	TTGATATTTATTTCA**A**GGTCAATAGAAATG
Mouse rs06 G	GTGATATTTATTTCA**G**GGTTAGTAGAAATG
Mouse rs06 A	GTGATATTTATTTCA**A**GGTTAGTAGAAATG
Human SF1 mut	TTGATATTTATTTCA**G**TTTCAATAGAAATG
GSE	TTCATGGGCTGACCTTGTCGTCACCATCAC

CHAPTER 2: DISTAL ENHANCER POTENTIATES ACTIVIN- AND GNRH-INDUCED TRANSCRIPTION OF *FSHB*

Abstract

Follicle-stimulating hormone (FSH) is critical for fertility. Transcription of *FSHB*, the gene encoding the beta subunit, is rate-limiting in FSH production and is regulated by both gonadotropin-releasing hormone (GnRH) and activin. Activin signals through SMAD transcription factors. While the mechanisms and importance of activin signaling in mouse *Fshb* transcription are well-established, activin regulation of human *FSHB* is less well understood. We previously reported a novel enhancer of *FSHB* which contains a fertility-associated single nucleotide polymorphism (rs10031006) and requires a region resembling a full (8 base-pair) SMAD binding element (SBE). Here, we investigated the role of the putative SBE within the enhancer in activin and GnRH regulation of *FSHB*. In mouse gonadotrope-derived LβT2 cells, the upstream enhancer potentiated activin induction of both the human and mouse *FSHB* proximal promoters and conferred activin responsiveness to a minimal promoter. Activin induction of the enhancer required the SBE and was blocked by the inhibitory SMAD7, confirming involvement of the classical SMAD signaling pathway. GnRH induction of *FSHB* was also potentiated by the enhancer and dependent on the SBE, consistent with known activin/GnRH synergy regulating *FSHB* transcription. In DNA pull-down, the enhancer SBE bound SMAD4, and chromatin immunoprecipitation demonstrated SMAD4 enrichment at the enhancer in native chromatin. Combined activin/GnRH treatment elevated levels of the active transcriptional histone marker, histone 3 lysine 27 acetylation at the enhancer. Overall, this study indicates that the enhancer is directly targeted by activin signaling and identifies a novel,

evolutionarily conserved mechanism by which activin and GnRH can regulate *FSHB* transcription.

Introduction

Follicle-stimulating hormone (FSH) is a key regulator of hormone synthesis and fertility in both sexes. In females, FSH regulates oocyte maturation, pre-ovulatory expression of luteinizing hormone (LH) receptor on ovarian granulosa cells, and granulosa cell synthesis of aromatase, an enzyme which catalyzes the conversion of androgens to estrogen (13-15). In males, FSH regulates spermatogenesis and Sertoli cell differentiation and proliferation (11, 12). The importance of FSH in reproduction is underscored by loss-of function (LOF) mutations, which result in infertility in both sexes (10). FSH is a heterodimeric glycoprotein hormone consisting of a unique β-subunit (*FSHB*) and an α-subunit common to LH, human chorionic gonadotropin, and thyroid-stimulating hormone. Produced within gonadotrope cells in the anterior pituitary, FSH synthesis is rate-limited by transcription of the *FSHB* gene (17, 18). Women with *FSHB* LOF mutations fail to initiate puberty and are anovulatory (35-38). Similarly, female *Fshb* knock-out mutant mice are infertile and anovulatory, with reduced uterine and ovarian size (41). Men with *FSHB* LOF mutations are azoospermatic, and a subset fail to initiate puberty (37, 39, 40). While male *Fshb* knock-out mutant mice are fertile, it is evident that FSH is important for spermatogenesis across species as these mice have reduced sperm counts and motility (41).

During the human menstrual cycle, FSH levels oscillate, with a midcycle peak at the time of the LH surge and a second peak during the late luteal/early follicular phase to initiate follicular maturation (32). Comparable peaks in rodents correspond to the proestrus LH surge

and the secondary surge during estrus (33). FSH synthesis and release is driven, in part, by gonadotropin-releasing hormone (GnRH) from the hypothalamus and activins and their inhibitors produced by the ovaries and within the pituitary (5, 8, 9).

Activins belong to the TGFβ family of signaling proteins. In gonadotropes, activins bind to their transmembrane type II receptor (likely Activin receptor type-2A) (103), a serine/threonine kinase that recruits and phosphorylates type I receptor partners, Activin receptor type-1B and/or Activin receptor type-1C (104, 105). The type I receptors then phosphorylate SMAD2/3 effector proteins within the cytoplasm, which complex with the common SMAD, SMAD4, and translocate to the nucleus (106). The SMAD complex acts as a transcription factor and recognizes a 4 base-pair (bp) SMAD-binding element (SBE), GTCT, or a higher affinity, 8 bp SBE which is a palindromic repeat of the 4 bp SBE (GTCTAGAC). SMADs upregulate mouse *Fshb* transcription in cooperation with Forkhead box protein L2 (FOXL2) (7, 34, 107, 108). The combined actions of SMADs and FOXL2 are essential for mouse *Fshb* expression as conditional deletion of SMAD4 and FOXL2 in gonadotropes results in FSH deficiency and female infertility in a mouse model (45, 109). Activin signaling is opposed by structurally-related inhibins, which compete for receptor binding, as well as follistatin, which binds and sequesters activin (5, 8, 9, 110). Activin and GnRH have been demonstrated to synergistically induce *FSHB* transcription (111, 112).

While activins regulate mouse *Fshb* through a full, 8 bp SBE at -260/-267 in the *Fshb* promoter and through several 4 bp SBEs dependent on adjacent FOXL2 binding-elements (34, 56, 107, 108, 113), the mechanisms of human *FSHB* regulation by activins remain less clear since the 8 bp SBE is rodent specific. The human -1027/+7 *FSHB* proximal promoter does contain several FOXL2 binding sites which contribute to activin induction and are adjacent to

putative SBEs (34, 114). Even so, the human *FSHB* promoter is less responsive to activin as compared to the rodent *Fshb* promoter (34, 56, 73, 111). Clinical evidence does support a role for activin in human FSH regulation. Among other observations, FSH deficiency has been observed in individuals with inhibin-secreting tumors (115-118), and postmenopausal women administered an experimental activin inhibitor had reduced FSH levels following treatment (119). For this reason, investigating additional regulatory elements outside the -1028/+7 *FSHB* promoter could identify additional mechanisms of activin action on *FSHB* regulation in humans.

We recently discovered a novel enhancer of *FSHB* located within a highly evolutionarily conserved region spanning ~450 base pairs and located ~26 Kb upstream of the *FSHB* transcriptional start site in human (chr11:30,204,683-30,205,132, hg38 assembly) (120). The analogous region from mouse also enhances mouse *Fshb* transcription and is located ~17 Kb upstream of the *Fshb* transcriptional start site (chr2:107,076,909-107,077,358, mm10 assembly). Within mouse pituitary, the enhancer was accessible exclusively in gonadotropes and was associated with enrichment of the enhancer marker, histone 3 lysine 4 monomethylation, and the active transcriptional marker, histone 3 lysine 27 acetylation (54, 120).

The human upstream enhancer contains a single nucleotide polymorphism (SNP), which was the most statistically significant variant identified in polycystic ovary syndrome (PCOS) GWAS studies, rs11031006 (G/A) (19, 20). In addition to PCOS, the 130 Kb locus at chromosome 11p14.1 containing rs11031006 was also associated with female fertility traits including LH and FSH levels, LH/FSH ratio, testosterone levels, age of natural menopause, and dizygotic twinning (19-23, 27, 44, 94). Compared to the major allele (G), we recently demonstrated that the minor allele (A) increased *FSHB* transcription in luciferase assays, likely via the creation of a stronger binding site for the transcription factor, Steroidogenic-factor

1/NR5A1 (SF1), a basal regulator of *FSHB* transcription (120). Besides the SF1 binding site, two additional sites within the enhancer were necessary for its activity. One of these sites (256-265) highly resembles an 8 bp SBE (7/8 base pair match).

Based on the presence of the putative SBE, we hypothesized that the enhancer is responsive to activin and that the response would depend on SMAD binding to the identified consensus motif. Consistent with this hypothesis, we found that the upstream enhancer potentiated activin induction of *FSHB* only when the SBE was intact. Furthermore, SMAD signaling is required for activin potentiation of the enhancer since transfection of the inhibitory SMAD7 reduced enhancer activity. We also determined that the enhancer requires the intact SBE to potentiate GnRH induction of *FSHB,* consistent with known mechanisms of synergy between activin- and GnRH-responsive elements. In DNA pull-down, SMAD4 bound to an oligonucleotide including the SBE but was not detected when the SBE was mutated. In agreement, SMAD4 was enriched at the enhancer in chromatin immunoprecipitation of gonadotrope-derived LβT2 cells treated with combined activin and GnRH. The combined activin/GnRH treatment also elevated levels of the active transcriptional histone marker, histone 3 lysine 27 acetylation, at the enhancer. Overall, our findings identify a novel role for the *FSHB* upstream enhancer as a hormone-responsive element and indicate that activin regulation of *FSHB* transcription may also involve the enhancer as well as the proximal promoter.

Methods

Plasmids

The human -1028/+7 *FSHB* luciferase reporter plasmid (-1028/+7 *FSHB*-luc) in a pGL3 backbone (Promega) was provided by Daniel Bernard (56). The SMAD7 expression vector in a

pcDNA3 backbone (Invitrogen) was provided by Aristidis Moustakas (121). The mouse -1000/-1 *Fshb* promoter luciferase reporter (m*Fshb*-luc), -81/+52 herpes thymidine kinase promoter luciferase reporter (TK-luc), hEnh/G:h*FSHB*-luc, hEnh/A:h*FSHB*-luc, hEnh/G:TK-luc, Δ256-265:h*FSHB*-luc, RVmEnh/G:m*Fshb*-luc, and RVmEnh/A:m*Fshb*-luc were previously described (120). The human hEnh/G:h*FSHB*-luc and hEnh/A:h*FSHB*-luc constructs contain a 450 base-pair enhancer from 26 Kb upstream of the *FSHB* transcriptional start site (chr11:30,204,683-30,205,132, hg38 assembly) cloned into the KpnI/SacI sites of h*FSHB*-luc, directly upstream of the -1028/+7 *FSHB* promoter. At the rs11031006 SNP site, hEnh/G:h*FSHB*-luc and hEnh/A:h*FSHB*-luc contain the major (G) and minor (A) alleles of rs11031006, respectively. The hEnh/G:TK-luc construct contains the same human 450 base-pair major allele enhancer cloned into the KpnI/SacI sites upstream of the TK promoter. Δ256-265 represents a 10 base-pair deletion within the 450 base-pair major allele enhancer (chr11:30,204,938-30,204,947, hg38 assembly). The mouse RVmEnh/G:m*Fshb*-luc and RVmEnh/A:m*Fshb*-luc contain a 450 base-pair enhancer from 17 Kb upstream of the *Fshb* transcriptional start site (chr2:107,076,909-107,077,358, mm10) cloned into the KpnI/SacI sites of m*Fshb*-luc, directly upstream of the proximal promoter and in the reverse orientation as we previously determined that it had higher activity than in the forward orientation. At the base equivalent to the human rs11031006 SNP site, mEnh/G:*Fshb*-luc has the mouse wild-type base (G), equivalent to the human major allele, whereas mEnh/A:*Fshb*-luc has been mutated to A, equivalent to the human minor allele.

Construction of the enhancer SMAD site mutation plasmid (mutSMAD:h*FSHB*-luc) was performed using the Quikchange II Site-Directed Mutagenesis Kit (Agilent, Cat # 200523) according to the manufacturer's protocol. The hEnh/G:*FSHB*-luc plasmid was used as a

template. Primer sequences are in Table 2.1. All plasmids were confirmed by Sanger sequencing (Eton Bioscience).

Cell Culture and Transient Transfection

LβT2 cells used in this study were validated by STR authentication using the CellCheck19 assay (IDEXX Bioanalytics). The STR profile was identical to "LβT2 Cell Stock 2" from a published reference for all nine of the four nucleotide repeat markers (122). Cells were negative for mycoplasma or interspecies contamination.

Cell culture was performed as described (120). Briefly, LβT2 cells cultured in Dulbecco's Modified Eagle Medium (DMEM) (Corning, cat # 10-013CV) supplemented with 10% fetal bovine serum (Omega Scientific, cat. # FB-01) and 1% penicillin-streptomycin (GE Life Sciences, cat. # SV30010) were maintained at 37°C, 5% CO_2. For luciferase assays, once reaching 80% confluency, LβT2 cells were dissociated by 0.25% trypsin-EDTA (Gibco, cat. # 25200056) and plated in 12-well plates at a density of $4.25x10^5$/well. The following morning, Polyjet (Sygnagen Laboratories, cat # SL100688) was used according to the manufacturer's protocol to co-transfect 500 ng/well of each luciferase reporter plasmid and 200 ng/well of a reporter plasmid encoding β-galactosidase driven by the herpes virus thymidine kinase promoter as an internal control of transfection efficiency. For the experiment including SMAD7, 200 ng/well of SMAD7 expression vector or pcDNA3 empty vector (Invitrogen) was also included. After five hours, media was replaced with serum-free DMEM and cells were incubated overnight. For each experimental replicate, three technical replicates were included for each condition.

Hormone Treatment and Luciferase Assay

For activin and GnRH luciferase experiments, approximately 24 hours following transfection, media was removed and replaced with serum-free DMEM containing vehicle (0.001% BSA), 10 ng/uL Activin A (Calbiochem, cat # 114700), and/or 10 nM GnRH (Sigma-Aldrich, cat # L7134) for a six-hour treatment. For follistatin treatment, approximately 24 hours following transfection, serum-free DMEM containing either vehicle or follistatin (Novus Biologicals cat # 4889-FN) was added to each well without removal of media. Final concentrations per well were 0.0025% BSA and 250 ng/mL follistatin. Cells were harvested after a 24-hour treatment.

Luciferase assays were performed as previously described (120). Briefly, cells were washed with 1x phosphate-buffered saline (PBS) and agitated for five minutes in lysis buffer (0.1 M potassium phosphate [pH 7.8] and 0.2% Triton-X-100) at room temperature. Lysates were split into two 96-well plates. To measure luciferase activity, lysates in the first plate were treated with 4x volume luciferase buffer (25 mM TrisHCl [pH 7.8], 15 mM MgSO4, 10 mM ATP, and 65 μM luciferin). To measure β-galactosidase activity, the second plate was assayed with Galacto-Light Plus reagents (Tropix, cat. # T1009) according to the manufacturer's protocol. For both assays, luminosity was measured in each well over one second following a one second delay using a Veritas Microplate Luminometer (Turner BioSystems).

For analysis, luciferase values were normalized to β-galactosidase values from the same tissue culture well ("normalized luciferase values"). Results are expressed as "relative luciferase values" (RLU), which is defined as the triplicate average of "normalized luciferase values" relative to pGL3 backbone levels from the same hormone treatment group and experimental replicate.

DNA pull-down

DNA precipitation was performed as previously described (56, 123). Following overnight incubation in serum-free DMEM, 10 cm plates of LβT2 cells at approximately 80% confluency were treated with 25 ng/mL Activin A (Calbiochem, cat # 114700) for 1 hour. Protein was collected in 1 mL FLAG buffer (300 mM NaCl, 20 mM Tris [pH 7.5], 1% Triton, 1 mM PMSF [Active Motif Cat # 37495], 1x protease inhibitor [Sigma, Cat # P8340]). Lysates were briefly vortexed, incubated on ice for 15 minutes, and spun at 15,000g for 15 minutes at 4°C before collecting supernatant. 30 µL Streptavidin-coated magnetic beads (Promega, cat # Z5481) were washed twice in 2X B&W buffer (10 mM Tris [pH 7.5], 1 mM EDTA, 2M NaCl) and incubated with 100 ng/sample Biotin conjugated DNA oligonucleotides for 15 minutes at room temperature in 1X binding buffer (5% glycerol, 20 mM Tris [pH 7.5], 1 mM EDTA, 1 mM DTT, 0.15% Triton, 100 mM NaCl, 4 mM MgCl). DNA oligonucleotide sequences are listed in Table 2.2. Beads were washed once in 2X B&W buffer, washed once in 1X binding buffer, and then blocked in 1X binding buffer with 1% BSA for 30 minutes at room temperature. Beads were resuspended in 50 µL 1X binding buffer and incubated for 1 hour at 4°C with cell lysate in the following 500 µL reaction: 100 µL lysate (in FLAG buffer), 150 µL 3X binding buffer, 10 µg Poly DI/DC (Sigma Aldrich, cat # P4929), 50 µL beads. Beads were washed 5x in 1X binding buffer and eluted by boiling for 5 minutes in 40 µL 1X Laemmli buffer with 200mM DTT. 30 µL/sample was run on a 4-20% polyacrylamide gel (Biorad, cat # 4561094), transferred to a PVDF membrane, blocked for 15 minutes at room temperature in TBS Blocking Buffer (Thermo, cat # 37542), and incubated overnight in SMAD 4 primary antibody (Cell Signaling, cat #38454) (124) at 1:1000 in TBS Blocking buffer with 0.4% Tween. Visualization was

performed with goat anti-rabbit IgG-HRP (Santa Cruz, cat# sc-2004) (125) at 1:10,000 for 1 hour at room temperature. Imaging was done with a Syngene PXi chemiluminescent detector.

Chromatin Immunoprecipitation (ChIP)

ChIP was performed using the ChIP-IT High Sensitivity kit (Active Motif, cat # 53040). For SMAD4 ChIP, LβT2 cells at approximately 80% confluency in 10 cm tissue culture dishes were treated for 16 hours with 25 ng/mL Activin A (Calbiochem, cat # 114700) and 50 nM GnRH (Sigma-Aldrich, cat # L7134) in serum-free DMEM. Adherent cells were washed twice with PBS. PBS supplemented with 1 mM $MgCl_2$ was added to the plate before adding disuccinimidyl glutarate (DSG) (Thermo Scientific, cat # 20593) in DMSO to a final concentration of 2 mM. Cells were fixed 45 minutes in DSG, then washed twice with PBS. Cells were fixed for an additional 10 minutes in PBS containing 1% formaldehyde.

For histone H3 lysine 27 acetylation (H3K27Ac) ChIP, LβT2 cells at approximately 80% confluency were treated 16 hours with 25 ng/mL Activin A and 50 nM GnRH or vehicle (0.0075% BSA) in serum-free DMEM. Cells were fixed with "Complete Cell Fixation Solution" (Active Motif) containing 1.3% formaldehyde for 10 minutes.

For both SMAD4 and H3K27Ac ChIP, chromatin was processed according to the manufacturer's instructions with a few minor modifications, as previously described (120). Chromatin was sonicated in 300 µL aliquots in 1.5 mL Bioruptor Pico Microtubes (Diagenode, cat. # C30010016) using the Bioruptor Pico (Diagenode, cat. # B01060010), 30 seconds on/30 seconds off for 15 minutes total. 30 µg of chromatin was used per reaction. For SMAD4, 4 µg of SMAD4 antibody (Cell Signaling, cat. # 46535) (126) or normal rabbit IgG (Cell Signaling, cat # 2729) (64) were used per reaction. For H3K27Ac, 5 µg of H3K27Ac antibody (Active Motif, cat

93133) (62) or normal rabbit IgG (Cell Signaling, cat # 2729) (64) were used per reaction. Input was collected from the flow-through of the IgG immunoprecipitation. Input and samples were treated with Proteinase K, purified using the QIAquick PCR Purification kit (Qiagen, cat. # 28104) and eluted in a total volume of 100 μL.

Quantitative PCR Analysis

DNA from input and immunoprecipitated samples were measured using iQ SYBR Green Supermix (Bio-Rad Laboratories, cat # 1708880) in a CFX Connect Detection System (Bio-Rad Laboratories). A standard curve of serial input dilutions was constructed for each plate and used to compute the concentration of each sample as % input. A dissociation curve was performed following PCR to ensure the presence of a single product. Three technical replicates were included per experiment. Primer design was previously described (120); sequences are listed in Table 2.1.

Statistical Analysis

For luciferase assays and SMAD4 ChIP, ANOVA followed by post-hoc Tukey-Kramer honestly significant difference test (Tukey's HSD) was performed in Prism 8 (GraphPad). Residuals were checked for normality using the Shapiro-Wilk test with $P > 0.05$ as the threshold. When needed and as indicated, data were transformed by a Box-Cox transformation in JMP Pro 15 (SAS) or a power transformation and reanalyzed in Prism 8. All transformed data subsequently met the residual normality threshold. $P < 0.05$ was used as the threshold for statistical significance. For H3K27Ac ChIP, two-tailed Student's t-tests adjusted with the Holm-Šídák method for multiple comparison were performed in Prism 8.

Results

The upstream enhancer potentiates activin induction of the FSHB promoter

To determine whether activin treatment increases *FSHB* transcription driven by the enhancer, human and mouse constructs containing the enhancer cloned upstream of the proximal promoter were transfected into LβT2 cells treated with 10 ng/mL Activin A or vehicle and compared to the promoter alone. At this dose, the human -1028/+7 *FSHB* promoter alone was not responsive to activin treatment, while expression from the enhancer/promoter construct was upregulated 1.7 fold by activin treatment (Fig. 2.1A). The mouse -1000/-1 *Fshb* promoter alone was responsive to 10 ng/mL activin (3.9-fold increase compared to untreated promoter), but addition of the mouse enhancer amplified activin induction, with a 7.1-fold increase in response to activin compared to the untreated enhancer/promoter construct (Fig. 2.1B). For both human and mouse, activin treatment and the enhancer synergistically induced *FSHB* transcription as determined by three-way ANOVA ($P < 0.05$).

The enhancer also potentiates GnRH induction of the FSHB promoter and activin/GnRH synergy

Because activin acts synergistically with GnRH to induce transcription from the *FSHB* proximal promoter (111, 112), we hypothesized that GnRH induction of *FSHB* transcription would be potentiated by the activin-responsive enhancer. Human and mouse constructs containing the enhancer plus promoter and promoter alone were treated with vehicle or 10 nM GnRH alone or in combination with 10 ng/mL activin. Validating this hypothesis, the human enhancer increased GnRH induction of the human *FSHB* promoter, with the human promoter-only construct induced 1.4 fold by GnRH treatment compared to 2.0 fold when the enhancer was

present (Fig. 2.1A). Additionally, combined activin/GnRH treatment of the promoter alone increased transcription 1.8 fold, as compared to 4.6 fold in the presence of the enhancer. Similarly, the mouse *Fshb* promoter alone was induced 3.1 fold by GnRH alone and 13.2 fold with combined activin/GnRH treatment, while the enhancer/promoter construct was induced 13.3 fold by GnRH alone and 78.5 fold with the combined activin/GnRH treatment (Fig. 2.1B). For both human and mouse, the synergistic interaction of GnRH and the enhancer and the three-way enhancer/activin/GnRH interaction were statistically significant by three-way ANOVA ($P < 0.05$).

The rs11031006 SNP increases activin induction of mouse Fshb enhancer, but not GnRH induction or induction of the human FSHB enhancer by either hormone

In untreated LβT2 cells, the rs11031006 SNP minor allele (A) increased enhancer activation of basal transcription from the human and mouse *FSHB* promoters as compared to the major allele (G), likely due to increased binding of the SF1 transcription factor to the enhancer (120). To evaluate whether activin or GnRH treatment would alter this effect, human and mouse constructs containing the minor allele (A) or equivalent mutation in mouse were treated with 10 ng/mL Activin A or 10 nM GnRH (Fig. 2.2). For the human constructs, while basal transcription was increased by conversion to the minor allele as previously reported, there was no interaction effect on activin induction of the enhancer (Fig. 2.2A). In contrast, the mouse minor allele equivalent did further potentiate activin signaling (6.3 fold vs 8.0 fold for the major vs. minor alleles, respectively) (Fig. 2.2B). For both species, there was no interaction effect between the minor allele and GnRH on *FSHB* induction (Fig. 2.2C and 2.2D). Overall, there was no interaction effect between the human rs11031006 minor allele and activin or GnRH induction of

the human *FSHB* promoter, but there was a species-specific interaction between the mouse minor allele equivalent within the enhancer and activin induction of *Fshb*.

The enhancer is sufficient to mediate activin, but not GnRH, induction of a minimal promoter

Given that the human and mouse enhancers with the major allele similarly potentiated activin and GnRH induction of *FSHB* (Fig. 2.1), the human enhancer was used in subsequent experiments aimed at mechanistic interrogation. The *FSHB* proximal promoter contains several transcription factor binding sites necessary for basal and hormone-mediated transcription of *FSHB*, each of which could interact with the enhancer to contribute to transcriptional activity. To determine whether the enhancer alone is truly activin responsive, a minimal herpes virus thymidine kinase promoter (*TK*) was used in place of the human -1028/+7 *FSHB* promoter. In vehicle treatment conditions, the enhancer increased transcription relative to the minimal TK promoter alone, consistent with our previous report that the *FSHB* enhancer is not promoter specific in LβT2 cells (120). While the minimal promoter alone was not affected by activin treatment, transcription from the human enhancer construct was induced 1.3 fold by activin (Fig. 2.3A). In contrast, the enhancer was not sufficient to confer GnRH responsiveness (Fig. 2.3B), indicating that elements within the *FSHB* proximal promoter are necessary for the increase in GnRH induction mediated by the enhancer.

The 256-265 site is necessary for activin and GnRH induction

We hypothesized that activin action on the enhancer is mediated by a previously predicted SBE within 256-265 (Fig. 2.4A) (120). If so, then deletion of this element within the enhancer construct should reduce transcriptional activation attributed to activin treatment. To

investigate whether the SBE contributes to activin induction of *FSHB*, LβT2 cells transfected with constructs containing a deletion of 256-265 within the enhancer cloned upstream of the proximal *FSHB* promoter (hΔ256-265hEnh+p) were treated with 10 ng/μL Activin A (Fig. 2.4B). As previously demonstrated (120), basal transcriptional activity of the Δ256-265 enhancer was reduced to promoter-only levels. Furthermore, there was no response to activin treatment, indicating that the 256-265 site is necessary for both basal and activin-stimulated transcriptional activity regulated by the enhancer (Fig. 2.4C). As a deletion could also reduce transcriptional activation by creating a new binding site for a repressor or by changing the spacing between other regulatory elements, a specifically mutated SMAD site (Human SBE mutation) construct was also studied (Fig. 2.4A). Basal transcriptional activity of the mutant was reduced compared to the wild-type enhancer, although it was still elevated above promoter-only levels (Fig. 2.4D). Comparable to the deletion construct, transcription was not increased in response to activin treatment (Fig. 2.4E).

Because the enhancer also potentiated GnRH induction of *FSHB* but was not sufficient to mediate GnRH induction of a minimal promoter (Fig. 2.1A and 2.3B), we hypothesized that GnRH potentiation mediated by the enhancer may require synergy with activin-responsive elements. For this reason, we investigated whether deletion or mutation of the SBE within the *FSHB* enhancer would affect GnRH potentiation. Compared to the intact enhancer construct, deletion of the SMAD site modestly reduced transcriptional activation by GnRH (Fig. 2.4F), although it was still elevated above promoter-only levels (Fig. 2.4G). Results obtained from the SMAD mutation construct were comparable (Fig. 2.4H and 2.4I). Overall, the putative SBE within 256-265 contributes to transcriptional activation of the enhancer in response to both

activin and GnRH treatment, although the overall effect of the enhancer and SBE on GnRH induction is weaker as compared to activin.

Follistatin represses enhancer-mediated FSHB transcription

Deletion of the putative SBE 256-265 within the enhancer was sufficient to reduce transcription to promoter-only levels (Fig. 2.4B), suggesting that activin activation and subsequent binding of SMADs is necessary for enhancer activity. Because LβT2 cells synthesize and secrete activin (127), untreated cells are continuously exposed to activin signaling, limiting the evaluation of the necessity of activin signaling for enhancer activity. To circumvent this limitation, transcriptional activity of the human enhancer was measured in the presence of the activin repressor, follistatin. Follistatin represses activin signaling by sequestering activin, preventing it from associating with its cell surface receptor (110). Follistatin treatment had no effect on transcription from the *FSHB* promoter alone but reduced activity from the human enhancer construct to promoter-only levels (Fig. 2.5A), demonstrating that activin signaling is necessary for enhancer activity.

Classical SMAD signaling is required for activin induction of the FSHB enhancer

We next sought to determine whether the classical activin signaling pathway mediated by phosphorylation of SMAD transcription factors is required, as would be expected if activin induction of the enhancer results from SMAD binding. SMAD7 acts as a dominant-negative inhibitor of SMAD phosphorylation by binding to the TGFβ type I receptor, blocking its ability to associate with and phosphorylate other SMAD proteins (128). While SMAD7 overexpression had no effect on transcription from the *FSHB* promoter alone, it reduced both basal and activin-

treated transcriptional activity from the enhancer to 0.8- and 0.6-fold, respectively, compared to transfection of the empty expression vector (Fig. 2.5B), indicating that the classical SMAD signaling pathway is necessary for basal and activin-regulated enhancer activity.

SMAD4 binds to the enhancer

To identify whether SMADs could bind to the putative SBE at 256-265, DNA-pull down was performed using biotin-labelled, 30 bp DNA double-stranded oligonucleotides spanning 241-270 of the human *FSHB* enhancer to capture proteins from whole cell lysates of LβT2 cells treated for one hour with 25 ng/mL Activin A (Fig. 2.6A). While SMAD4 was detected by an oligonucleotide representing the endogenous sequence, it was not captured when the putative SBE was mutated (same mutation as indicated in Fig. 2.4A). Similar results were obtained with oligonucleotides spanning 248-277 of the mouse *Fshb* enhancer to capture the analogous region.

To verify that SMADs can bind to the upstream enhancer in native chromatin, we performed ChIP using an antibody against the common SMAD, SMAD4 (Fig. 2.6B). As compared to the negative control region (chromosome 14 gene desert), SMAD4 binding was enriched at the *Fshb* enhancer and positive control *Hsd17b1* promoter (129), although this assay was not sensitive enough to detect it at the *Fshb* proximal promoter.

Activin and GnRH treatment elevates H3K27Ac at the enhancer

The histone marker H3K27Ac is associated with active transcription (54). To determine whether activin and GnRH treatment could increase H3K27Ac enrichment near the *Fshb* enhancer, ChIP was performed on LβT2 cells treated with a combination of 25 ng/mL Activin A and 50 nM GnRH and compared to vehicle (Fig. 2.7). While the *Fshb* proximal promoter was

unaffected by the treatment, H3K27Ac at the *Fshb* enhancer was increased 2 fold as compared to vehicle. These results support a role for activin and GnRH in increasing enhancer activity.

Discussion

While activin has long been recognized as an activator of human *FSHB* transcription, the mechanism has remained somewhat elusive given the lack of conservation of the rodent 8 bp SBE within the proximal promoter and the relatively weaker induction of the human *FSHB* proximal promoter by activin (34, 56, 73, 111). We identified a role for a recently discovered upstream enhancer of *FSHB* in activin and GnRH regulation of *FSHB* and determined that an imperfect, full SMAD site within the enhancer is necessary for its function. The ability of the upstream element to regulate activin- and GnRH-stimulated *FSHB* transcription is conserved between human and mouse. Through DNA-pull down and ChIP experiments, we confirmed that SMAD4 can bind to this element. Furthermore, combined activin and GnRH treatment increased H3K27Ac recruitment at the upstream enhancer, supporting the role of the enhancer as a hormone-responsive regulator of *FSHB* transcription.

The *FSHB* enhancer described here likely acts in cooperation with the *FSHB* promoter and other regulatory elements. A randomly integrated, 10 Kb human transgene encoding *FSHB* flanked by 4 Kb of upstream and 2 Kb of downstream sequence was previously demonstrated to restore fertility to an *Fshb* knock-out mouse but could not compensate for a loss of FOXL2 and SMAD4 function, suggesting that one or both factors act on the 10 Kb transgene to regulate human *FSHB* expression in this mouse model (87, 130). Interestingly, activin induction of the human transgene was weaker than the mouse gene in primary pituitary cultures, potentially reflecting that additional elements not included in the transgene are needed for full activin

induction. Our results confirm the presence of an additional activin-responsive element within the upstream enhancer that was not included within the 10 Kb transgene and support a mechanism which includes direct regulation by SMAD binding to the enhancer.

On the human *FSHB* proximal promoter, activin action is dependent on FOXL2 binding sites located immediately adjacent to SMAD half-site binding elements. In a search using the "Find Individual Motif Occurrences" (FIMO) tool (131) with the JASPAR (132) FOXL2 binding matrix (MA1607.1) as input and $P<10^{-4}$ as the cutoff for match discovery, no putative binding sites were identified within the human enhancer, although the more general Forkhead class (MF0005.1) binding matrix did identify one match within the human enhancer from 288-296. As deletion of this element did not affect activity of the enhancer in basal conditions but deletion of the SMAD element at 256-265 within the enhancer did (120), we focused our investigation on the latter. Given that the 256-265 enhancer SMAD site contains only a single mismatch as compared to the full 8 bp canonical SBE, it is indeed possible that FOXL2 is not required for SMAD binding at this locus. Similarly, the full SMAD site within the mouse proximal promoter is not immediately adjacent to a FOXL2 element but contributes to SMAD induction of *Fshb* (56, 73, 113). Additionally, the SMAD site on the human enhancer is adjacent to another element which is required for basal enhancer activity that is a perfect match to the consensus site for the transcription factor PTX1, which has been shown to directly interact with SMADs in gonadotropes (29, 86).

Direct regulation of the enhancer by activin is supported by the necessity of the intact SBE within the enhancer, detection of SMAD4 binding to the enhancer in ChIP and DNA pull-down, and sufficiency of the enhancer to confer activin responsiveness to a minimal promoter. In contrast, GnRH potentiation mediated by the enhancer requires the *FSHB* proximal promoter,

which has previously been reported to be strongly responsive to GnRH in both species even in the absence of the enhancer (111, 112), although we did observe variability in the strength of GnRH induction of the human *FSHB* promoter in our experiments (compare Fig. 2.1A to Figs. 2.4F,H). Furthermore, combined activin/GnRH synergy was also potentiated by the enhancer, and GnRH induction was dependent upon the SMAD full site. We therefore conclude that GnRH is most likely acting at the proximal promoter and synergizing with activin-responsive elements on the enhancer, although we have not formally ruled out the possibility that GnRH effector proteins (such as FOS/JUN) could directly bind to the enhancer.

We had previously reported that the active transcriptional marker H3K27Ac was enriched at the enhancer in chromatin from whole pituitary, but we were unable to detect significant enrichment in untreated LβT2 cells. We hypothesized that this difference may be due to hormone action required for activation of the enhancer. In this study, H3K27Ac was detectable in LβT2 chromatin at the enhancer even with vehicle treatment. This difference may be due to technical differences between the two experiments, such as media composition at the time of fixation or sonication duration or to variability intrinsic to the LβT2 cell line (122). Regardless of this difference, our current findings do reveal that activin and GnRH treatment results in accumulation of H3K27Ac, supporting our hypothesis that these factors activate the enhancer.

Given that the direction of the rs11031006 effect on basal *FSHB* transcription was counter to our initial hypothesis based upon FSH levels in PCOS patients (increasing, rather than decreasing, *FSHB* transcription), we had previously speculated that the rs11031006 SNP might interfere with activin or GnRH induction of the enhancer. This does not seem to be the case. In mouse, a mutation analogous to the human rs11031006 minor allele synergistically increased activin induction, although this effect was not observed with the human constructs, potentially

reflective of species-specific differences between the human and mouse SF1 and SMAD elements. While the human major allele SF1 site containing rs11031006 matched 7/8 base pairs to the SF1 consensus, the mouse sequence contains an additional mismatch, resulting in a potentially greater increase in SF1 binding with conversion to the minor allele equivalent (120). Similarly, the mouse SMAD site also contains an additional mismatch with the SMAD consensus. Together, SMAD binding to the mouse *Fshb* enhancer may be more dependent on anchoring by other factors, and the stability of a complex containing both SF1 and SMAD could be more dramatically increased by conversion to the rs11031006 minor allele equivalent. While not synergistic, the effect of the rs11031006 minor allele from human was additive with activin and GnRH signaling, suggesting that it does still increase *FSHB* transcription above major allele levels as a result of increased basal transcription. Whether this effect could impact human fertility remains to be investigated.

In summary, we determined that the FSHB enhancer potentiates activin and GnRH induction of FSHB transcription, dependent on a SBE at 256-265. With respect to both basal and activin/GnRH regulation, the function of the *FSHB* enhancer is conserved between human and mouse, presenting an opportunity for future investigations of the enhancer and rs11031006 SNP with mouse models.

Our findings contribute to a greater understanding of the mechanisms of *FSHB* regulation. FSH plays an indispensable role in human reproduction through regulation of puberty and fertility (35-41), but also contributes to nonreproductive functions, such as bone density and adiposity (133-135). While FSH insufficiency is associated with anovulation and conditions such as PCOS, elevated FSH levels can contribute to bone loss in postmenopausal women and premature ovarian failure (16, 134), and therefore both extremes are consequential for human

health. As FSH synthesis is rate-limited by *FSHB* transcription (17, 18), understanding how the *FSHB* gene is regulated may provide valuable insight for novel therapeutic targets.

Acknowledgements

This work was supported by National Institutes of Health (NIH) Eunice Kennedy Shriver National Institute of Child Health and Human Development (NICHD) Grants R01 HD082567, HD100580, and HD072754 to P.L.M., as well as P50 HD012303 (to P.L.M. and V.G.T.) as part of the National Centers for Translational Research in Reproduction and Infertility. P.L.M. was also partially supported by NIH P30 DK063491, P30 CA023100, and P42 ES010337. S.C.B. was partially supported by NIH F31 HD096838 and NIH T32 NS061847. J.C. was partially supported by NIH T32 HD007203 and K12 GM026584. V.G.T. was partially supported by NIH R01 HD095412. The content is solely the responsibility of the authors and does not necessarily represent the official views of the National Institutes of Health.

Chapter 2 has been resubmitted for publication in *Endocrinology* (Bohaczuk, Stephanie. C.; Cassin, Jessica; Slaiwa, Theresa I.; Thackray, Varykina. G.; Mellon, Pamela. L. 2021. Distal Enhancer Potentiates Activin- and GnRH-Induced Transcription of FSHB. *Endocrinology* [Resubmitted]). The dissertation author was the primary investigator and author of this paper. Jessica Cassin contributed the DNA pull-down. Theresa Slaiwa provided technical assistance with the follistatin luciferase experiment. Varykina Thackray assisted with experimental design and paper composition. Pamela Mellon supervised the project and provided advice.

Figures

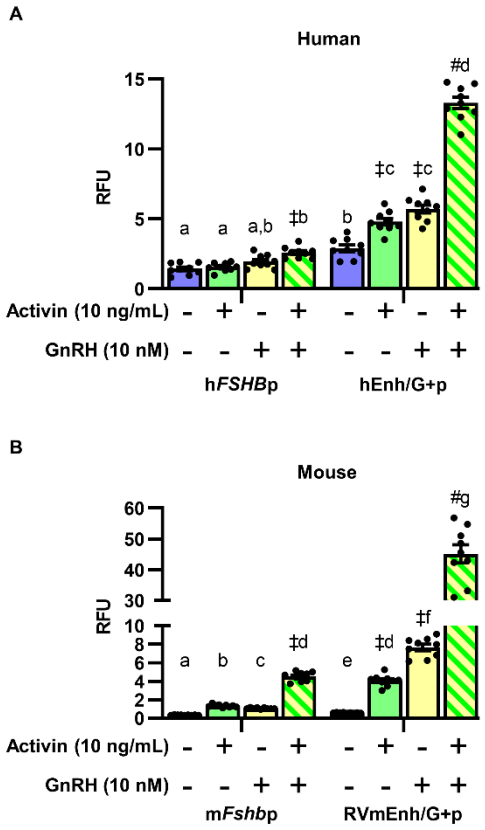

Figure 2.1: The upstream enhancer potentiates activin and GnRH induction of *FSHB* promoter. A) Luciferase expression from reporter constructs driven by the human -1028/+7 *FSHB* promoter alone (h*FSHB*p) or downstream of the human major allele enhancer (hEnh/G+p) in LβT2 cells treated with vehicle, 10 ng/mL activin, 10 nM GnRH, or both (n=9). B) Luciferase expression from reporter constructs driven by the mouse -1000/-1 *Fshb* promoter alone (m*Fshb*p) or downstream of the reverse orientation mouse major allele enhancer (RVmEnh/G+p) in LβT2 cells treated with vehicle, 10 ng/mL activin, 10 nM GnRH, or both (n=9). Each bar represents mean ± SEM. Data were analyzed by three-way ANOVA, post-hoc Tukey HSD. Different letters denote significant differences among groups $P < 0.05$. ‡ indicates a significant two-way factor interaction ($P < 0.05$) and # indicates a significant three-way factor interaction. A Box-Cox transform was used on B prior to analysis. RLU, relative luciferase units. p, promoter.

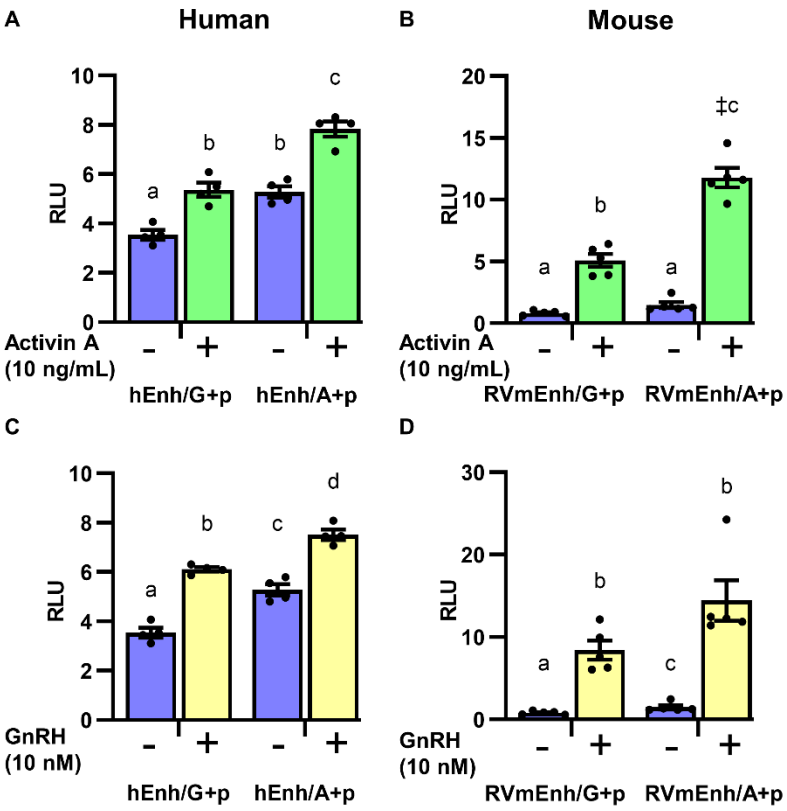

Figure 2.2: The rs11031006 SNP has a species-specific effect on activin, but not GnRH, induction of *FSHB*. A) Luciferase expression from reporter constructs driven by the human -1028/+7 *FSHB* promoter downstream of the human major allele enhancer (hEnh/G+p) or minor allele enhancer (hEnh/A+p) in LβT2 cells treated with vehicle or 10 ng/mL activin (n=4). B) Luciferase expression from reporter constructs driven by the mouse -1000/-1 *Fshb* promoter downstream of the mouse major allele enhancer (RVmEnh/G+p) or minor allele enhancer (RVmEnh/A+p) in LβT2 cells treated with vehicle or 10 ng/mL activin (n=5). C) Luciferase expression from the human constructs as in A, transfected into LβT2 cells treated with vehicle or 10 nM GnRH (n=4). The same vehicle control groups as in A were used for comparison. D) Luciferase expression from the mouse constructs as in B, transfected into LβT2 cells treated with vehicle or 10 nM GnRH (n=5). The same vehicle control groups as in B were used for comparison. Each bar represents mean ± SEM. Tukey's HSD was used for post-hoc analysis. Different letters denote significant differences among groups $P < 0.05$. ‡ indicates a significant two-way ANOVA factor interaction ($P < 0.05$). A reciprocal cube root transformation was used on D prior to analysis. RLU, relative luciferase units. p, promoter.

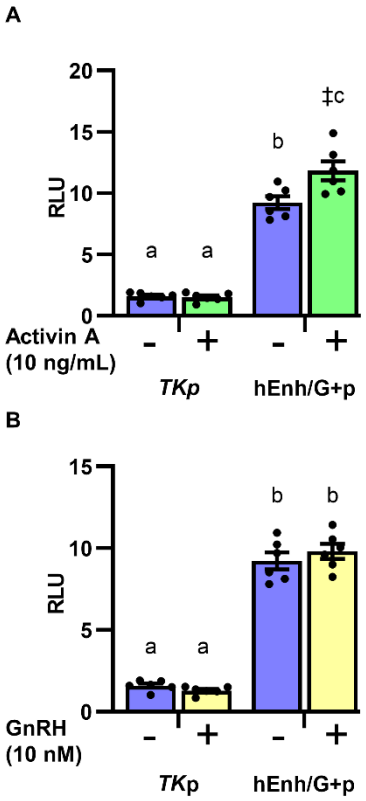

Figure 2.3: The *FSHB* enhancer confers activin, but not GnRH, responsiveness to a heterologous promoter. A) Luciferase expression from a reporter driven by the TK minimal promoter alone (*TK*p) or downstream of the human major allele enhancer (hEnh/G+p) in LβT2 cells treated with vehicle or 10 ng/mL activin (n=6). B) Luciferase expression from the same constructs as in A, transfected into LβT2 cells treated with vehicle or 10 nM GnRH (n=6). The same vehicle control groups as in A were used for comparison. Each bar represents mean ± SEM. Data were analyzed by two-way ANOVA, post-hoc Tukey HSD. Different letters denote significant differences among groups $P < 0.05$. ‡ indicates a significant two-way ANOVA factor interaction ($P < 0.05$). RLU, relative luciferase units. p, promoter.

Figure 2.4: The 256-265 site is required for maximal activin and GnRH induction via the *FSHB* enhancer. A) Sequence comparison of the SMAD consensus with the putative SBE within the human enhancer at 256-265, the equivalent site within the mouse enhancer at 263-272, and the human SBE mutation construct. Bases mismatched with the SMAD consensus sequence are bolded. B-I) Luciferase expression from transfection of LβT2 cells with reporter constructs driven by the human -1028/+7 *FSHB* promoter alone (h*FSHB*p), downstream of the full human major allele enhancer (hEnh/G+p), or downstream of the human major allele enhancer with deletion (hΔ256-265+p) or mutation (hSBEmut+p) of the putative SBE and treatment as indicated. B) SBE deletion construct (hΔ256-265+p) with vehicle or 10 ng/mL activin treatment (n=6). C) Data from B expressed as fold induction (activin-treated/vehicle). D) SBE mutation construct (hSBEmut+p) with vehicle or 10 ng/mL activin treatment (n=5). E) Data from D expressed as fold induction (activin-treated/vehicle). F) SBE deletion construct (hΔ256-265+p) with vehicle or 10 nM GnRH treatment (n=6). The same vehicle control groups as in B were used for comparison. G) Data from F expressed as fold induction (GnRH-treated/vehicle). H) SBE mutation construct (hSBEmut+p) with vehicle or 10 nM GnRH treatment (n=5). The same vehicle control groups as in D were used for comparison. I) Data from H expressed as fold induction (GnRH-treated/vehicle). Each bar represents mean ± SEM. Data were analyzed by two-way (B, D, F, and H) or one-way (C, E, G, and I) ANOVA, post-hoc Tukey HSD. Different letters denote significant differences among groups $P < 0.05$. A Box-Cox transform was used on F and H prior to analysis. RLU, relative luciferase units. p, promoter. SBE, SMAD-binding element.

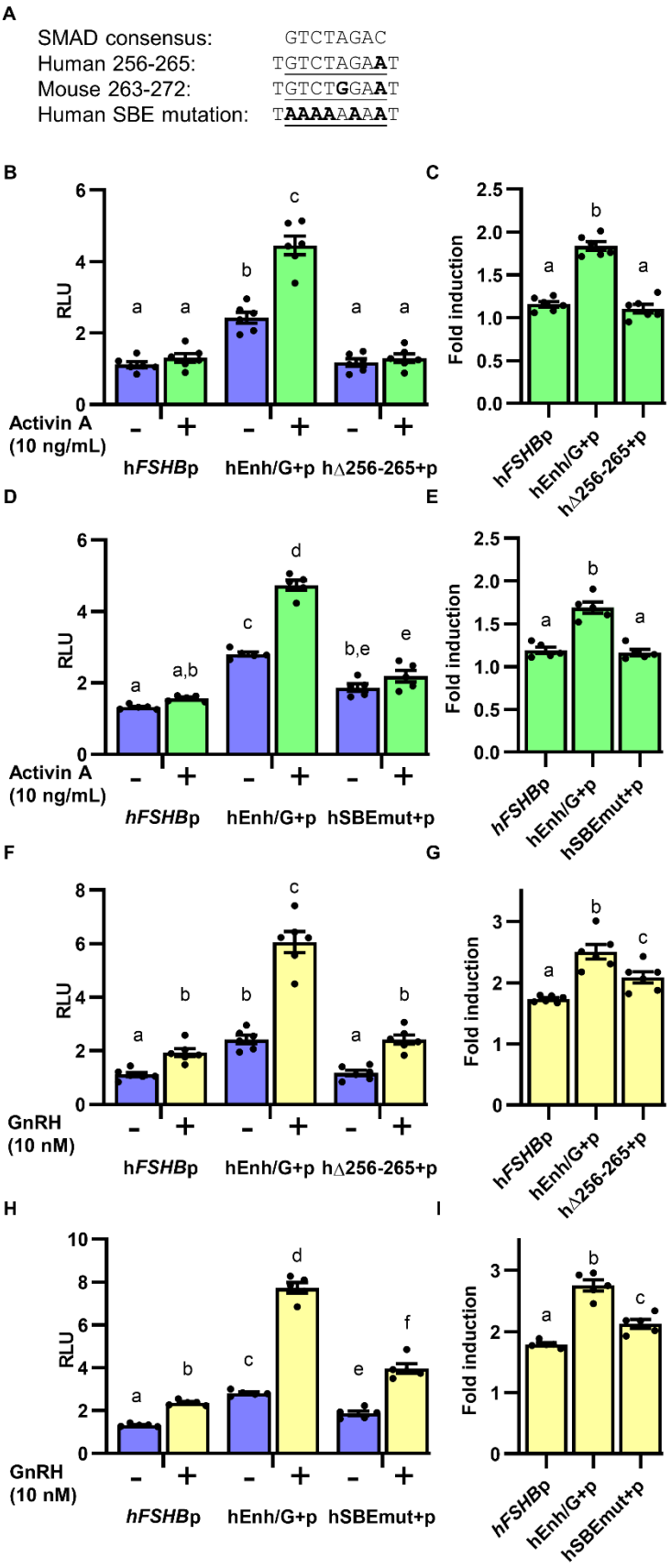
A
SMAD consensus: GTCTAGAC
Human 256-265: TGTCTAGAAT
Mouse 263-272: TGTCTGGAAT
Human SBE mutation: TAAAAAAAAT
B
RLU
Activin A (10 ng/mL)
hFSHBp
hEnh/G+p
hΔ256-265+p
C
Fold induction
D
RLU
Activin A (10 ng/mL)
hFSHBp
hEnh/G+p
hSBEmut+p
E
Fold induction
F
RLU
GnRH (10 nM)
hFSHBp
hEnh/G+p
hΔ256-265+p
G
Fold induction
H
RLU
GnRH (10 nM)
hFSHBp
hEnh/G+p
hSBEmut+p
I
Fold induction

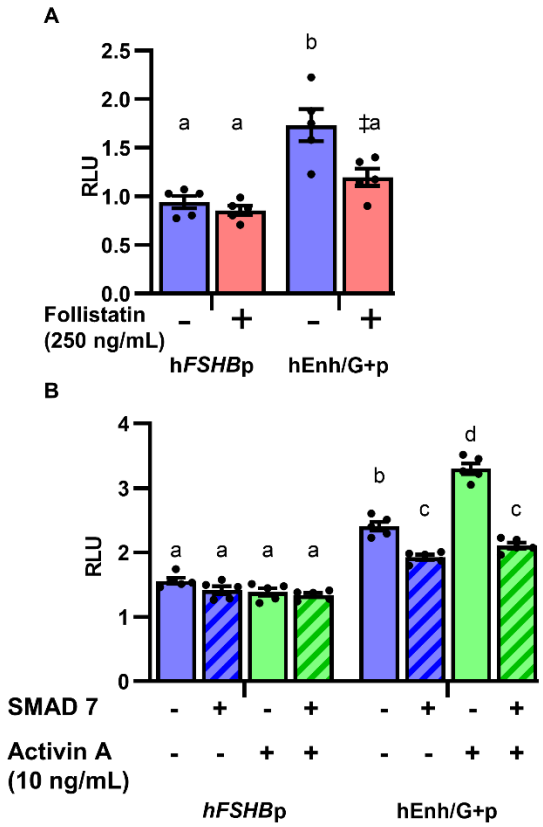

Figure 2.5: The classical SMAD signaling pathway is required for activin induction of the *FSHB* enhancer. A) Luciferase expression from reporter constructs driven by the human -1028/+7 *FSHB* promoter alone (h*FSHB*p) or downstream of the major allele enhancer (hEnh/G+p) in LβT2 cells treated with vehicle or 250 ng/mL follistatin (n=5). ‡ indicates a significant two-way ANOVA factor interaction ($P < 0.05$). B) Luciferase expression from reporter constructs as in A, co-transfected with 200 ng/well of a SMAD7 expression vector or empty vector in LβT2 cells. Each bar represents mean ± SEM. Data were analyzed by two-way (A) or three-way (B) ANOVA, post-hoc Tukey HSD. Different letters denote significant differences among groups $P < 0.05$. RLU, relative luciferase units. p, promoter.

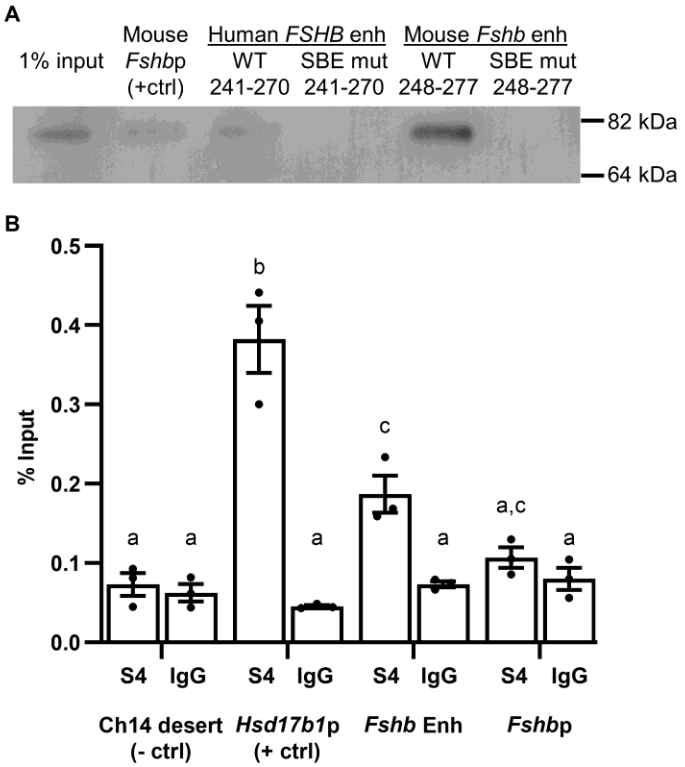

Figure 2.6: SMAD4 binds to the *FSHB* enhancer. A) Biotin-labelled 30 bp double-stranded oligonucleotides from the indicated regions of the human and mouse *FSHB* enhancers containing the wild-type (WT) or mutant SBE (SBE mut) were used in DNA pull-down of protein from activin-treated LβT2 whole cell lysates. Following precipitation of DNA/protein complexes with streptavidin magnetic beads, proteins were eluted and analyzed by Western blot with a SMAD4 antibody. Input is shown for comparison. Image is representative of four replicates. B) ChIP-qPCR using a SMAD4 antibody (S4) and normal rabbit IgG control to compare binding at the negative control region (Chromosome 14 gene desert), positive control region (*Hsd17b1* promoter), *Fshb* enhancer, and *Fshb* proximal promoter in LβT2 cells treated overnight with 25 ng/mL Activin A and 50 nM GnRH (n=3). Data were analyzed by two-way ANOVA, post-hoc Tukey HSD. Different letters denote significant differences among groups $P < 0.05$. S4, SMAD4 antibody. p, promoter. Enh, enhancer. Ch14, chromosome 14.

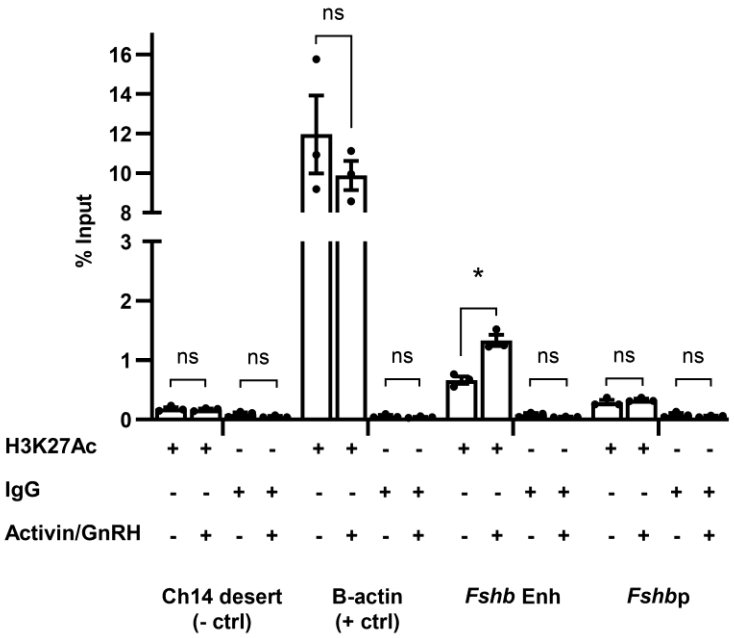

Figure 2.7: H3K27Ac increases at the *Fshb* enhancer following activin and GnRH treatment. ChIP-qPCR was performed using an H3K27Ac antibody to compare enrichment at the negative control (Chromosome 14 gene desert), positive control (b-actin intron 1), *Fshb* enhancer, and *Fshb* proximal promoter regions between activin/GnRH and vehicle treatment groups in LβT2 cells. Enrichment using a normal rabbit IgG control is shown for each treatment and region for comparison (n=3). At each locus, the vehicle-treated group served as a control for the GnRH/activin-treated group and was compared by two-tailed Student's t-test. *P* values are adjusted with the Holm-Šídák method for multiple comparisons. * indicates $P < 0.05$. p, promoter. Enh, enhancer. Ch14, chromosome 14.

Tables

Table 2.1: Primer sequences

Site-directed mutagenesis		
Human SMAD mutation	FW:	GGTAGTTTTGTACAGTGGATTATTATAAAA AAAATTTAATAGCACTCTGCTCTTTGATAT
	RV:	ATATCAAAGAGCAGAGTGCTATTAAATTTT TTTTATAATAATCCACTGTACAAAACTACC
qPCR (mouse)		
Fshb enhancer	FW:	TGCTCACTGCAAGAAGAGACAG
	RV:	ATAAATATCACAGGGCAGAGCAA
Fshb proximal promoter	FW:	CCCTGTGGATTTACTGGGTGT
	RV:	CGAGGCTTGATCTCCCTGTC
β-actin intron 1	FW:	GGTTTGGACAAAGACCCAGA
	RV:	GCCGTATTAGGTCCATCTTGAG
Ch14 gene desert	FW:	GTCACAGAAACGCAAAGGTTTA
	RV:	CCCAAAGTCATGTTGTACTTGATAG
Hsd17b1 promoter	FW:	CTGTGGGCAGGAGCAGA
	RV:	GCAAGCAAGCGAGCATGAA

Table 2.2: DNA pull-down oligonucleotide sequences

m*Fshb* proximal promoter	FW:	Biotin-CAGAAAGAATAGTCTAGACTCTAGAGTCAC
	RV:	GTGACTCTAGAGTCTAGACTATTCTTTCTG
hFSHB enhancer (241-270)	FW:	Biotin-TACAGTGGATTATTATGTCTAGAATTTAAT
	RV:	ATTAAATTCTAGACATAATAATCCACTGTA
SMAD mut hFSHB enhancer (241-270)	FW:	Biotin-TACAGTGGATTATTATAAAAAAAATTTAAT
	RV:	ATTAAATTTTTTTTATAATAATCCACTGTA
mFshb enhancer (248-277)	FW:	Biotin-TACAGCAGATTATTATGTCTGGAATTTAAT
	RV:	ATTAAATTCCAGACATAATAATCTGCTGTA
SMAD mut mFshb enhancer (248-277)	FW:	Biotin-TACAGCAGATTATTATAAAAAAAATTTAAT
	RV:	ATTAAATTTTTTTTATAATAATCTGCTGTA

CHAPTER 3: FERTILITY IS NOT IMPAIRED BY DELETION OF OR POINT MUTATION WITHIN AN UPSTREAM FSHB ENHANCER IN MICE

Abstract

Follicle-stimulating hormone (FSH) is necessary for fertility in both sexes as a regulator of gametogenesis and hormone synthesis. Humans with loss-of-function mutations within the gene encoding the FSH beta subunit (*FSHB*) are infertile. Similarly, female *Fshb* knock-out mice are infertile and fail to ovulate, whereas males are subfertile. We recently reported the discovery and characterization of an upstream enhancer of *FSHB* located 26 Kb upstream of the transcriptional start site in humans (17 Kb in mouse) that also amplifies activin and gonadotropin-releasing hormone induction of *FSHB.* Notably, the upstream enhancer contains a fertility-associated single nucleotide polymorphism, rs11031006 (G/A), and the minor allele (A) increased enhancer activity *in vitro* as compared to the major allele (G), likely through the creation of a higher affinity SF1 binding site. To investigate the role of the novel enhancer and rs11031006 variant *in vivo*, we created two mouse models, one containing a deletion of the upstream enhancer and one with a G>A point mutation at the rs11031006-equivalent base. A full characterization of the enhancer deletion model revealed no apparent differences in fertility or serum FSH/LH levels, although first estrus was slightly, but significantly, delayed in juvenile females homozygous for the deletion. As additional enhancers could compensate for the loss of the enhancer at 17 Kb, we investigated several additional conserved regions upstream of *Fshb* for enhancer activity. We identified an element located approximately 12 Kb upstream of the *Fshb* transcriptional start site which increased *Fshb* transcription in a luciferase assay. A partial characterization of the rs11031006 variant model revealed no differences in the timing of puberty in either sex, and a pilot study of adult males revealed no significant differences in

serum FSH/LH levels or sperm number or motility, although variability limited a robust conclusion. Overall, the mouse 17 Kb enhancer may be necessary for early FSH expression but is dispensable in adult mice.

Introduction

Follicle-stimulating hormone (FSH) is a dimeric glycoprotein hormone which is necessary for female and male fertility. It is produced by gonadotrope cells within the anterior pituitary along with the other pituitary gonadotropin, luteinizing hormone (LH). FSH consists of an alpha subunit (αGSU) common to LH, human chorionic gonadotropin, and thyroid-stimulating hormone, as well as a unique beta subunit (FSHβ) which confers receptor specificity. Transcription of the gene encoding the beta subunit (*FSHB*) is the rate limiting step in FSH synthesis (17, 18).

In females, FSH is required for oocyte maturation beyond the antral stage (41). As such, both female mice and women with loss-of-function mutations within the *FSHB* gene are infertile and anovulatory (10, 41). Men with *FSHB* loss-of-function mutations are azoospermatic (10). While *Fshb* knock-out male mice are fertile, epididymal sperm numbers and motility are reduced 75% and 40%, respectively (41). Mouse models of FSH insufficiency, arising from pituitary-specific deletion of *Fshb* regulatory factors including FOXL2 and SMAD4 range in phenotypic severity from subfertile to completely infertile (45, 109, 136). Overall, it is apparent that FSH is necessary for both sexes and both species for normal fertility.

While loss-of-function mutations in *FSHB* are rare, FSH deficiency is commonly observed in some patients with polycystic ovary syndrome (PCOS). Genome-wide association studies (GWAS) of PCOS identified a locus encompassing the gene encoding *FSHB* in

association with PCOS, FSH levels, LH levels, and the LH/FSH ratio, potentially indicating that *FSHB* dysregulation could contribute to PCOS etiology (19-22). The same locus has also been associated with other traits of fertility including age of natural menopause and dizygotic twinning, each of which have been related to FSH levels (23, 24). The lead single nucleotide polymorphism to emerge from several studies is rs11031006 (G/A) (19, 20). rs11031006 resides within an ~450 base pair element that is evolutionarily conserved between species, located 26 Kb upstream of the *FSHB* transcriptional start site (TSS) in human and 17 Kb upstream in mouse.

We recently reported that the conserved element is an enhancer of mouse and human *FSHB* transcription, as indicated by induction of *FSHB* in luciferase assay, chromatin accessibility exclusively in gonadotropes, and the presence of the active enhancer histone signature of histone 3 lysine 4 monomethylation and histone 3 lysine 27 acetylation (120). The rs11031006 variant minor allele increased transcription as compared to the major allele, likely through the creation of a higher affinity binding site for the transcription factor Steroidogenic factor 1 (SF1) (120). Both the human and mouse enhancers potentiate activin and GnRH induction of *FSHB*, dependent upon the presence of a SMAD binding element within the enhancer (Chapter 2).

In this study, we created two mouse models to evaluate the role of the 17 Kb *Fshb* enhancer and the rs11031006 (rs06) variant *in vivo*. For the enhancer deletion mouse line, we found that adult FSH/LH levels and fertility were normal, although first estrus was slightly but significantly delayed in mice homozygous for the enhancer deletion (ΔE/ΔE). To determine if additional enhancers might be able to compensate for the loss of the 17 Kb enhancer, we evaluated several conserved regions between the *Fshb* TSS and the 17 Kb for enhancer activity and identified an element approximately 12 Kb upstream of the *Fshb* proximal promoter which

enhanced *Fshb* transcription. Overall, these results indicate that the 17Kb *Fshb* enhancer is not necessary for adult fertility and may be compensated by the presence of additional upstream enhancers of *Fshb*. For the rs06 variant mouse line, there were no differences in male or female puberty. A pilot study of adult males revealed no significant differences in FSH/LH serum levels or sperm production, although further investigation including a larger sample size and female mice is required for a full evaluation of fertility.

Methods

Animal Housing

All experiments were performed in accordance with University of California, San Diego, Institutional Animal Care and Use Committee regulations. Mice were group housed (up to 5 per cage) with *ad libitum* access to food and water on a 12:12 light-dark cycle.

CRISPR crRNA design and injection

For both the enhancer deletion (ΔE) and rs11031006 minor allele (rs06) lines, CRISPR RNAs (crRNAs) were designed in Benchling using the CRISPR design tool. Sequences are listed in Table 3.1. For the ΔE line, two crRNAs were used to target each end of the enhancer. To generate the CRISPR injection mix, each crRNA (synthesized by Integrated DNA Technologies) was annealed to an equal molar ratio of trans-activating CRISPR RNA (tracrRNA) (Integrated DNA Technologies) and incubated with Alt-R S.p. HiFi Cas9 Nuclease V3 (Integrated DNA technologies) for a final concentration of 0.6 μM of each crRNA complex in IDTE pH 7.5 (Integrated DNA Technologies). Zygotes from C57BL/6NHsd mice (Envigo) were injected by the UC San Diego Transgenics Core. Genotyping was performed by PCR of a tail clip using the

FW/RV Ext del primers (Table 3.2), which anneal on either side of the deletion. As the deletion band outcompeted the WT band in samples from heterozygous mice, an additional primer set, FW/RV Int del, was used to distinguish between mice that were heterozygous and homozygous for the deletion. For the founder, the PCR product representing the deletion band amplified by the FW/RV Ext del primers was verified by Sanger Sequencing (Eton Biosciences).

For the rs06 line, a single crRNA was designed adjacent to the rs11031006 equivalent base in mouse. A single-stranded DNA containing a point mutation (G>A) at the rs11031006 equivalent base and 45 base pairs of flanking sequence from the mouse genome served as a template for homologous recombination (Table 3.1). The CRISPR injection mix was formulated and injected as above with the addition of 0.6 μM repair template.

Pubertal onset

Vaginal opening and preputial separation served as markers for pubertal onset and were assessed daily following weaning, typically at 21 days, as previously described (137).

First Estrus and Adult Estrous Cycling

Vaginal smears were collected daily by vaginal lavage with sterile PBS and visualized with methylene blue. For first estrus, cycling began on the day of vaginal opening and continued until estrus was identified. For adult cycling, 12-week-old females were cycled for 21 days. Vaginal smears were collected daily by vaginal lavage with sterile PBS and visualized by methylene blue staining. Cycle stage was determined as previously described (138).

Sperm analysis

Adult mice were euthanized by isofluorane overdose. To measure motility, the right caudal epididymis was collected in M2 media (Sigma-Aldrich), sliced in half, and squeezed gently with forceps to release sperm. Sperm was incubated for 15 minutes at room temperature, mixed, and motile sperm were counted using a hemocytometer. The hemocytometer was heated at 55°C for 5 minutes to immobilize sperm and intact (heads and tails) sperm were counted. % motility was determined by dividing the motile sperm over intact sperm. To measure total sperm, the left caudal epididymis was minced in M2 media using scissors. After approximately one hour incubation at room temperature, tissue was strained using a 70 μM filter. Sperm were diluted in water to immobilize them, and sperm heads were counted with a hemocytometer for total sperm count.

Ovariectomy (ovx)

Female adult mice were anesthetized with isoflurane. Ovaries were surgically excised through an incision in the back. 0.1 mg/kg buprenorphine was administered subcutaneously to all animals as an analgesic on the day of surgery and again on subsequent days as necessary. On the day of tissue collection, animals were euthanized by CO_2 inhalation. Uterine size was visually assessed to confirm estradiol deficiency.

Tissue and Serum Collection

Adult mice were euthanized by CO_2 (females) or isofluorane overdose (males). Blood was collected from the inferior vena cava, incubated for one hour at room temperature, and centrifuged for 15 minutes at 2000 x g. Serum was collected from the supernatant. FSH and LH levels were measured by the UVA Ligand Core radioimmunoassay. For intact animals, the right

ovary was carefully dissected, stripped of extraneous tissue, and weighed. The left ovary was removed from the uterus, and the uterus was removed and weighed.

Fertility Assays

Adult female mice were paired with virgin, wild-type C57BL/6NHsd males (Envigo) for 120 days. The date of each litter and total number of pups was recorded. The days to first litter, total number of litters, average pups per litter, and total number of pups are reported and reflect both live and dead pups.

Plasmids, Cell Culture, and Luciferase Assay

The mouse -1000/-1 *Fshb* promoter luciferase reporter (m*Fshb*-luc), and forward/reverse 17 Kb mouse *Fshb* enhancer plasmids (mEnh/G:m*Fshb*-luc, and RVmEnh/G:m*Fshb*-luc) plasmids were previously described (120). All other plasmids were constructed by PCR amplification of the target site from C57BL/6 mouse genomic DNA and cloning into the KpnI/SacI sites in the m*Fshb*-luc plasmid, except for region C2 which contained an endogenous SacI site and was cloned into the KpnI/MluI sites instead. Regions and primer sequences are specified in Table 3.3. For cloning the forward orientation plasmids, the KpnI restriction site (GGTACC) was included upstream of the FW primer sequence and the SacI (GAGCTC) or MluI (ACGCGT) restriction site was included upstream of the RV primer sequence. The restriction sites were switched to clone the reverse orientation plasmids. Cell culture and luciferase assay were performed as previously described (120). For analysis, luciferase values were normalized to β-galactosidase values from the same tissue culture well ("normalized luciferase values"). Results are expressed as "relative luciferase values" (RLU), which is defined as the triplicate

average of “normalized luciferase values” relative to pGL3 backbone levels from the same hormone treatment group and experimental replicate.

Statistical Analysis

Differences were analyzed via Student t-test or ANOVA as indicated. One-way ANOVA was followed by post-hoc Dunnett test. Residuals were checked for normality using the Shapiro-Wilk test with $P > 0.05$ as the threshold. Prism 8 (GraphPad) was used for all analysis, and $p < 0.05$ was the threshold for statistical significance.

Results

Validation of the enhancer deletion mouse line

To generate the 17 Kb enhancer deletion mouse line (ΔE), we designed two crRNAs to target each end of the enhancer (Fig. 3.1A). The crRNA binding sites were removed by the deletion, preventing additional cleavage. A founder with a deletion that extended slightly past the 17 Kb enhancer (ch2:107076837-107077613, mm10) was selected. Genotyping was performed using two primer sets (Fig. 3.1B). One set binds fully outside of the deleted region (Ext del) and amplifies a 1,288 bp product from the wild-type allele and a 510 bp product from the ΔE allele. As the ΔE allele PCR product often outcompeted the 1,288 bp product in heterozygous mice, a second primer set with one primer binding site falling within the deleted region (Int del) was used to distinguish heterozygous mice from homozygous ΔE/ΔE. The enhancer deletion allele band amplified using the Ext del primer set was sequenced from the founder.

Female serum FSH and LH are not different in ΔE/ΔE mice

Serum was collected from adult female mice in diestrus. There were no significant differences between wild-type and ΔE/ΔE mice in serum FSH (Fig. 3.2A), serum LH (Fig. 3.2B), or the LH/FSH ratio (Fig. 3.2C). Compensation within the hypothalamic-pituitary-gonadal axis could mask an effect on circulating FSH levels, although no differences were detected in body weight (Fig. 3.2D), ovarian weight (Fig. 3.2E), or uterine weight (Fig. 3.2F), suggesting normal estradiol levels. Still, we performed ovariectomy to fully remove ovarian feedback from the model and to determine if there could be a difference in maximal FSH induction, but we did not detect any differences in serum FSH (Fig. 3.2G), serum LH (Fig. 3.2H), or the FSH/LH ratio (Fig. 3.2I).

Female ΔE/ΔE mice cycle normally and are fertile

Although there were no differences in serum FSH or LH levels in diestrus or with ovariectomy, we considered the possibility that differences in FSH expression in conditions not measured (i.e., different cycle stages or during development) could have an impact on fertility. For this reason, we performed estrous cycling and a fertility assay on wild-type and ΔE/ΔE females. Representative cycling is shown in Fig. 3.3A. A full cycle was defined as the first day of estrus until the first day of estrus in the subsequent cycle. There were no differences in the total number of cycles completed in 21 days (Fig. 3.3B), the average cycle length (Fig. 3.3C), or the percentage of time spent in each cycle stage (Fig. 3.3D).

For the fertility assay, the dates of each new litter and the number of pups (both live and dead) were recorded for 120 days. There were no differences in the average number of pups (Fig. 3.3E), total number of pups (Fig. 3.3F), total number of litters (Fig. 3.3G), time to first litter (Fig.

3.3H), or average interval between litters (Fig. 3.3I). Overall, these results indicate that fertility is normal in ΔE/ΔE females.

Male serum FSH and LH levels are not different in ΔE/ΔE mice

To investigate whether there could be a sex-specific requirement for the 17 Kb *Fshb* enhancer, serum FSH and LH levels were measured in adult male ΔE/ΔE mice. As in females, there were no differences detected in either hormone between genotypes (Fig. 3.4 A-C). Body and testes weights were also unaffected by genotype (Fig. 3.4D, E).

Sperm counts are normal in ΔE/ΔE mice

Although no differences were expected given normal FSH serum levels in adult males, we performed sperm counts to address the possibility that deletion of the enhancer could reduce FSH during development and lead to deficiencies in the generation of sperm in adults. We measured the total number of sperm (Fig. 3.4F) and percentage of motile sperm (Fig. 3.4G) within the caudal epididymis but found no differences between genotypes, overall indicating that adult male ΔE/ ΔE do not have any observable reproductive phenotypes.

First estrus is delayed in female ΔE/ΔE mice but male puberty is normal

Given that there were no differences in FSH serum levels or fertility in adult ΔE/ΔE mice, we next evaluated juvenile mice to determine if there might be differences at other developmental time points. “Mini puberty” occurs during infancy and is characterized by a large spike in serum FSH and LH content. In females, mini-puberty has been shown to regulate development of the first wave of ovulated oocytes (139), and so we speculated that first estrus

could be impaired by deletion of the 17Kb *Fshb* enhancer. To determine if there were any differences in pubertal onset, we measured the age and weight of vaginal opening in females (Fig. 3.5A, B) but found no differences. Beginning on the day of vaginal opening, we collected vaginal smears for cytology to evaluate the day of first estrus. As compared to wild-type mice, age of first estrus was significantly delayed in ΔE/ΔE mice (Fig. 3.5C). There was also a significant difference in the number of days between vaginal opening and first estrus (Fig. 3.5D). In males, there were no differences in pubertal onset as measured by the timing of preputial separation (Fig. 3.5E) or body weight at preputial separation (Fig. 3.5F). Overall, these results indicate a delay in first estrus in ΔE/ΔE mice, although further investigation is necessary to determine if, and when, during development, FSH levels could differ in ΔE/ΔE mice to give rise to this phenotype.

An evolutionarily-conserved element located 12 Kb upstream of the Fshb transcriptional start site enhances Fshb expression

Because deletion of the enhancer at 17 Kb upstream of *Fshb* did not impair FSH levels or fertility, we considered the possibility that additional upstream enhancers of *Fshb* could compensate for the deletion. Evolutionary sequence conservation can be used to predict regulatory regions as sequence conservation can indicate an important biological function. Five conserved regions (C1-C5) between the 17 Kb enhancer and the *Fshb* transcriptional start site were cloned upstream of the *Fshb* proximal promoter in both the forward and reverse orientation in a luciferase reporter plasmid to assess enhancer activity (Fig. 3.6A). One region, C2, located approximately 12 Kb upstream of the *Fshb* TSS, enhanced transcription in the forward orientation (Fig. 3.6B) and was previously shown to be accessible in scATAC-seq (120).

Overall, these results support the presence of additional *Fshb* enhancers, which could potentially compensate for deletion of the 17 Kb enhancer.

Validation of the rs06 (A) point mutation mouse line

At the base equivalent to the human rs11031006 (G/A) variant, the mouse genome is consistent with the human major allele (G). To introduce the minor allele variant (A), a single crRNA was used along with a single-stranded repair template containing 45 bp of homology flanking the G>A point mutation at the rs11031006-equivalent site (Fig. 3.7A). Cas9 requires a protospacer adjacent motif (PAM) sequence of NGG in order to bind and cleave DNA. As the rs11031006 equivalent base falls within an NGG motif, we used this to our advantage such that the PAM site would be eliminated following G>A mutation, thereby preventing the site from being targeted again for cleavage once successfully mutated. Routine genotyping was performed by fluorescent Sanger sequencing to assess the presence of each allele (Fig. 3.7B). In addition, the founder was sequenced past the homology arms on either end to confirm that no additional indels were present at the *Fshb* locus.

Puberty is normal in rs06 A/A mice

As first estrus was delayed in the ΔE/ΔE mice, we evaluated puberty in the rs06 mouse line. In females, there were no differences in the age of vaginal opening, weight at vaginal opening, age of first estrus, or length of the interval between vaginal opening and first estrus (Fig. 3.8A-D). In males, there were no differences in the age of preputial separation or weight at preputial separation (Fig. 3.8E and F).

A pilot study of adult male rs06 A/A mice reveals no significant differences in FSH/LH serum levels or sperm production

In a pilot study of n=3 per group, we evaluated fertility in adult male mice. There were no significant differences between the rs06 G/G control group or rs06 A/A group in FSH levels, LH levels, or the LH/FSH ratio (Fig. 3.9 A-C), although high variability within both groups limited a robust conclusion with this sample size. Body and testes weight (Fig. 3.9D,E), as well as sperm motility and total sperm count (Fig. 3.9F,G), did not differ between genotypes.

Discussion

In a mouse deletion model of the *Fshb* enhancer at 17 Kb, serum FSH levels and fertility were normal in adults, although there was a significant delay in first estrus. It is not unusual that loss of a single enhancer does not fully recapitulate the phenotype of a knock-out animal. Phenotypes associated with deletion of a single enhancer vary and have been described as having a subset of the knock-out phenotype or no obvious impairments. For example, *Arx* loss-of-function causes severe neurological defects (140, 141). *Arx* is regulated by multiple "ultraconserved" (perfect sequence conservation) enhancers (142). Dickel, et al. (2018), showed that individual deletions of two ultraconserved enhancers led to decreased neuron density or decreased body weight, while deletion of both resulted in both decreased neuronal density and decreased body weight, suggesting that each enhancer has a unique effect on gene regulation with the resulting phenotypes reflecting temporal and spatial differences in ARX expression (143). A similar effect may explain why mice lacking the 17 Kb enhancer of *Fshb* have delayed first estrus but no apparent differences in adult fertility, although further characterization,

including measurement of serum and pituitary FSH levels in juvenile mice, will be necessary to validate the observed effect.

In another model of enhancer deletion, Osterwalder, et al., report that deletion of individual enhancers of the *Gli3* gene, which regulates forelimb development, had no measurable effect, but deletion of two enhancers that overlap in spatial and temporal expression resulted in limb malformations (144). For this reason, we investigated the possibility of additional enhancers of *Fshb*. An evolutionarily conserved region located 12 Kb upstream of the *Fshb* TSS and located within a region of chromatin accessible in gonadotropes as determined by scATAC-seq (120) also enhanced *Fshb* expression in transfections into LβT2 cells. Future research investigating deletion of the 12 Kb enhancer alone and in combination with the 17 Kb enhancer will provide additional information relevant to understand enhancers within the context of *Fshb* regulation.

In addition to the enhancer deletion mouse model, we also performed a preliminary investigation of the rs11031006 minor allele mouse and did not identify any apparent phenotypes affecting puberty. In a pilot study of adult male mice, FSH/LH serum levels and sperm production were not significantly different, although high variability and small sample size limited a conclusive interpretation. Further characterization of this mouse line, including a female fertility assay, is required to fully understand whether the rs11031006 variant affects fertility. Although the homozygous enhancer deletion did not affect adult fertility, we previously demonstrated that the rs1031006 minor allele increased SF1 binding as compared to the major allele *in vitro*. For this reason, the rs06 A/A mouse may represent a gain-of-function mutation and a phenotype may still arise.

Finally, mouse models can provide valuable insight for human health and disease but can be limited by species-specific differences. While the sequence of the enhancer is conserved between species and *in vitro* assays revealed functional similarities with respect to hormone induction, other differences in *Fshb* regulation could still contribute to the resulting phenotype. We previously demonstrated that both the human and mouse *FSHB* enhancers potentiate activin and GnRH induction of *FSHB* (Chapter 2). While the mouse proximal promoter alone is robustly responsive to activin, the human proximal promoter is not (34, 56, 73, 111). It is plausible that human *FSHB* expression would require the 26 Kb enhancer but that the equivalent mouse 17 Kb enhancer would be dispensable due to compensation by the proximal promoter. Therefore, it is still an open question whether the enhancer or the rs11031006 variant might affect *FSHB* transcription differently within humans.

Acknowledgements

This work was supported by National Institutes of Health (NIH) Eunice Kennedy Shriver National Institute of Child Health and Human Development (NICHD) Grants R01 HD082567, HD100580, and HD072754 to P.L.M., as well as P50 HD012303 (to P.L.M. and V.G.T.) as part of the National Centers for Translational Research in Reproduction and Infertility. P.L.M. was also partially supported by NIH P30 DK063491, P30 CA023100, and P42 ES010337. S.C.B. was partially supported by NIH F31 HD096838 and NIH T32 NS061847. V.G.T. was partially supported by NIH R01 HD095412. The content is solely the responsibility of the authors and does not necessarily represent the official views of the National Institutes of Health.

Chapter 3 is currently in preparation for submission of this material for publication. (Bohaczuk, Stephanie C.; Slaiwa, Theresa I.; Thackray, Varykina G.; Mellon, Pamela L. Mouse

Fertility Is Not Impaired by Deletion of or Point Mutation within an Upstream *Fshb* Enhancer). The dissertation author was the primary investigator and author of this paper. Theresa Slaiwa provided technical assistance. Varykina Thackray assisted with experimental design. Pamela Mellon supervised the project and provided advice.

Figures

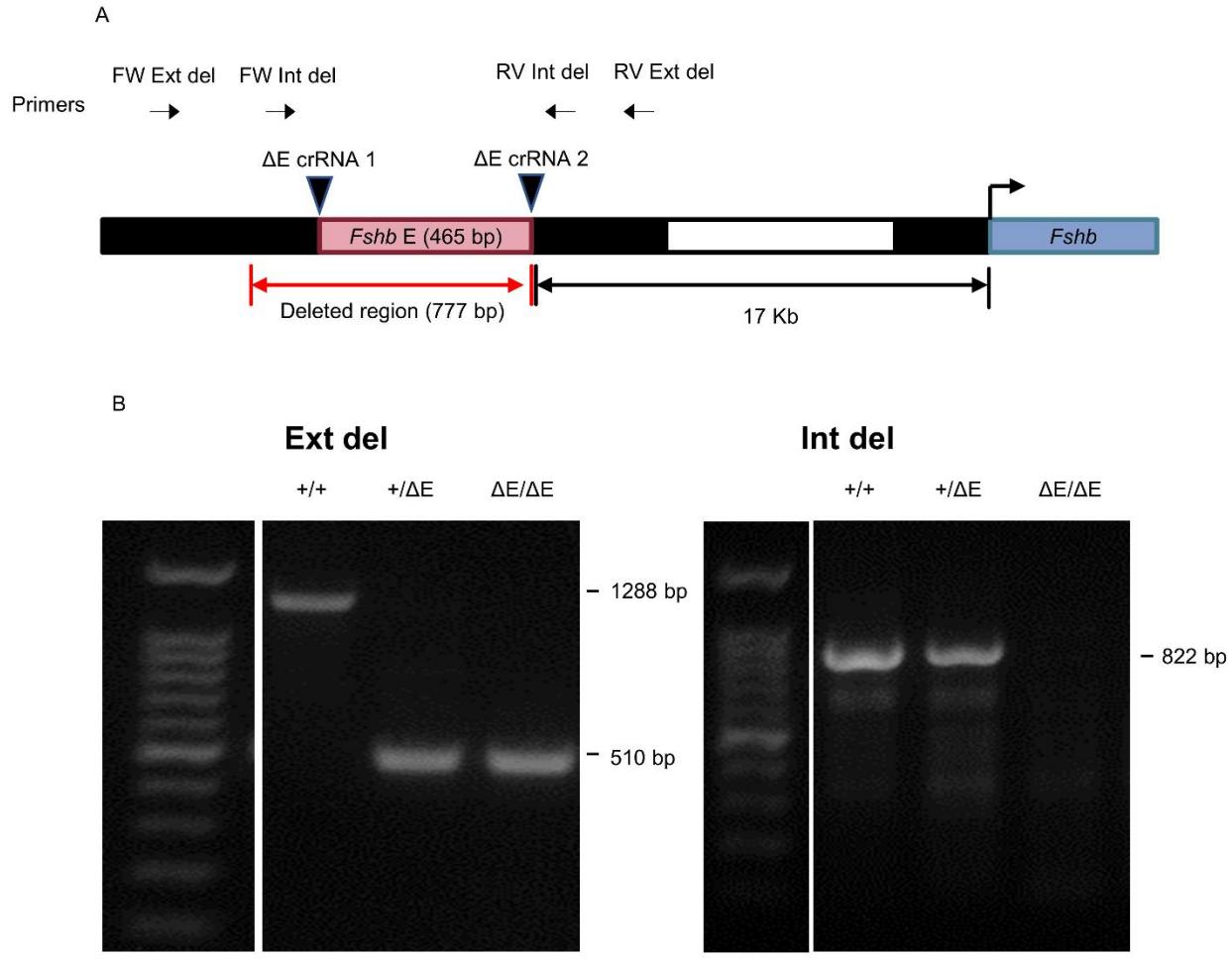

Figure 3.1: Generation of the *Fshb* enhancer deletion mouse line (ΔE). A) A diagram of the crRNA cleavage sites, deleted region, and genotyping primer binding sites. B) A representative PCR of genotyping. +/+, wild-type, +/ΔE, heterozygous for enhancer deletion, ΔE/ΔE, homozygous for enhancer deletion. E, enhancer. bp, base pair.

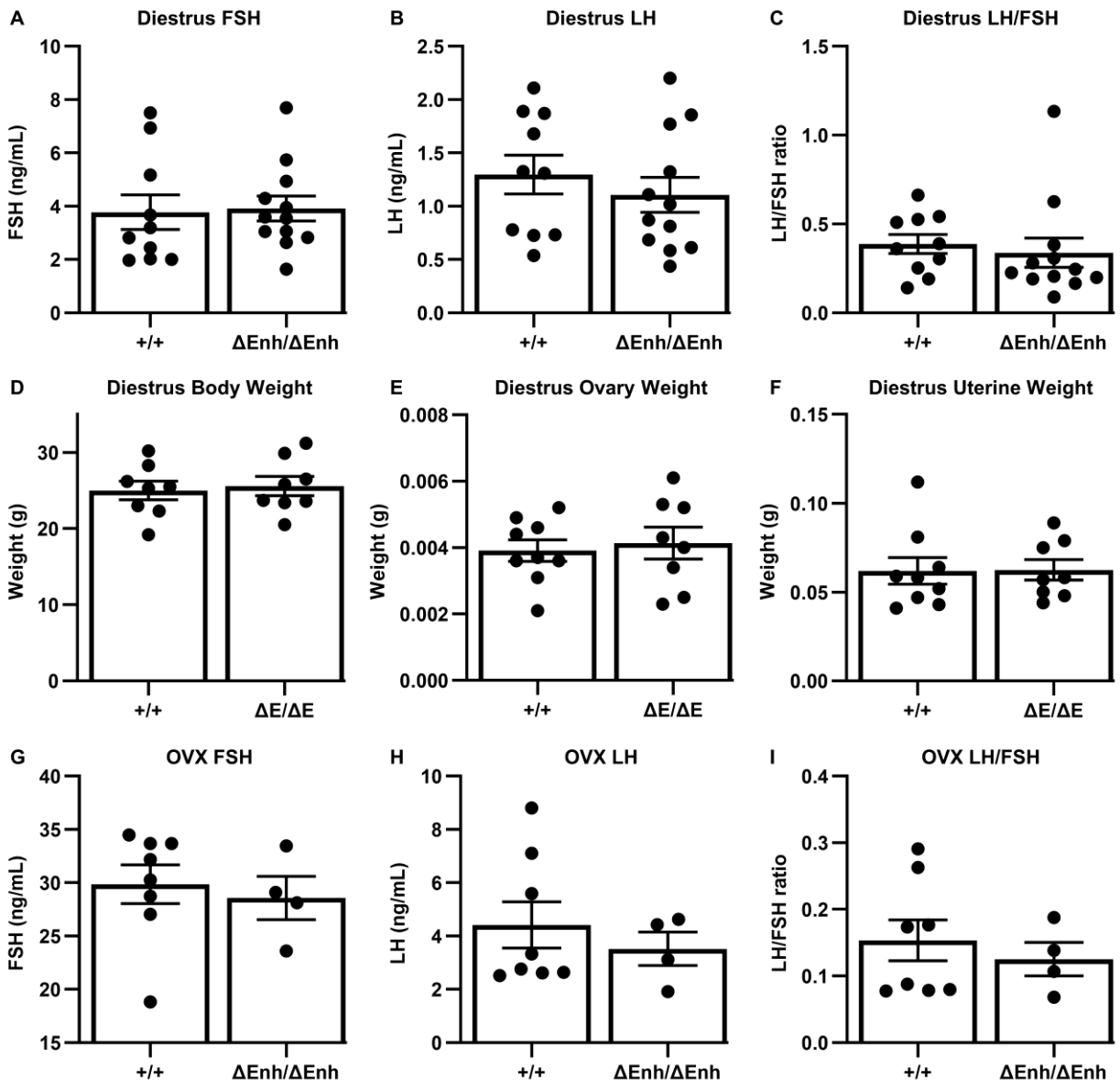

Figure 3.2: Serum FSH/LH levels and ovarian, uterine, and body weights are normal in female ΔE/ΔE mice. From adult female mice, A) diestrus serum FSH B) diestrus serum LH, C) diestrus LH/FSH ratio, D) diestrus body weight E) diestrus ovarian weight (right ovary), F) diestrus uterine weight, G) ovariectomized serum FSH, H) ovariectomized serum LH, and I) ovariectomized LH/FSH ratio were not different between wild-type and ΔE/ΔE mice by two-tailed Student's t-test. FSH, follicle-stimulating hormone. LH, luteinizing hormone. OVX, ovariectomized.

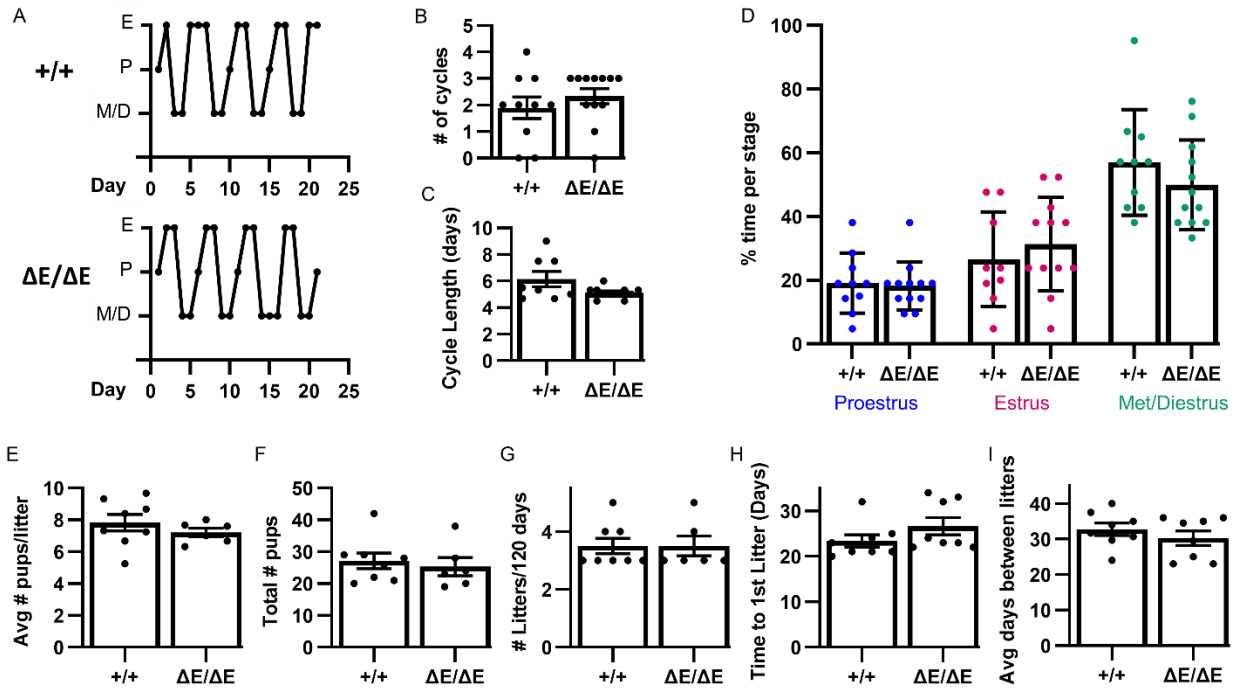

Figure 3.3: Female ΔE/ΔE mice are fertile. A) Representative estrus cycle staging in adult females of each genotype. B) Number of cycles in 21 days, C) average cycle length, and D) % of time spent in each cycle stage are shown. E-I) A fertility assay was conducted with female wild-type or ΔE/ΔE mice mated to wild-type males. E) average pup count per litter, F) total number of pups, G) total number of litters, H) time to first litter, and I) average interval between litters in 120 days were compared. There were no differences between wild-type and ΔE/ΔE mice by two-tailed Student's t-test.

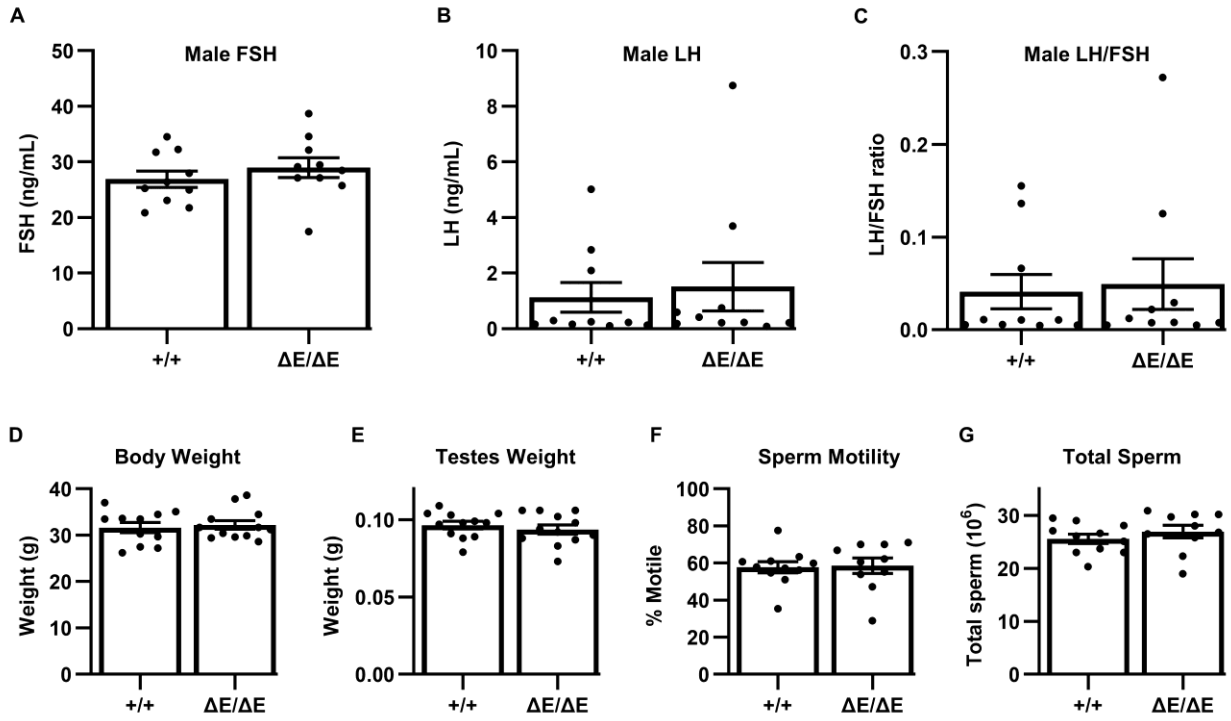

Figure 3.4: Serum FSH/LH levels, testes weight, body weight and sperm are normal in male ΔE/ΔE mice. From adult male mice, A) serum FSH, B) serum LH, C) body weight, D) testes weight, E) total epididymal sperm count, and F) epididymal sperm motility were not different between wild-type and ΔE/ΔE mice by two-tailed Student's t-test.

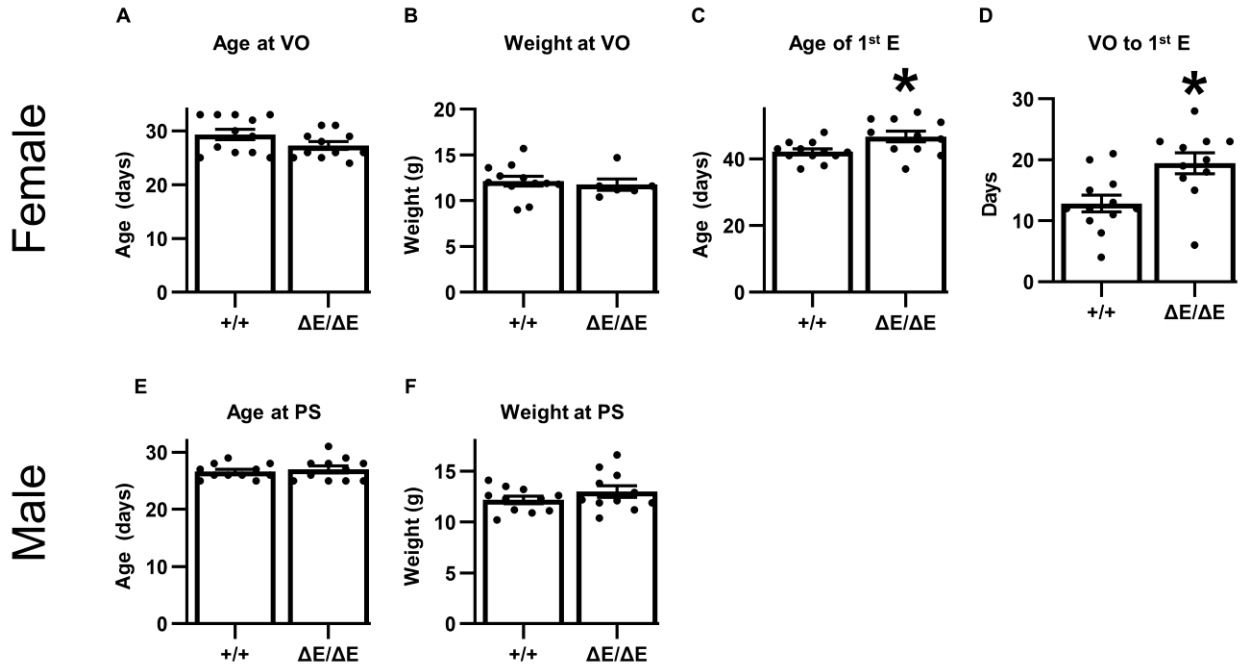

Figure 3.5: First estrus is delayed in female ΔE/ΔE mice, but male puberty is normal. From juvenile female mice, A) age at vaginal opening, B) weight on the day of vaginal opening. C) age at first estrus, and D) days between vaginal opening and first estrus are shown. From juvenile male mice, E) age at preputial separation and F) weight on the day of preputial separation are shown. Data were analyzed by two-tailed Student's t-test. Significant differences between groups (P<0.05) are indicated by *. VO, vaginal opening. PS, preputial separation.

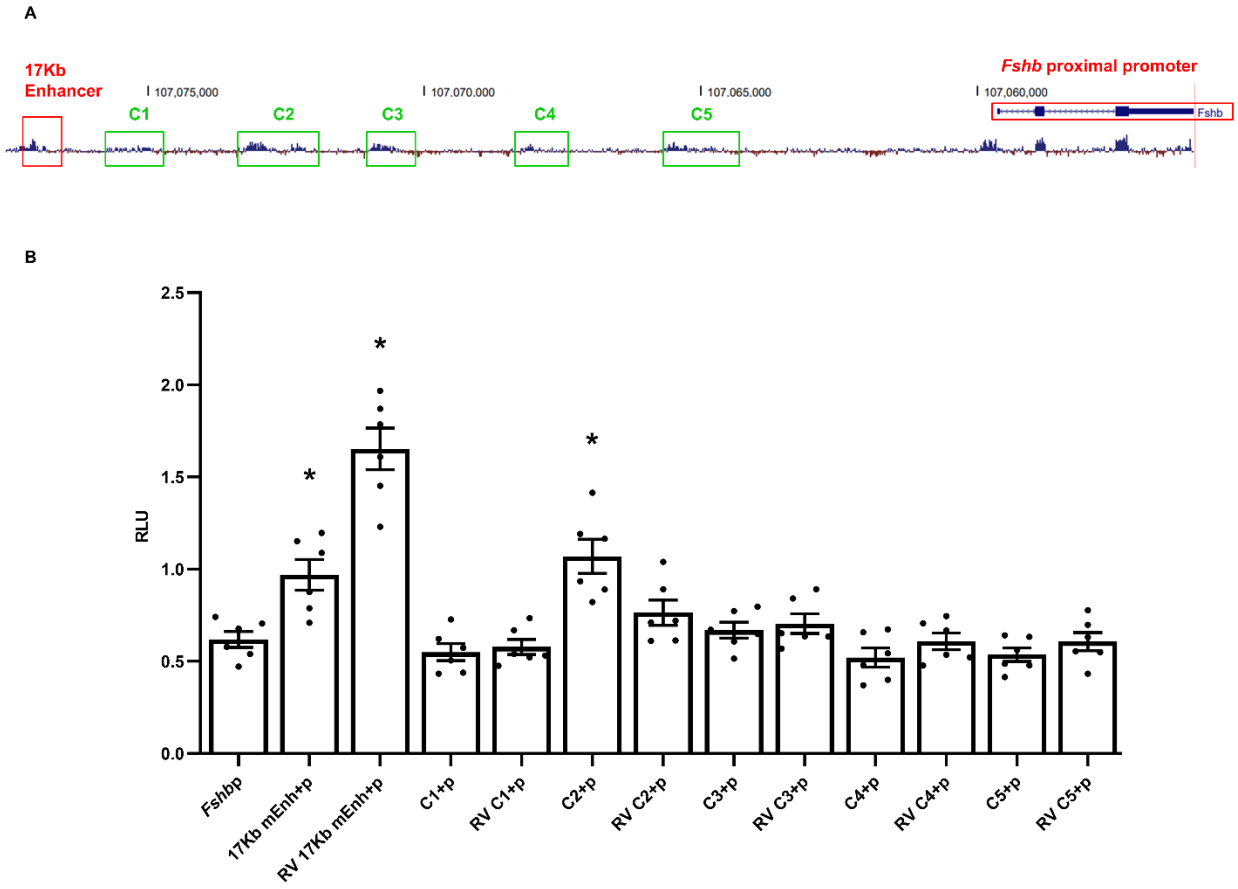

Figure 3.6: A conserved element ~12 Kb upstream of the *Fshb* transcriptional start site (C2) enhances *Fshb* transcription. A) A diagram of conservation upstream of *Fshb* (UCSC genome browser, mm10). Five conserved regions (green boxes, C1-C5) located between the mouse *Fshb* enhancer at 17 Kb and the *Fshb* transcriptional start site, were evaluated for enhancer activity. B) Luciferase expression from reporter constructs driven by the mouse -1000/-1 *Fshb* promoter alone (*Fshb*p) or downstream of the indicated element. Values represent mean ± SEM. Data were analyzed by one-way ANOVA, post-hoc Dunnett multiple comparisons test. * indicates P<0.05 from comparison to the *Fshb* promoter alone.

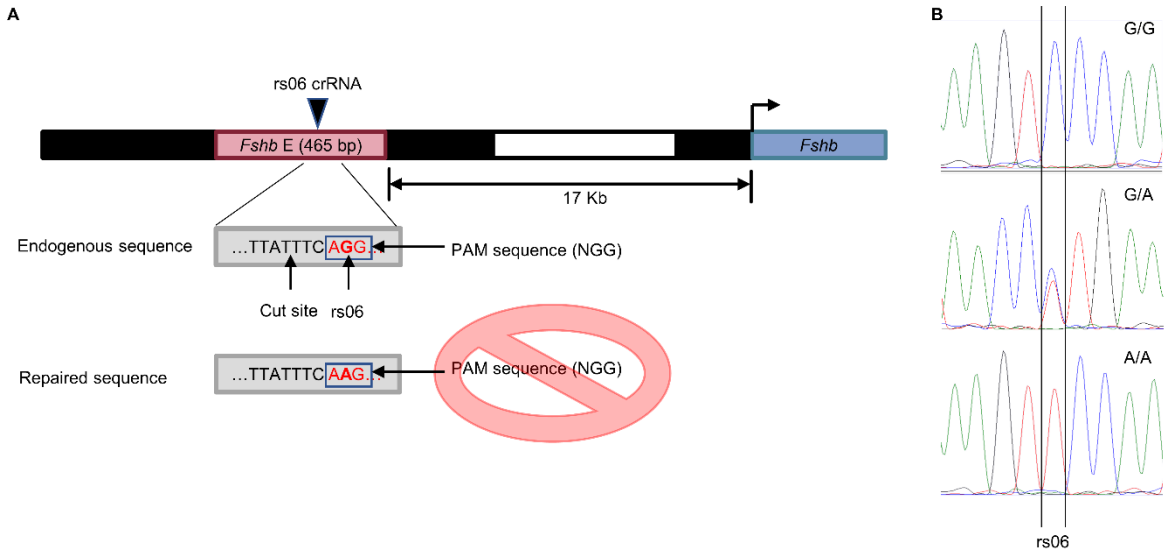

Figure 3.7: Generation of the rs06(A) mouse line. A) A diagram of the crRNA cleavage site. The G>A point mutation at the rs06 base mutates the PAM site necessary for cleavage by Cas9, preventing DNA from being cut again once repaired. B) Representative DNA sequencing chromatograms of the rs06 point mutation, for genotyping. G/G, wild-type (equivalent to human major allele); G/A, heterozygous; A/A, homozygous for rs06 G>A mutation (equivalent to human minor allele). E, enhancer. PAM, protospacer adjacent motif.

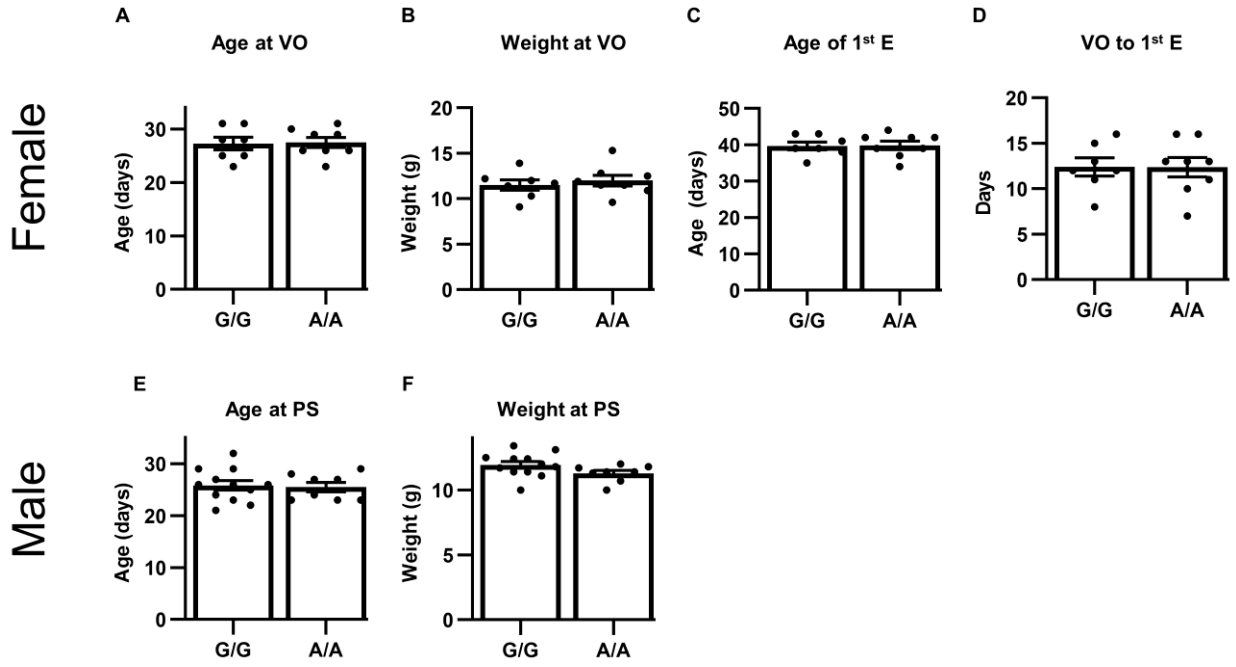

Figure 3.8: Puberty is normal in rs06 A/A female and male mice. From juvenile female mice, A) age at vaginal opening, B) weight on the day of vaginal opening. C) age at first estrus, and D) days between vaginal opening and first estrus are shown. From juvenile male mice, E) age at preputial separation and F) weight on the day of preputial separation are shown. There were no differences between rs06 G/G and rs06 A/A mice by two-tailed Student's t-test. VO, vaginal opening. PS, preputial separation.

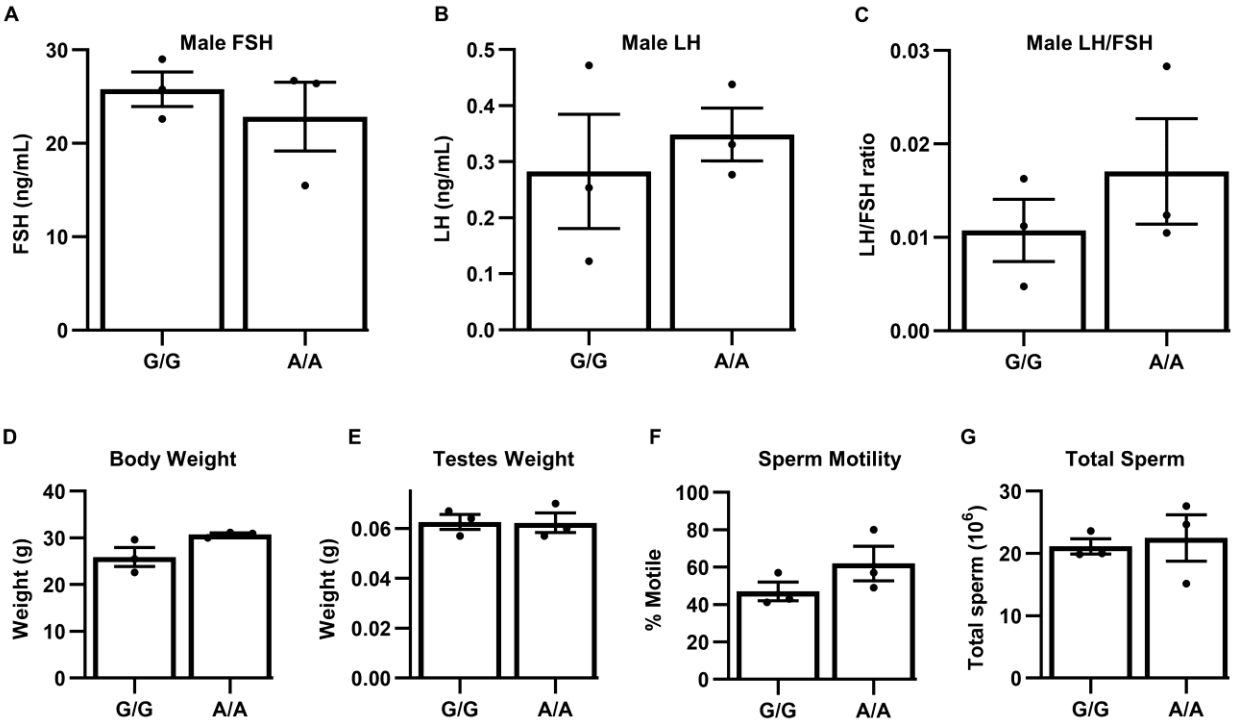

Figure 3.9: Serum FSH/LH levels, testes weight, body weight and sperm are not different in male rs06 A/A mice. From adult male mice, A) serum FSH, B) serum LH, C) LH/FSH ratio, D) body weight, E) testes weight, F) epididymal sperm motility and G) total epidydimal sperm count did not differ between rs06 G/G (wild-type) and rs06 A/A mice by two-tailed Student's t-test.

Tables

Table 3.1: crRNA and repair template sequences

crRNAs		
Name	Cut site (mm10)	Sequence (5’ to 3’)
ΔE, crRNA1	ch2:107076840	AAACAUGAGAAAGACUAACA
ΔE, crRNA1	ch2:107077384	ACACUCCUUGAAGUCUGCCC
Rs06	ch2:107,077,058	UGCCCUGUGAUAUUUAUUUC
Repair template		
rs06	chr2:107,077,008-107,077,098	TATGTCTGGAATTTAATATTGCTCTGCCCTGTGATATTTATTTCA**A**GGTTAGTAGAAATGTAGCTACCTCCTGTAATGACAAATGAACTAT

Table 3.2: Genotyping primer sequences

Name	Sequence (5’ to 3’)
FW Ext del	TGACAAGCACCAGGAGTTGA
RV Ext del	TGGGACTTGTGAGACAGTGT
FW Int del	ACGAAATTGACATCTGTTGCA
RV Int del	ATGATGGGTGTGGGACGTTA

Table 3.3: Conserved region primer sequences

Name	Span (mm10)	Primer Sequence	
C1	chr2:107074862-107075858	FW	GGGAACCAGGTCTTTAGCTG
		RV	CCTTTCTGATGGTTTGCTGA
C2	chr2:107072083-107073413	FW	TCAGCCTTCCTTCGTAAACC
		RV	TGAGGCCAACCCTATGTTTC
C3	chr2:107070312-107071417	FW	GAGGGGGAGAGAGAGAGCAT
		RV	AGCCCATCTCCTTCCAGAGT
C4	chr2:107067807+107068425	FW	TTCCAACACCTGGGAGAAAG
		RV	GCACTTTGGAAGGCTGAAAC
C5	chr2:107064477-107065796	FW	TCCCAGTGTCTTCTGTGTGTG
		RV	CTCCTTTCATTTGTTCATGTGAC

REFERENCES

1. Shupnik MA. Gonadotropin gene modulation by steroids and gonadotropin-releasing hormone. *Biol Reprod.* 1996;**54**(2):279-286.

2. Weiss J, Jameson JL, Burrin JM, Crowley WF, Jr. Divergent responses of gonadotropin subunit messenger RNAs to continuous *versus* pulsatile gonadotropin-releasing hormone *in vitro*. *Mol Endocrinol.* 1990;**4**(4):557-564.

3. Haisenleder D, Dalkin A, Ortolano G, Marshall J, Shupnik M. A pulsatile gonadotropin-releasing hormone stimulus is required to increase transcription of the gonadotropin subunit genes: Evidence for differential regulation of transcription by pulse frequency *in vivo*. *Endocrinology.* 1991;**128**:509-517.

4. Bedecarrats GY, Kaiser UB. Differential regulation of gonadotropin subunit gene promoter activity by pulsatile gonadotropin-releasing hormone (GnRH) in perifused L beta T2 cells: role of GnRH receptor concentration. *Endocrinology.* 2003;**144**(5):1802-1811.

5. Bilezikjian LM, Blount AL, Leal AM, Donaldson CJ, Fischer WH, Vale WW. Autocrine/paracrine regulation of pituitary function by activin, inhibin and follistatin. *Mol Cell Endocrinol.* 2004;**225**(1-2):29-36.

6. Roberts VJ, Sawchenko PE, Vale W. Expression of inhibin/active subunit messenger ribonucleic acids during rat embryogenesis. *Endocrinology.* 1991;**128**:3122-3129.

7. Lebrun JJ, Takabe K, Chen Y, Vale W. Roles of pathway-specific and inhibitory Smads in activin receptor signaling. *Mol Endocrinol.* 1999;**13**(1):15-23.

8. Nakamura T, Takio K, Eto Y, Shibai H, Titani K, Sugino H. Activin-binding protein from rat ovary is follistatin. *Science.* 1990;**247**(4944):836-838.

9. Shimonaka M, Inouye S, Shimasaki S, Ling N. Follistatin binds to both activin and inhibin through the common subunit. *Endocrinology.* 1991;**128**(6):3313-3315.

10. Siegel ET, Kim HG, Nishimoto HK, Layman LC. The molecular basis of impaired follicle-stimulating hormone action: evidence from human mutations and mouse models. *Reprod Sci.* 2013;**20**(3):211-233.

11. Oduwole OO, Peltoketo H, Huhtaniemi IT. Role of follicle-stimulating hormone in spermatogenesis. *Front Endocrinol (Lausanne).* 2018;**9**:763.

12. Meroni SB, Galardo MN, Rindone G, Gorga A, Riera MF, Cigorraga SB. Molecular mechanisms and signaling pathways involved in Sertoli cell proliferation. *Front Endocrinol (Lausanne).* 2019;**10**:224.

13. Blake JA, Richardson JE, Bult CJ, Kadin JA, Eppig JT, Mouse Genome Database G. The Mouse Genome Database (MGD): the model organism database for the laboratory mouse. *Nucleic Acids Res.* 2002;**30**(1):113-115.

14. Zeleznik AJ, Midgley JAR, Reichert JLE. Granulosa cell maturation in the rat: increased binding of human chorionic gonadotropin following treatment with follicle-stimulating hormone in vivo. *Endocrinology.* 1974;**95**(3):818-825.

15. Steinkampf MP, Mendelson CR, Simpson ER. Regulation by follicle-stimulating hormone of the synthesis of aromatase cytochrome P-450 in human granulosa cells. *Mol Endocrinol.* 1987;**1**(7):465-471.

16. Chand AL, Harrison CA, Shelling AN. Inhibin and premature ovarian failure. *Hum Reprod Update.* 2010;**16**(1):39-50.

17. Ortolano GA, Haisenleder DJ, Dalkin AC, Iliff-Sizemore SA, Landefeld TD, Maurer RA, Marshall JC. Follicle-stimulating hormone beta subunit messenger ribonucleic acid concentrations during the rat estrous cycle. *Endocrinology.* 1988;**123**(6):2946-2948.

18. Halvorson LM, Weiss J, Bauer-Dantoin AC, Jameson JL. Dynamic regulation of pituitary follistatin messenger ribonucleic acids during the rat estrous cycle. *Endocrinology.* 1994;**134**(3):1247-1253.

19. Hayes MG, Urbanek M, Ehrmann DA, Armstrong LL, Lee JY, Sisk R, Karaderi T, Barber TM, McCarthy MI, Franks S, Lindgren CM, Welt CK, Diamanti-Kandarakis E, Panidis D, Goodarzi MO, Azziz R, Zhang Y, James RG, Olivier M, Kissebah AH, Stener-Victorin E, Legro RS, Dunaif A. Genome-wide association of polycystic ovary syndrome implicates alterations in gonadotropin secretion in European ancestry populations. *Nat Commun.* 2015;**6**:7502.

20. Day FR, Hinds DA, Tung JY, Stolk L, Styrkarsdottir U, Saxena R, Bjonnes A, Broer L, Dunger DB, Halldorsson BV, Lawlor DA, Laval G, Mathieson I, McCardle WL, Louwers Y, Meun C, Ring S, Scott RA, Sulem P, Uitterlinden AG, Wareham NJ, Thorsteinsdottir U, Welt C, Stefansson K, Laven JS, Ong KK, Perry JR. Causal mechanisms and balancing selection inferred from genetic associations with polycystic ovary syndrome. *Nat Commun.* 2015;**6**:8464.

21. Day F, Karaderi T, Jones MR, Meun C, He C, Drong A, Kraft P, Lin N, Huang H, Broer L, Magi R, Saxena R, Laisk T, Urbanek M, Hayes MG, Thorleifsson G, Fernandez-Tajes J, Mahajan A, Mullin BH, Stuckey BGA, Spector TD, Wilson SG, Goodarzi MO, Davis L, Obermayer-Pietsch B, Uitterlinden AG, Anttila V, Neale BM, Jarvelin MR, Fauser B, Kowalska I, Visser JA, Andersen M, Ong K, Stener-Victorin E, Ehrmann D, Legro RS, Salumets A, McCarthy MI, Morin-Papunen L, Thorsteinsdottir U, Stefansson K, Styrkarsdottir U, Perry JRB, Dunaif A, Laven J, Franks S, Lindgren CM, Welt CK. Large-scale genome-wide meta-analysis of polycystic ovary syndrome suggests shared genetic architecture for different diagnosis criteria. *PLoS Genet.* 2018;**14**(12):e1007813.

22. Tian Y, Zhao H, Chen H, Peng Y, Cui L, Du Y, Wang Z, Xu J, Chen ZJ. Variants in FSHB Are associated with polycystic ovary syndrome and luteinizing hormone level in Han Chinese women. *J Clin Endocrinol Metab.* 2016;**101**(5):2178-2184.

23. Day FR, Ruth KS, Thompson DJ, Lunetta KL, Pervjakova N, Chasman DI, Stolk L, Finucane HK, Sulem P, Bulik-Sullivan B, Esko T, Johnson AD, Elks CE, Franceschini N, He C, Altmaier E, Brody JA, Franke LL, Huffman JE, Keller MF, McArdle PF, Nutile T, Porcu E, Robino A, Rose LM, Schick UM, Smith JA, Teumer A, Traglia M, Vuckovic D, Yao J, Zhao W, Albrecht E, Amin N, Corre T, Hottenga JJ, Mangino M, Smith AV, Tanaka T, Abecasis GR, Andrulis IL, Anton-Culver H, Antoniou AC, Arndt V, Arnold AM, Barbieri C, Beckmann MW, Beeghly-Fadiel A, Benitez J, Bernstein L, Bielinski SJ, Blomqvist C, Boerwinkle E, Bogdanova NV, Bojesen SE, Bolla MK, Borresen-Dale AL, Boutin TS, Brauch H, Brenner H, Bruning T, Burwinkel B, Campbell A, Campbell H, Chanock SJ, Chapman JR, Chen YI, Chenevix-Trench G, Couch FJ, Coviello AD, Cox A, Czene K, Darabi H, De Vivo I, Demerath EW, Dennis J, Devilee P, Dork T, Dos-Santos-Silva I, Dunning AM, Eicher JD, Fasching PA, Faul JD, Figueroa J, Flesch-Janys D, Gandin I, Garcia ME, Garcia-Closas M, Giles GG, Girotto GG, Goldberg MS, Gonzalez-Neira A, Goodarzi MO, Grove ML, Gudbjartsson DF, Guenel P, Guo X, Haiman CA, Hall P, Hamann U, Henderson BE, Hocking LJ, Hofman A, Homuth G, Hooning MJ, Hopper JL, Hu FB, Huang J, Humphreys K, Hunter DJ, Jakubowska A, Jones SE, Kabisch M, Karasik D, Knight JA, Kolcic I, Kooperberg C, Kosma VM, Kriebel J, Kristensen V, Lambrechts D, Langenberg C, Li J, Li X, Lindstrom S, Liu Y, Luan J, Lubinski J, Magi R, Mannermaa A, Manz J, Margolin S, Marten J, Martin NG, Masciullo C, Meindl A, Michailidou K, Mihailov E, Milani L, Milne RL, Muller-Nurasyid M, Nalls M, Neale BM, Nevanlinna H, Neven P, Newman AB, Nordestgaard BG, Olson JE, Padmanabhan S, Peterlongo P, Peters U, Petersmann A, Peto J, Pharoah PD, Pirastu NN, Pirie A, Pistis G, Polasek O, Porteous D, Psaty BM, Pylkas K, Radice P, Raffel LJ, Rivadeneira F, Rudan I, Rudolph A, Ruggiero D, Sala CF, Sanna S, Sawyer EJ, Schlessinger D, Schmidt MK, Schmidt F, Schmutzler RK, Schoemaker MJ, Scott RA, Seynaeve CM, Simard J, Sorice R, Southey MC, Stockl D, Strauch K, Swerdlow A, Taylor KD, Thorsteinsdottir U, Toland AE, Tomlinson I, Truong T, Tryggvadottir L, Turner ST, Vozzi D, Wang Q, Wellons M, Willemsen G, Wilson JF, Winqvist R, Wolffenbuttel BB, Wright AF, Yannoukakos D, Zemunik T, Zheng W, Zygmunt M, Bergmann S, Boomsma DI, Buring JE, Ferrucci L, Montgomery GW, Gudnason V, Spector TD, van Duijn CM, Alizadeh BZ, Ciullo M, Crisponi L, Easton DF, Gasparini PP, Gieger C, Harris TB, Hayward C, Kardia SL, Kraft P, McKnight B, Metspalu A, Morrison AC, Reiner AP, Ridker PM, Rotter JI, Toniolo D, Uitterlinden AG, Ulivi S, Volzke H, Wareham NJ, Weir DR, Yerges-Armstrong LM, Consortium P, kConFab I, Investigators A, Generation S, Consortium EP-I, LifeLines Cohort S, Price AL, Stefansson K, Visser JA, Ong KK, Chang-Claude J, Murabito JM, Perry JR, Murray A. Large-scale genomic analyses link reproductive aging to hypothalamic signaling, breast cancer susceptibility and BRCA1-mediated DNA repair. *Nat Genet.* 2015;**47**(11):1294-1303.

24. Lambalk CB, Boomsma DI, De Boer L, De Koning CH, Schoute E, Popp-Snijders C, Schoemaker J. Increased levels and pulsatility of follicle-stimulating hormone in mothers of hereditary dizygotic twins. *J Clin Endocrinol Metab.* 1998;**83**(2):481-486.

25. The Genomes Project C. A global reference for human genetic variation. *Nature.* 2015;**526**(7571):68-74.

26. Pau CT, Mosbruger T, Saxena R, Welt CK. Phenotype and tissue expression as a function of genetic risk in polycystic ovary syndrome. *PLoS ONE.* 2017;**12**(1):e0168870.

27. Mbarek H, Steinberg S, Nyholt DR, Gordon SD, Miller MB, McRae AF, Hottenga JJ, Day FR, Willemsen G, de Geus EJ, Davies GE, Martin HC, Penninx BW, Jansen R, McAloney K, Vink JM, Kaprio J, Plomin R, Spector TD, Magnusson PK, Reversade B, Harris RA, Aagaard K, Kristjansson RP, Olafsson I, Eyjolfsson GI, Sigurdardottir O, Iacono WG, Lambalk CB, Montgomery GW, McGue M, Ong KK, Perry JRB, Martin NG, Stefansson H, Stefansson K, Boomsma DI. Identification of common genetic variants influencing spontaneous dizygotic twinning and female fertility. *Am J Hum Genet.* 2016;**98**(5):898-908.

28. Alarid ET, Windle JJ, Whyte DB, Mellon PL. Immortalization of pituitary cells at discrete stages of development by directed oncogenesis in transgenic mice. *Development.* 1996;**122**(10):3319-3329.

29. Lamba P, Khivansara V, D'Alessio AC, Santos MM, Bernard DJ. Paired-like homeodomain transcription factors 1 and 2 regulate follicle-stimulating hormone beta-subunit transcription through a conserved cis-element. *Endocrinology.* 2008;**149**(6):3095-3108.

30. West BE, Parker GE, Savage JJ, Kiratipranon P, Toomey KS, Beach LR, Colvin SC, Sloop KW, Rhodes SJ. Regulation of the follicle-stimulating hormone beta gene by the LHX3 LIM-homeodomain transcription factor. *Endocrinology.* 2004;**145**(11):4866-4879.

31. Jacobs SB, Coss D, McGillivray SM, Mellon PL. Nuclear factor Y and steroidogenic factor 1 physically and functionally interact to contribute to cell-specific expression of the mouse Follicle-stimulating hormone-beta gene. *Mol Endocrinol.* 2003;**17**(8):1470-1483.

32. Reed BG, Carr BR 2018 The normal menstrual cycle and the control of ovulation. In: Endotext [Internet]: MDText. com, Inc.

33. Woodruff TK, Besecke LM, Groome N, Draper LB, Schwartz NB, Weiss J. Inhibin A and inhibin B are inversely correlated to follicle-stimulating hormone, yet are discordant during the follicular phase of the rat estrous cycle, and inhibin A is expressed in a sexually dimorphic manner. *Endocrinology.* 1996;**137**(12):5463-5467.

34. Corpuz PS, Lindaman LL, Mellon PL, Coss D. FoxL2 is required for activin induction of the mouse and human follicle-stimulating hormone beta-subunit genes. *Mol Endocrinol.* 2010;**24**(5):1037-1051.

35. Matthews CH, Borgato S, Beck-Peccoz P, Adams M, Tone Y, Gambino G, Casagrande S, Tedeschini G, Benedetti A, Chatterjee VK. Primary amenorrhoea and infertility due to a mutation in the beta-subunit of follicle-stimulating hormone. *Nat Genet.* 1993;**5**(1):83-86.

36. Layman LC, Lee EJ, Peak DB, Namnoum AB, Vu KV, van Lingen BL, Gray MR, McDonough PG, Reindollar RH, Jameson JL. Delayed puberty and hypogonadism caused by mutations in the follicle-stimulating hormone beta-subunit gene. *N Engl J Med.* 1997;**337**(9):607-611.

37. Layman LC, Porto AL, Xie J, da Motta LA, da Motta LD, Weiser W, Sluss PM. FSH beta gene mutations in a female with partial breast development and a male sibling with normal puberty and azoospermia. *J Clin Endocrinol Metab.* 2002;**87**(8):3702-3707.

38. Berger K, Souza H, Brito VN, d'Alva CB, Mendonca BB, Latronico AC. Clinical and hormonal features of selective follicle-stimulating hormone (FSH) deficiency due to FSH beta-subunit gene mutations in both sexes. *Fertil Steril.* 2005;**83**(2):466-470.

39. Lindstedt G, Nystrom E, Matthews C, Ernest I, Janson PO, Chatterjee K. Follitropin (FSH) deficiency in an infertile male due to FSHbeta gene mutation. A syndrome of normal puberty and virilization but underdeveloped testicles with azoospermia, low FSH but high lutropin and normal serum testosterone concentrations. *Clin Chem Lab Med.* 1998;**36**(8):663-665.

40. Phillip M, Arbelle JE, Segev Y, Parvari R. Male hypogonadism due to a mutation in the gene for the beta-subunit of follicle-stimulating hormone. *N Engl J Med.* 1998;**338**(24):1729-1732.

41. Kumar TR, Wang Y, Lu N, Matzuk MM. Follicle stimulating hormone is required for ovarian follicle maturation but not male fertility. *Nat Genet.* 1997;**15**(2):201-204.

42. Fauser BC, Tarlatzis BC, Rebar RW, Legro RS, Balen AH, Lobo R, Carmina E, Chang J, Yildiz BO, Laven JS, Boivin J, Petraglia F, Wijeyeratne CN, Norman RJ, Dunaif A, Franks S, Wild RA, Dumesic D, Barnhart K. Consensus on women's health aspects of polycystic ovary syndrome (PCOS): the Amsterdam ESHRE/ASRM-Sponsored 3rd PCOS Consensus Workshop Group. *Fertil Steril.* 2012;**97**(1):28-38 e25.

43. Revised 2003 consensus on diagnostic criteria and long-term health risks related to polycystic ovary syndrome. *Fertil Steril.* 2004;**81**(1):19-25.

44. Ruth KS, Campbell PJ, Chew S, Lim EM, Hadlow N, Stuckey BG, Brown SJ, Feenstra B, Joseph J, Surdulescu GL, Zheng HF, Richards JB, Murray A, Spector TD, Wilson SG,

Perry JR. Genome-wide association study with 1000 genomes imputation identifies signals for nine sex hormone-related phenotypes. *Eur J Hum Genet.* 2016;**24**(2):284-290.

45. Fortin J, Boehm U, Deng CX, Treier M, Bernard DJ. Follicle-stimulating hormone synthesis and fertility depend on SMAD4 and FOXL2. *FASEB J.* 2014;**28**(8):3396-3410.

46. Shi Y, Zhao H, Cao Y, Yang D, Li Z, Zhang B, Liang X, Li T, Chen J, Shen J, Zhao J, You L, Gao X, Zhu D, Zhao X, Yan Y, Qin Y, Li W, Yan J, Wang Q, Geng L, Ma J, Zhao Y, He G, Zhang A, Zou S, Yang A, Liu J, Li B, Wan C, Shi J, Yang J, Jiang H, Xu JE, Qi X, Sun Y, Zhang Y, Hao C, Ju X, Zhao D, Ren CE, Li X, Zhang W, Zhang J, Wu D, Zhang C, He L, Chen ZJ. Genome-wide association study identifies eight new risk loci for polycystic ovary syndrome. *Nat Genet.* 2012;**44**(9):1020-1025.

47. Chen ZJ, Zhao H, He L, Shi Y, Qin Y, Li Z, You L, Zhao J, Liu J, Liang X, Zhao X, Sun Y, Zhang B, Jiang H, Zhao D, Bian Y, Gao X, Geng L, Li Y, Zhu D, Sun X, Xu JE, Hao C, Ren CE, Zhang Y, Chen S, Zhang W, Yang A, Yan J, Ma J, Zhao Y. Genome-wide association study identifies susceptibility loci for polycystic ovary syndrome on chromosome 2p16.3, 2p21 and 9q33.3. *Nat Genet.* 2011;**43**(1):55-59.

48. Grigorova M, Punab M, Ausmees K, Laan M. FSHB promoter polymorphism within evolutionary conserved element is associated with serum FSH level in men. *Hum Reprod.* 2008;**23**(9):2160-2166.

49. Grigorova M, Punab M, Poolamets O, Kelgo P, Ausmees K, Korrovits P, Vihljajev V, Laan M. Increased prevalance of the -211 T allele of follicle stimulating hormone (FSH) beta subunit promoter polymorphism and lower serum FSH in infertile men. *J Clin Endocrinol Metab.* 2010;**95**(1):100-108.

50. Tuttelmann F, Laan M, Grigorova M, Punab M, Sober S, Gromoll J. Combined effects of the variants FSHB -211G>T and FSHR 2039A>G on male reproductive parameters. *J Clin Endocrinol Metab.* 2012;**97**(10):3639-3647.

51. Rull K, Grigorova M, Ehrenberg A, Vaas P, Sekavin A, Nommemees D, Adler M, Hanson E, Juhanson P, Laan M. FSHB -211 G>T is a major genetic modulator of reproductive physiology and health in childbearing age women. *Hum Reprod.* 2018;**33**(5):954-966.

52. Ferlin A, Vinanzi C, Selice R, Garolla A, Frigo AC, Foresta C. Toward a pharmacogenetic approach to male infertility: polymorphism of follicle-stimulating hormone beta-subunit promoter. *Fertil Steril.* 2011;**96**(6):1344-1349 e1342.

53. Benson CA, Kurz TL, Thackray VG. A human FSHB promoter SNP associated with low FSH levels in men impairs LHX3 binding and basal FSHB transcription. *Endocrinology.* 2013;**154**(9):3016-3021.

54. Creyghton MP, Cheng AW, Welstead GG, Kooistra T, Carey BW, Steine EJ, Hanna J, Lodato MA, Frampton GM, Sharp PA, Boyer LA, Young RA, Jaenisch R. Histone H3K27ac separates active from poised enhancers and predicts developmental state. *Proc Natl Acad Sci U S A.* 2010;**107**(50):21931-21936.

55. Simon JA, Kingston RE. Mechanisms of polycomb gene silencing: knowns and unknowns. *Nat Rev Mol Cell Biol.* 2009;**10**(10):697-708.

56. Lamba P, Santos MM, Philips DP, Bernard DJ. Acute regulation of murine follicle-stimulating hormone beta subunit transcription by activin A. *J Mol Endocrinol.* 2006;**36**(1):201-220.

57. Thackray VG, McGillivray SM, Mellon PL. Androgens, progestins, and glucocorticoids induce follicle-stimulating hormone beta-subunit gene expression at the level of the gonadotrope. *Mol Endocrinol.* 2006;**20**(9):2062-2079.

58. Spady TJ, Shayya R, Thackray VG, Ehrensberger L, Bailey JS, Mellon PL. Androgen regulates follicle-stimulating hormone beta gene expression in an activin-dependent manner in immortalized gonadotropes. *Mol Endocrinol.* 2004;**18**(4):925-940.

59. Li LA, Chiang EF, Chen JC, Hsu NC, Chen YJ, Chung BC. Function of steroidogenic factor 1 domains in nuclear localization, transactivation, and interaction with transcription factor TFIIB and c-Jun. *Mol Endocrinol.* 1999;**13**(9):1588-1598.

60. Novoradovsky A, Zhang V, Ghosh M, Hogrefe H, Sorge JA, Gaasterland T 2005 Computational principles of primer design for site directed mutagenesis. Technical Proceedings of 2005 NSTI Nanotechnology Conference and Trade Show, 2005, pp 532-535

61. Maaten Lvd, Hinton G. Visualizing data using t-SNE. *J Mach Learn Res.* 2008;**9**(Nov):2579-2605.

62. RRID:AB_2561016.

63. RRID:AB_2561020.

64. RRID:AB_1031062.

65. RRID:AB_2615075.

66. RRID:AB_2793712.

67. Owczarzy R, Tataurov AV, Wu Y, Manthey JA, McQuisten KA, Almabrazi HG, Pedersen KF, Lin Y, Garretson J, McEntaggart NO, Sailor CA, Dawson RB, Peek AS. IDT SciTools: a suite for analysis and design of nucleic acid oligomers. *Nucleic Acids Res.* 2008;**36**(Web Server issue):W163-169.

68. Ye J, Coulouris G, Zaretskaya I, Cutcutache I, Rozen S, Madden TL. Primer-BLAST: a tool to design target-specific primers for polymerase chain reaction. *BMC Bioinformatics.* 2012;**13**:134.

69. RRID:AB_310756.

70. RRID:AB_737197.

71. Pennacchio LA, Bickmore W, Dean A, Nobrega MA, Bejerano G. Enhancers: five essential questions. *Nat Rev Genet.* 2013;**14**(4):288-295.

72. Turner BM. Reading signals on the nucleosome with a new nomenclature for modified histones. *Nat Struct Mol Biol.* 2005;**12**(2):110-112.

73. Bernard DJ, Tran S. Mechanisms of activin-stimulated FSH synthesis: the story of a pig and a FOX. *Biol Reprod.* 2013;**88**(3):78.

74. Bohaczuk ST, VG; Shen, J; Skowronska-Krawczyk, D; Mellon, PL. Data from: FSHB transcription is regulated by a novel 5' distal enhancer with a fertility-associated single nucleotide polymorphism. UC San Diego, Dataset. Dryad Digital Repository 2020. Deposited 12 September 2020. https://doi.org/10.6075/J09885DG.

75. Koch CM, Andrews RM, Flicek P, Dillon SC, Karaoz U, Clelland GK, Wilcox S, Beare DM, Fowler JC, Couttet P, James KD, Lefebvre GC, Bruce AW, Dovey OM, Ellis PD, Dhami P, Langford CF, Weng Z, Birney E, Carter NP, Vetrie D, Dunham I. The landscape of histone modifications across 1% of the human genome in five human cell lines. *Genome Res.* 2007;**17**(6):691-707.

76. Graham KE, Nusser KD, Low MJ. LbetaT2 gonadotroph cells secrete follicle stimulating hormone (FSH) in response to active A. *J Endocrinol.* 1999;**162**(3):R1-5.

77. Zentner GE, Tesar PJ, Scacheri PC. Epigenetic signatures distinguish multiple classes of enhancers with distinct cellular functions. *Genome Res.* 2011;**21**(8):1273-1283.

78. Rhodes SJ, Chen R, DiMattia GE, Scully KM, Kalla KA, Lin SC, Yu VC, Rosenfeld MG. A tissue-specific enhancer confers Pit-1-dependent morphogen inducibility and autoregulation on the pit-1 gene. *Genes Dev.* 1993;**7**(6):913-932.

79. Busygina TV, Ignatieva EV, Osadchuk AV. Consensus sequence of transcription factor SF-1 binding site and putative binding site in the 5' flanking regions of genes encoding mouse steroidogenic enzymes 3betaHSDI and Cyp17. *Biochemistry (Mosc).* 2003;**68**(4):377-384.

80. Jameson JL. Of mice and men: The tale of steroidogenic factor-1. *J Clin Endocrinol Metab.* 2004;**89**(12):5927-5929.

81. Jorgensen JS, Nilson JH. AR suppresses transcription of the LHbeta subunit by interacting with steroidogenic factor-1. *Mol Endocrinol.* 2001;**15**(9):1505-1516.

82. Barnhart KM, Mellon PL. The orphan nuclear receptor, steroidogenic factor-1, regulates the glycoprotein hormone alpha-subunit gene in pituitary gonadotropes. *Mol Endocrinol.* 1994;**8**(7):878-885.

83. Ruf-Zamojski F, Fribourg M, Ge Y, Nair V, Pincas H, Zaslavsky E, Nudelman G, Tuminello SJ, Watanabe H, Turgeon JL, Sealfon SC. Regulatory architecture of the LbetaT2 gonadotrope cell underlying the response to gonadotropin-releasing hormone. *Front Endocrinol (Lausanne).* 2018;**9**:34.

84. Tremblay JJ, Lanctot C, Drouin J. The pan-pituitary activator of transcription, Ptx1 (pituitary homeobox 1), acts in synergy with SF-1 and Pit1 and is an upstream regulator of the Lim-homeodomain gene Lim3/Lhx3. *Mol Endocrinol.* 1998;**12**(3):428-441.

85. Tremblay JJ, Marcil A, Gauthier Y, Drouin J. Ptx1 regulates SF-1 activity by an interaction that mimics the role of the ligand-binding domain. *EMBO J.* 1999;**18**(12):3431-3441.

86. Coss D, Thackray VG, Deng CX, Mellon PL. Activin regulates luteinizing hormone beta-subunit gene expression through Smad-binding and homeobox elements. *Mol Endocrinol.* 2005;**19**(10):2610-2623.

87. Kumar TR, Low MJ, Matzuk MM. Genetic rescue of follicle-stimulating hormone beta-deficient mice. *Endocrinology.* 1998;**139**(7):3289-3295.

88. Gallagher MD, Chen-Plotkin AS. The post-GWAS era: from association to function. *Am J Hum Genet.* 2018;**102**(5):717-730.

89. Maurano MT, Humbert R, Rynes E, Thurman RE, Haugen E, Wang H, Reynolds AP, Sandstrom R, Qu H, Brody J, Shafer A, Neri F, Lee K, Kutyavin T, Stehling-Sun S, Johnson AK, Canfield TK, Giste E, Diegel M, Bates D, Hansen RS, Neph S, Sabo PJ, Heimfeld S, Raubitschek A, Ziegler S, Cotsapas C, Sotoodehnia N, Glass I, Sunyaev SR, Kaul R, Stamatoyannopoulos JA. Systematic localization of common disease-associated variation in regulatory DNA. *Science.* 2012;**337**(6099):1190-1195.

90. Iyer AK, Miller NL, Yip K, Tran BH, Mellon PL. Enhancers of GnRH transcription embedded in an upstream gene use homeodomain proteins to specify hypothalamic expression. *Mol Endocrinol.* 2010;**24**(10):1949-1964.

91. Visel A, Bristow J, Pennacchio LA. Enhancer identification through comparative genomics. *Semin Cell Dev Biol.* 2007;**18**(1):140-152.

92. Woolfe A, Goodson M, Goode DK, Snell P, McEwen GK, Vavouri T, Smith SF, North P, Callaway H, Kelly K, Walter K, Abnizova I, Gilks W, Edwards YJ, Cooke JE, Elgar

G. Highly conserved non-coding sequences are associated with vertebrate development. *PLoS Biol.* 2005;**3**(1):e7.

93. Edwards SL, Beesley J, French JD, Dunning AM. Beyond GWASs: illuminating the dark road from association to function. *Am J Hum Genet.* 2013;**93**(5):779-797.

94. Ruth KS, Day FR, Tyrrell J, Thompson DJ, Wood AR, Mahajan A, Beaumont RN, Wittemans L, Martin S, Busch AS, Erzurumluoglu AM, Hollis B, O'Mara TA, McCarthy MI, Langenberg C, Easton DF, Wareham NJ, Burgess S, Murray A, Ong KK, Frayling TM, Perry JRB. Using human genetics to understand the disease impacts of testosterone in men and women. *Nat Med.* 2020;**26**(2):252-258.

95. Witchel SF, Tena-Sempere M. The Kiss1 system and polycystic ovary syndrome: lessons from physiology and putative pathophysiologic implications. *Fertil Steril.* 2013;**100**(1):12-22.

96. Ibáñez L, Valls C, Cols M, Ferrer A, Marcos MV, De Zegher F. Hypersecretion of FSH in infant boys and girls born small for gestational age. *J Clin Endocrinol Metab.* 2002;**87**(5):1986-1988.

97. Melo AS, Vieira CS, Barbieri MA, Rosa ESAC, Silva AA, Cardoso VC, Reis RM, Ferriani RA, Silva-de-Sá MF, Bettiol H. High prevalence of polycystic ovary syndrome in women born small for gestational age. *Hum Reprod.* 2010;**25**(8):2124-2131.

98. Kuiri-Hänninen T, Kallio S, Seuri R, Tyrväinen E, Liakka A, Tapanainen J, Sankilampi U, Dunkel L. Postnatal developmental changes in the pituitary-ovarian axis in preterm and term infant girls. *J Clin Endocrinol Metab.* 2011;**96**(11):3432-3439.

99. Grossman MP, Nakajima ST, Fallat ME, Siow Y. Müllerian-inhibiting substance inhibits cytochrome P450 aromatase activity in human granulosa lutein cell culture. *Fertil Steril.* 2008;**89**(5 Suppl):1364-1370.

100. Dewailly D, Robin G, Peigne M, Decanter C, Pigny P, Catteau-Jonard S. Interactions between androgens, FSH, anti-Mullerian hormone and estradiol during folliculogenesis in the human normal and polycystic ovary. *Hum Reprod Update.* 2016;**22**(6):709-724.

101. Garg D, Tal R. The role of AMH in the pathophysiology of polycystic ovarian syndrome. *Reprod Biomed Online.* 2016;**33**(1):15-28.

102. Cimino I, Casoni F, Liu X, Messina A, Parkash J, Jamin SP, Catteau-Jonard S, Collier F, Baroncini M, Dewailly D, Pigny P, Prescott M, Campbell R, Herbison AE, Prevot V, Giacobini P. Novel role for anti-Mullerian hormone in the regulation of GnRH neuron excitability and hormone secretion. *Nat Commun.* 2016;**7**:10055.

103. Matzuk MM, Kumar TR, Bradley A. Different phenotypes for mice deficient in either activins or activin receptor type II. *Nature.* 1995;**374**(6520):356-560.

104. Lee KB, Khivansara V, Santos MM, Lamba P, Yuen T, Sealfon SC, Bernard DJ. Bone morphogenetic protein 2 and activin A synergistically stimulate follicle-stimulating hormone beta subunit transcription. *J Mol Endocrinol.* 2007;**38**(1-2):315-330.

105. Thackray VG, Mellon PL. Synergistic induction of follicle-stimulating hormone beta-subunit gene expression by gonadal steroid hormone receptors and smad proteins. *Endocrinology.* 2008;**149**(3):1091-1102.

106. Bernard DJ. Both SMAD2 and SMAD3 mediate activin-stimulated expression of the follicle-stimulating hormone beta subunit in mouse gonadotrope cells. *Mol Endocrinol.* 2004;**18**(3):606-623.

107. Lamba P, Fortin J, Tran S, Wang Y, Bernard DJ. A novel role for the forkhead transcription factor FOXL2 in activin A-regulated follicle-stimulating hormone beta subunit transcription. *Mol Endocrinol.* 2009;**23**(7):1001-1013.

108. Tran S, Lamba P, Wang Y, Bernard DJ. SMADs and FOXL2 synergistically regulate murine FSHbeta transcription via a conserved proximal promoter element. *Mol Endocrinol.* 2011;**25**(7):1170-1183.

109. Li Y, Schang G, Wang Y, Zhou X, Levasseur A, Boyer A, Deng CX, Treier M, Boehm U, Boerboom D, Bernard DJ. Conditional deletion of FOXL2 and SMAD4 in gonadotropes of adult mice causes isolated FSH deficiency. *Endocrinology.* 2018;**159**(7):2641-2655.

110. Thompson TB, Lerch TF, Cook RW, Woodruff TK, Jardetzky TS. The structure of the follistatin:activin complex reveals antagonism of both type I and type II receptor binding. *Dev Cell.* 2005;**9**(4):535-543.

111. Wang Y, Fortin J, Lamba P, Bonomi M, Persani L, Roberson MS, Bernard DJ. Activator protein-1 and smad proteins synergistically regulate human follicle-stimulating hormone beta-promoter activity. *Endocrinology.* 2008;**149**(11):5577-5591.

112. Coss D, Hand CM, Yaphockun KK, Ely HA, Mellon PL. p38 mitogen-activated protein kinase is critical for synergistic induction of the FSH(beta) gene by gonadotropin-releasing hormone and activin through augmentation of c-Fos induction and Smad phosphorylation. *Mol Endocrinol.* 2007;**21**(12):3071-3086.

113. Suszko MI, Lo DJ, Suh H, Camper SA, Woodruff TK. Regulation of the rat follicle-stimulating hormone beta-subunit promoter by activin. *Mol Endocrinol.* 2003;**17**(3):318-332.

114. Bernard DJ, Fortin J, Wang Y, Lamba P. Mechanisms of FSH synthesis: what we know, what we don't, and why you should care. *Fertil Steril.* 2010;**93**(8):2465-2485.

115. Lappohn RE, Burger HG, Bouma J, Bangah M, Krans M. Inhibin as a marker for granulosa cell tumor. *Acta Obstet Gynecol Scand Suppl.* 1992;**155**:61-65.

116. Healy DL, Burger HG, Mamers P, Jobling T, Bangah M, Quinn M, Grant P, Day AJ, Rome R, Campbell JJ. Elevated serum inhibin concentrations in postmenopausal women with ovarian tumors. *N Engl J Med.* 1993;**329**(21):1539-1542.

117. Krishnan A, Murdock C, Allard J, Cisar M, Reid E, Nieman L, Segars J. Pseudo-isolated FSH deficiency caused by an inhibin B-secreting granulosa cell tumour: case report. *Hum Reprod.* 2003;**18**(3):502-505.

118. Decoudier B, Hécart AC, Hoeffel C, Graesslin O, Joseph K, Amiot-Chapoutot F, Delemer B. Isolated FSH deficiency revealing a granulosa cell tumor. *Ann Endocrinol (Paris).* 2010;**71**(6):543-547.

119. Ruckle J, Jacobs M, Kramer W, Pearsall AE, Kumar R, Underwood KW, Seehra J, Yang Y, Condon CH, Sherman ML. Single-dose, randomized, double-blind, placebo-controlled study of ACE-011 (ActRIIA-IgG1) in postmenopausal women. *J Bone Miner Res.* 2009;**24**(4):744-752.

120. Bohaczuk SC, Thackray VG, Shen J, Skowronska-Krawczyk D, Mellon PL. FSHB transcription is regulated by a novel 5' distal enhancer with a fertility-associated single nucleotide polymorphism. *Endocrinology.* 2021;**162**(1):1-12.

121. RRID:Addgene_80893.

122. Ruf-Zamojski F, Ge Y, Pincas H, Shan J, Song Y, Hines N, Kelley K, Montagna C, Nair P, Toufaily C, Bernard DJ, Mellon PL, Nair V, Turgeon JL, Sealfon SC. Cytogenetic, genomic, and functional characterization of pituitary gonadotrope cell lines. *J Endocr Soc.* 2019;**3**(5):902-920.

123. Choy L, Derynck R. Transforming growth factor-beta inhibits adipocyte differentiation by Smad3 interacting with CCAAT/enhancer-binding protein (C/EBP) and repressing C/EBP transactivation function. *J Biol Chem.* 2003;**278**(11):9609-9619.

124. RRID:AB_2728776.

125. RRID:AB_631746.

126. RRID:AB_2736998.

127. Pernasetti F, Vasilyev VV, Rosenberg SB, Bailey JS, Huang HJ, Miller WL, Mellon PL. Cell-specific transcriptional regulation of follicle-stimulating hormone-beta by activin and gonadotropin-releasing hormone in the LbetaT2 pituitary gonadotrope cell model. *Endocrinology.* 2001;**142**(6):2284-2295.

128. Hayashi H, Abdollah S, Qiu Y, Cai J, Xu YY, Grinnell BW, Richardson MA, Topper JN, Gimbrone MA, Jr., Wrana JL, Falb D. The MAD-related protein Smad7 associates with the TGFbeta receptor and functions as an antagonist of TGFbeta signaling. *Cell.* 1997;**89**(7):1165-1173.

129. Bak B, Carpio L, Kipp JL, Lamba P, Wang Y, Ge RS, Hardy MP, Mayo KE, Bernard DJ. Activins regulate 17beta-hydroxysteroid dehydrogenase type I transcription in murine gonadotrope cells. *J Endocrinol.* 2009;**201**(1):89-104.

130. Ongaro L, Schang G, Zhou Z, Kumar TR, Treier M, Deng CX, Boehm U, Bernard DJ. Human follicle-stimulating hormone ß subunit expression depends on FOXL2 and SMAD4. *Endocrinology.* 2020;**161**(5

131. Grant CE, Bailey TL, Noble WS. FIMO: scanning for occurrences of a given motif. *Bioinformatics.* 2011;**27**(7):1017-1018.

132. Fornes O, Castro-Mondragon JA, Khan A, van der Lee R, Zhang X, Richmond PA, Modi BP, Correard S, Gheorghe M, Baranasic D, Santana-Garcia W, Tan G, Cheneby J, Ballester B, Parcy F, Sandelin A, Lenhard B, Wasserman WW, Mathelier A. JASPAR 2020: update of the open-access database of transcription factor binding profiles. *Nucleic Acids Res.* 2020;**48**(D1):D87-D92.

133. Kumar TR. Extragonadal actions of FSH: a critical need for novel genetic models. *Endocrinology.* 2017;**159**(1):2-8.

134. Sun L, Peng Y, Sharrow AC, Iqbal J, Zhang Z, Papachristou DJ, Zaidi S, Zhu LL, Yaroslavskiy BB, Zhou H, Zallone A, Sairam MR, Kumar TR, Bo W, Braun J, Cardoso-Landa L, Schaffler MB, Moonga BS, Blair HC, Zaidi M. FSH directly regulates bone mass. *Cell.* 2006;**125**(2):247-260.

135. Liu P, Ji Y, Yuen T, Rendina-Ruedy E, DeMambro VE, Dhawan S, Abu-Amer W, Izadmehr S, Zhou B, Shin AC, Latif R, Thangeswaran P, Gupta A, Li J, Shnayder V, Robinson ST, Yu YE, Zhang X, Yang F, Lu P, Zhou Y, Zhu LL, Oberlin DJ, Davies TF, Reagan MR, Brown A, Kumar TR, Epstein S, Iqbal J, Avadhani NG, New MI, Molina H, van Klinken JB, Guo EX, Buettner C, Haider S, Bian Z, Sun L, Rosen CJ, Zaidi M. Blocking FSH induces thermogenic adipose tissue and reduces body fat. *Nature.* 2017;**546**(7656):107-112.

136. Li Y, Schang G, Boehm U, Deng CX, Graff J, Bernard DJ. SMAD3 regulates follicle-stimulating hormone synthesis by pituitary gonadotrope cells in vivo. *J Biol Chem.* 2017;**292**(6):2301-2314.

137. Hoffmann HM. Determination of reproductive competence by confirming pubertal onset and performing a fertility assay in mice and rats. *J Vis Exp.* 2018140):e58352.

138. Cora MC, Kooistra L, Travlos G. Vaginal cytology of the laboratory rat and mouse: review and criteria for the staging of the estrous cycle using stained vaginal smears. *Toxicologic Pathology.* 2015;**43**(6):776-793.

139. François CM, Petit F, Giton F, Gougeon A, Ravel C, Magre S, Cohen-Tannoudji J, Guigon CJ. A novel action of follicle-stimulating hormone in the ovary promotes estradiol production without inducing excessive follicular growth before puberty. *Sci Rep.* 2017;**7**:46222.

140. Gecz J, Cloosterman D, Partington M. ARX: a gene for all seasons. *Curr Opin Genet Dev.* 2006;**16**(3):308-316.

141. Kitamura K, Yanazawa M, Sugiyama N, Miura H, Iizuka-Kogo A, Kusaka M, Omichi K, Suzuki R, Kato-Fukui Y, Kamiirisa K, Matsuo M, Kamijo S-i, Kasahara M, Yoshioka H, Ogata T, Fukuda T, Kondo I, Kato M, Dobyns WB, Yokoyama M, Morohashi K-i. Mutation of ARX causes abnormal development of forebrain and testes in mice and X-linked lissencephaly with abnormal genitalia in humans. *Nature Genetics.* 2002;**32**(3):359-369.

142. Bejerano G, Pheasant M, Makunin I, Stephen S, Kent WJ, Mattick JS, Haussler D. Ultraconserved elements in the human genome. *Science.* 2004;**304**(5675):1321-1325.

143. Dickel DE, Ypsilanti AR, Pla R, Zhu Y, Barozzi I, Mannion BJ, Khin YS, Fukuda-Yuzawa Y, Plajzer-Frick I, Pickle CS, Lee EA, Harrington AN, Pham QT, Garvin TH, Kato M, Osterwalder M, Akiyama JA, Afzal V, Rubenstein JLR, Pennacchio LA, Visel A. Ultraconserved enhancers are required for normal development. *Cell.* 2018;**172**(3):491-499.e415.

144. Osterwalder M, Barozzi I, Tissières V, Fukuda-Yuzawa Y, Mannion BJ, Afzal SY, Lee EA, Zhu Y, Plajzer-Frick I, Pickle CS, Kato M, Garvin TH, Pham QT, Harrington AN, Akiyama JA, Afzal V, Lopez-Rios J, Dickel DE, Visel A, Pennacchio LA. Enhancer redundancy provides phenotypic robustness in mammalian development. *Nature.* 2018;**554**(7691):239-243.